Ana Maria Freitas da Silva
Licenciatura em Ciências da Engenharia Química e Bioquímica

A SIMPLE CLOSED-LOOP MEMBRANE PROCESS FOR THE PURIFICATION OF ACTIVE PHARMACEUTICAL INGREDIENTS

Dissertação para obtenção do Grau de Mestre em
Engenharia Química e Bioquímica

Orientadores:	Professor Andrew G. Livingston (IC) Professor João G. Crespo (FCT-UNL)
Co-orientador:	Jeong F. Kim (IC)

IMPERIAL COLLEGE LONDON
Faculty of Engineering
Department of Chemical Engineering and Chemical Technology

UNIVERSIDADE NOVA DE LISBOA
Faculdade de Ciências e tecnologia
Departamento de Química

Novembro 2012

Copyright Ana Maria Freitas da Silva, FCT-UNL, UNL

A Faculdade de Ciências e Tecnologia e a Universidade Nova de Lisboa tem o direito, perpétuo e sem limites geográficos, de arquivar e publicar esta dissertação através de exemplares impressos reproduzidos em papel ou de forma digital, ou por qualquer outro meio conhecido ou que venha a ser inventado, e de a divulgar através de repositórios científicos e de admitir a sua cópia e distribuição com objectivos educacionais ou de investigação, não comerciais, desde que seja dado crédito ao autor e editor.

ACKNOWLEDGMENT

First of all, I would like to thank Professor Andrew Livingston for receiving me in his research group.

I am deeply grateful to Jeong Kim, my daily supervisor, who helped me through the whole project, including writing this thesis.

I would like to thank all the other members of the Separation Engineering and Technology research group for their support during my stay at Imperial College.

I would like also to thank Professor João Crespo and Professor Isabel Coelhoso for being always available to help with any questions and showing interest in my work.

Last but not least, I would like to thank my family and friends for their emotional help, encouragement and understanding.

ABSTRACT

Here we present a simple closed-loop process for the purification of active pharmaceutical ingredients (API) that combines two Organic Solvent Nanofiltration (OSN) membranes, one for purification and another for solvent recovery. Its success depends on the membrane used for solvent recovery that should only let the solvent pass through it.

A mixture of Solvent Yellow 7 (MW=198.2g.mol^{-1}) (SY7) and Brilliant Blue R (MW=826.0g.mol^{-1}) (BBR) in *N,N*-dimethylformamide (DMF) – model mixture A - and a mixture of Martius Yellow (MW=274.16 g.mol^{-1}) (MY) and BBR in methanol (MeOH) – model mixture C -, were purified using the system proposed. Although the process operated as predicted, these mixtures were challenging in terms of separation so it was difficult to find a membrane tighter enough for the solvent recovery purpose. Thus, to achieve yields >90% it was necessary to disconnect the two membrane units at some point and continue the diafiltration with only the first membrane, using fresh solvent.

Experiments with model mixture A showed that the tighter the membrane used for solvent recovery, the small the volume of solvent required to achieve the target purity and yield. Experiments with model mixture C showed a maximum reduction of 59% in the MeOH usage, comparing to the amount of solvent required by a single membrane process to achieve the same yield and purity.

The effect of increasing the number of membranes for purification was assessed through simulations. It was found that the product yield can be increased from 1% to 97% by just increasing the number of membranes units from 1 to 3. However, the purity can drop from 99% to 54% due to the exponential increase of the overall rejections with the number of membrane units in the membrane cascade.

Keywords: Organic Solvent Nanofiltration (OSN), Active Pharmaceutical Ingredients (API), Solvent Recovery, Membrane Cascades

RESUMO

Apresenta-se aqui um processo simples em circuito fechado para a purificação de ingredientes farmacêuticos activos, que combina duas membranas de nanofiltração com solventes orgânicos, uma para purificação e outra para recuperação de solvente. O sucesso deste processo depende da membrana utilizada na recuperação de solvente, que deverá ser apenas permeável ao solvente.

Uma mistura de Solvent Yellow 7 (MW=198.2g.mol^{-1}) (SY7) e Brilliant Blue R (MW=826.0g.mol^{-1}) (BBR) em *N,N*-dimetilformamida (DMF) – mistura modelo A – e uma mistura de Martius Yellow (MW=274.16 g.mol^{-1}) (MY) e BBR em metanol (MeOH) – mistura modelo C-, foram purificadas utilizando o sistema proposto. Apesar do processo ter funcionado como previsto, estas misturas revelaram-se difíceis de separar, pelo que foi difícil encontrar uma membrana suficientemente densa para a recuperação de solvente. Assim, para alcançar um rendimento de produto >90%, foi necessário desconectar as duas membranas a dada altura e continuar a diafiltração com apenas a primeira membrana, utilizando solvente novo.

Experiências com a mistura modelo A demonstraram que quanto mais densa é a membrana utilizada na recuperação de solvente, menor o volume de solvente necessário para atingir o rendimento e a pureza desejados. Experiências com a mistura modelo C demonstraram uma redução máxima do consumo de MeOH em 59%, comparando com a quantidade de solvente exigida por um processo com uma única membrana para alcançar o mesmo rendimento e a mesma pureza.

O efeito de aumentar o número de membranas para purificação foi avaliado através de simulações. Verificou-se que o rendimento pode aumentar de 1% para 97% aumentando o número de membranas de 1 para 3. No entanto, a pureza pode diminuir de 99% para 54% devido ao aumento exponencial das rejeições globais com o número de membranas na cascata.

Termos chave: Nanofiltração com Solventes Orgânicos, Ingredientes Farmacêuticos Activos, Recuperação de Solventes, Cascatas de Membranas

TABLE OF CONTENTS

LIST OF FIGURES XV
LIST OF TABLES XXI
ABREVIATIONS XXV
NOMENCLATURE XXVI
GREEK SYMBOLS XXVII
SUBSCRIPTS XXVII

CHAPTER 1 LITERATURE REVIEW 1

1.1. Membrane technology 1
1.1.1. The Membrane 1
1.1.2. Membrane types 2
1.1.3. Membrane preparation techniques 3
1.1.4. Membrane processes 5
1.1.5. Membrane characterization 7
1.1.6. Transport in membranes 9
1.1.7. Strengths and limitations of membrane processes 11

1.2. Solvent use in the pharmaceutical industry 16
1.2.1. Solvent utilization 16
1.2.2. Waste minimization and solvent recovery 17
1.2.3. Use of membrane technology for solvent recovery 18

1.3. Membrane cascades 21
1.3.1. Module configurations and mode of operation 21
1.3.2. Membrane cascades configurations and modes of operation. 22
1.3.3. Membrane cascades applications 24

1.4. Implication of the Literature Review and Research Motivation 27

CHAPTER 2 MATERIALS & METHODS 28

2.1. Model mixtures 28

2.2. Membranes 30

2.2.1. Integrally Skinned Membranes 30
2.2.2. Thin Film Composite Membranes 32
2.2.3. Membrane performance 33

2.3. Membrane Filtration 34
2.3.1. Cross-flow Filtration 34
2.3.2. Experimental set-ups 35

2.4. Analytical Methods 38
2.4.1. UV/Vis Spectroscopy 38
2.4.2. High Pressure Liquid Chromatography (HPLC) 38

2.5. Process Modeling 39

CHAPTER 3 CLOSED-LOOP MEMBRANE PROCESS 40

3.1. Model Mixture A 41
3.1.1. Experimental 41
3.1.2. Results & Discussion 42
3.1.3. Conclusions 64

3.2. Model mixture B 66
3.2.1. Experimental 66
3.2.2. Results & Discussion 66
3.2.3. Conclusions 68

3.3. Model Mixture C 70
3.3.1. Experimental 70
3.3.2. Results & Discussion 72
3.3.3. Conclusions 96

CHAPTER 4 MEMBRANE CASCADE 97

4.1. Single membrane experiments 99
4.1.1. Experimental 99
4.1.2. Results & Discussion 100

4.2. Membrane cascade modelling 106

4.3. Conclusions 107

CHAPTER 5 CONCLUSION REMARKS AND FUTURE WORK 109

REFERENCES 110

APPENDIX A. HPLC CALIBRATION CURVES 118

APPENDIX B. EFFECT OF TEMPERATURE ON THE VISIBLE SPECTRA OF MY AND BBR COMPOUNDS 119

APPENDIX C. PROCESS MODELING 120

C.1 Single membrane system 120

C.2 Closed-loop membrane process 121

C.3 Membrane cascade 121

LIST OF FIGURES

Figure 1.1 Schematic representation of a membrane separation: component 1 selectively passes through the membrane, driven by a chemical or electrical potential gradient. Adapted from (Mulder, 1996). 1

Figure 1.2 Principal types of membranes. Adapted from (Baker, 2004, Mulder, 1996). 2

Figure 1.3 Typical rejection curves for membranes with a A) sharp cut-off and a B) diffuse cut-off. Adapted from (Mulder, 1996). 8

Figure 1.4 Schematic representation of the most important transport mechanisms through membranes: (a) the pore-flow model and (b) the solution-diffusion model (Baker, 2004). 10

Figure 1.5 Concentration polarization: concentration profile under steady-state conditions. 12

Figure 1.6 Flux as a function of the applied pressure both for pure water and for a solution: the flux of pure water increases lineary with applied pressure, considering that no compaction occurs; however when solutes are added to water the flux starts platteauing after a certain applied pressure (Mulder, 1996). 13

Figure 1.7 Typical pharmaceutical batch operation. Adapted from (Dunn, 2010). 16

Figure 1.8 The two basic module operations: (a) Dead-end and (b) Cross-flow (Mulder, 1996). 21

Figure 1.9 The arrangement of membrane units and stages in a cascade. Adapted from (Benedict, Pigford & Levi, 1981). 22

Figure 1.10 Modes of cascade operation: (a) simple cascade and (b) countercurrent recycle cascade. Adapted from (Villani & Becker, 1979). 23

Figure 2.1 Process diagram of the cross-flow cell rig used for membrane screening tests (F: Flow meter; P: Pressure gauge; T: Temperature thermocouple). 34

Figure 2.2 Schematics of the (a) front and (b) top views of the custom-made membrane cells used for the experimental set-ups of this work. Adapted from (Lin & Livingston, 2007). 35

Figure 2.3 Process diagram of the single membrane system (HPLC-P: HPLC pump; BPR: Back pressure regulator; PRV: Pressure relief valve; PI: Pressure gauge; TC: Temperature controller). 36

Figure 2.4 Process diagram of the closed loop system. (HPLC-P: HPLC pump; BPR: Back pressure regulator; PRV: Pressure relief valve; PI: Pressure gauge; TC: Temperature controller). 37

Figure 3.1 Schematic diagram of the closed-loop membrane process. 40

Figure 3.2 Photograph of the feed solution at the beginning (F0, 40 times diluted) and after 8 diafiltration volumes (F8, 8 times diluted) and of the permeate samples at each diafiltration volume (P1-P8, without dilution). 45

Figure 3.3 Calculated and experimental mass profiles of product (SY7) and waste (BBR) in (a) feed tank and (b) membrane cell for the purification of model mixture A using single membrane process with a PI2411 membrane disc at 30 bar and 22 °C. Curve fitting was done by assigning different values to RSY7: Model 1-RSY7=40.0%/RBBR=100.0%, Model 2-RSY7=52.0% /RBBR=100.0%; Model 3- RSY7=61.0%/RBBR=100.0%. 46

Figure 3.4 Yield and purity profiles for the purification of model mixture A using single membrane process with a PI2411 membrane disc at 30 bar and 22 °C. Curve fitting was done by assigning different values to RSY7: Model 1-RSY7=40.0%/RBBR=100.0%, Model 2-RSY7=52.0%/RBBR=100.0%; Model 3- RSY7=61.0%/RBBR=100.0%. 47

Figure 3.5 Calculated and experimental mass profiles of the product (SY7) and waste (BBR) in (a) feed tank, (b) membrane cell 1 and (c) membrane cell 2 for the purification of model mixture A using the closed-loop membrane process with a PI2411 and a DM150 membrane disc. Curve fitting was done by assigning different values to RSY7: Model 1- RSY7,1=83% and RSY7,2=95%, Model 2- RSY7,1=42.5% and RSY7,2=97%, Model 3- RSY7,1=59% and RSY7,2=95%.. 50

Figure 3.6 Yield and purity profiles for the purification of model mixture A using closed-loop membrane process with a PI2411 and a DM150 membrane discs. Curve fitting was done by assigning different values to RSY7: Model 1- RSY7,1=83%/RBBR,1=100.0% and RSY7,2=95%/RBBR,2=100.0%, Model 2- RSY7,1=42.5%/RBBR,1=100.0% and RSY7,2=97%/RBBR,2=100.0%, Model 3- RSY7,1=59%/RBBR,1=100.0% and RSY7,2=95%/RBBR,2=100.0%.. 52

Figure 3.7 Calculated and experimental mass profiles of the product (SY7) and waste (BBR) in (a) feed tank and (b) membrane cell 1 after disconnecting the second cell from the system PI24411/DM150 (RSY7=87%). 54

Figure 3.8 Yield and purity profiles for the purification of model mixture A after disconnecting the second cell from the system PI24411/DM150 (RSY7=87%). 55

Figure 3.9 Calculated and experimental mass profiles of the product (SY7) and waste (BBR) in (a) feed tank, (b) membrane cell 1 and (c) membrane cell 2 for the purification of model mixture A using closed-loop membrane process with a PI2411 and a TFC-MPD discs. Curve fitting was done by assigning different values to RSY7: Model 1- RSY7,1=83%/RBBR,1=100% and RSY7,2=64%/RBBR,2=100%, Model 2- RSY7,1=68%/RBBR,1=100% and RSY7,2=74%/RBBR,2=100%, Model 3- RSY7,1=93%/RBBR,1=100% and RSY7,2=91%/RBBR,2=100%.. 57

Figure 3.10 Yield and purity profiles for the purification of model mixture A using the closed-loop membrane process with a PI2411 and a TFC-MPD disc Curve fitting was done by assigning different values to RSY7: Model 1- RSY7,1=83%/RBBR,1=100% and RSY7,2=64%/RBBR,2=100%, Model 2- RSY7,1=68%/RBBR,1=100% and RSY7,2=74%/RBBR,2=100%, Model 3- RSY7,1=93%/RBBR,1=100% and RSY7,2=91%/RBBR,2=100%.. 59

Figure 3.11 Calculated and experimental mass profiles of the product (SY7) and waste (BBR) in (a) feed tank and (b) membrane cell 1 after disconnecting the second cell from the system PI24411/TFC-MPD. Curve fitting was done by assigning different values to RSY7: Model 1- RSY7=82%/RBBR=100%, Model 2- RSY7=72.0% /RBBR=100%. 61

Figure 3.12 Yield and purity profiles for the purification of model mixture A after disconnecting the second cell from the system PI24411/TFC-MPD. Curve fitting was done by assigning different values to RSY7: Model 1- RSY7=82% and RBBR=100%, Model 2- RSY7=72.0% and RBBR=100%. 62

Figure 3.13 Effect of product rejection in the solvent recovery stage in a closed-loop membrane process to the product yield. Simulations were performed assuming that RSY7,1=83% and RBBR,1=100%. 64

Figure 3.14 Calculated yield and purity profiles for the purification of model mixture B using the closed-loop membrane process with PI2211 membrane (RMY=74.6%/RBBR=100%) for purification and TFC-MPD membrane (RMY=96.5%/RBBR=99.7%) for solvent recovery. 68

Figure 3.15 Flux profiles over time at 10 bar and 27 °C for the membranes screened using model mixture C. The flux at time 0 is the flux of pure MeOH. 73

Figure 3.16 Calculated and experimental mass profiles of product (MY) and waste (BBR) in (a) feed tank and (b) membrane cell for the purification of model mixture C using single membrane process with a PI2211 disc at 30 bar and 22 °C. 78

Figure 3.17 Calculated and experimental concentration profiles in the permeate for the purification of model mixture C using the single membrane process with a PI2211 disc at 30 bar and 22 °C. 79

Figure 3.18 Photograph of the initial and final feed and of retentate and permeate samples at each diafiltration volume. Feed and retentate samples were 40 times diluted. 79

Figure 3.19 Yield and purity profiles for the purification of model mixture C using single membrane process with a PI2211 disc at 30 bar and 22 °C. 80

Figure 3.20 Calculated and experimental mass profiles of the product (MY) and waste (BBR) in (a) feed tank, (b) membrane cell 1 and (c) membrane cell 2 for the purification of model mixture C using the closed-loop membrane process with a PI2211 and a TFRO-SG disc at 25 °C. Curve fitting was done by assigning different values to the rejections: Model 1-RMY,1=74%,/RBBR,1=96%, and RMY,2=79%/RBBR,2=52%, Model 2-RMY,1=91%/RBBR,1=87% and RMY,2=96%/RBBR,2=76%. 83

Figure 3.21 Yield and purity profiles for the purification of model mixture C using closed-loop membrane process with a PI2211 and a TFRO-SG disc at 25 °C. Curve fitting was done by assigning different values to the rejections: Model 1- RMY,1=74%,/RBBR,1=96%, and RMY,2=79%/RBBR,2=52%, Model 2-RMY,1=91%/RBBR,1=87% and RMY,2=96%/RBBR,2=76%. 84

Figure 3.22 Yield and purity profiles for the purification of model mixture C after disconnecting the second cell from the system PI2211/TFRO-SG. 86

Figure 3.23 Experimental and calculated concentration profiles for the product (MY) and waste (BBR) in the permeate. 86

Figure 3.24 Calculated and experimental mass profiles of product (MY) and waste (BBR) in (a) feed tank and (b) membrane cell for the purification of model mixture C using single membrane process with a PBI 24xDBX disc at 21 bar and 23 °C. Curve fitting was done by assigning different values to RMY and RBBR: Model 1- RMY=95%/RBBR=100%; Model 2- RMY=94%/RBBR=98.5%; Model 3- RMY=96.5%/RBBR=98.5%. 89

Figure 3.25 Yield and purity profiles for the purification of model mixture C using single membrane process with a PBI 24xDBX disc at 21 bar and 23 °C. Curve fitting was done by assigning different values to RMY and RBBR: Model 1- RMY=95%/RBBR=100%; Model 2- RMY=94%/RBBR=98.5%; Model 3- RMY=96.5%/RBBR=98.5%. 90

Figure 3.26 Experimental and calculated concentration profiles for the product (MY) and waste (BBR) in the permeate. Curve fitting was done by assigning different values to RMY and RBBR: Model 1- RMY=95%/RBBR=100%; Model 2- RMY=94%/RBBR=98.5%; Model 3- RMY=96.5%/RBBR=98.5%. 91

Figure 3.27 Calculated and experimental mass profiles of the product (MY) and waste (BBR) in (a) feed tank, (b) membrane cell 1 and (c) membrane cell 2 for the purification of model mixture C using closed-loop membrane process with a PBI 24xDBX and a PBI 26xDBB disc. Curve fitting was done by assigning different values to RMY and RBBR: Model 1- RMY,1=91%, RBBR,1=97%, RMY,2=94% and RBBR,2=98%; Model 2- RMY,1=91% and RBBR,1=95%, RMY,2=94% and RBBR,2=90%. 93

Figure 3.28 Yield and purity profiles for the purification of model mixture C using closed-loop membrane process with a PI2211 and a TFRO-SG disc. Curve fitting was done by assigning different values to RMY and RBBR: Model 1- RMY,1=91%, RBBR,1=97%, RMY,2=94% and RBBR,2=98%; Model 2- RMY,1=91% and RBBR,1=95%, RMY,2=94% and RBBR,2=90%.. ... 94

Figure 3.29 Yield and purity profiles for the purification of model mixture C after disconnecting the second cell from the system PBI 24xDBX/PBI 26xDBB. Curve fitting was done by assigning different values to RMY and RBBR: Model 1- RMY,1=90%/RBBR,1=99%; Model 2- RMY,1=90%/RBBR,1=98%; 95

Figure 4.1 Schematic representation of the closed-loop membrane process integrating a cascade of n membrane units for purification. 97

Figure 4.2 Flux profiles over time at 10 bar and 25°C for the membranes screened using model mixture D1. The flux at time 0 is the flux of pure MeCN. 100

Figure 4.3 Rejection curves in for the membranes screened in MeCN at 10 bar and 25°C after a) 5 hours and b) 24 hours of continuous operation. 101

Figure 4.4 Flux profiles over time at 10 bar and 25°C for the membranes screened using model mixture D2. The flux at time 0 is the flux of pure MeCN. 102

Figure 4.5 Experimental and calculated mass profiles for the polymer (product) and monomer (waste) using the single membrane process with a PI2341 membrane at 10-15 bar and 21 °C. Calculated curves were obtained considering the an average of the calculated rejections, Rpolymer=95.5% and Rmonomer=94.6%. (Model 1) and corrected values, Rpolymer=92% and Rmonomer=84%. (Model 2). 105

Figure 4.6 Yield and purity profiles as a function of the number of membrane units used for purification. Simulations performed by assuming that Rpolymer=92% and Rmonomer=84%.. 106

LIST OF TABLES

Table 1.1 Classification of membrane processes according to their driving forces (Mulder, 1996). 5

Table 1.2 Comparison of various pressure driven membrane processes. Adapted from (Mulder, 1996). 6

Table 1.3 Comparison of solvent use at GSK based on overall manufacturing operations (1995-2000) and more recent pilot plant operations (2005) (Constable, Jimenez-Gonzalez & Henderson, 2007). 17

Table 2.1 Properties of the dyes used as model compounds. 29

Table 2.2 Summary of the membranes not prepared but used in this work 30

Table 2.3 Summary of the integrally skinned PI membranes prepared. 31

Table 2.4 Summary of the integrally skinned PBI membranes prepared. 32

Table 2.5 Summary of the TFC membranes prepared. 33

Table 3.1 Summary of the screening results for 14 cm^2 membrane discs using model mixture A (Mix A). 43

Table 3.2 Summary of the data recorded during the diafiltration of model mixture A using the single membrane process with a PI2411 membrane disc. 44

Table 3.3 Summary of the data recorded along the diafiltration of model mixture A using the closed-loop membrane process with a PI2411 membrane disc for purification and a DM150 membrane disc for solvent recovery. 49

Table 3.4 Summary of the data recorded along the diafiltration of model mixture A using the single membrane process with a PI2411 membrane disc after disconnected the cells. 53

Table 3.5 Summary of the data recorded along the diafiltration of model mixture A using the closed-loop process with a PI2411 membrane disc for purification and a TFC-MPD membrane disc for solvent recovery. 56

Table 3.6 Summary of the data recorded along the diafiltration of model mixture A using the single membrane process with a PI2411 membrane disc after disconnected the cells. 60

Table 3.7 Comparison between the three processes used to purify model mixture A. 63

Table 3.8 Summary of the screening data. 67

Table 3.9 Physical parameters of the solvents. 74

Table 3.10 Rejections after 5h and 24h of operation at 10 bar and 27°C for the membranes screened using model mixture C. 74

Table 3.11 Summary of the data recorded along the diafiltration of model mixture C using the single membrane process with a PI2211 membrane. 77

Table 3.12 Summary of the data recorded along the purification of model mixture C using the closed-loop membrane process with a PI2211 membrane disc for purification and a TFRO-SG membrane disc for solvent recovery. 81

Table 3.13 Summary of the data recorded along the purification of model mixture C using the single membrane process with a PI2211 membrane disc after disconnecting the second cell from the system. 85

Table 3.14 Comparison between the performance of the single membrane process with PI2211 membrane and the closed-loop membrane process with PI2211 and TFRO-SG membranes 87

Table 3.15 Summary of the data recorded along the purification of model mixture C using the single membrane process with a PBI 24xDBX membrane. 88

Table 3.16 Summary of the data recorded along the purification of model mixture C using the closed-loop membrane process with a PBI 24xDBX membrane disc for purification and a PBI 26xDBB membrane disc for solvent recovery. 92

Table 3.17 Summary of the data recorded along the diafiltration of model mixture C using the single membrane process with a PBI 24xDBX membrane disc after disconnected the cells. 95

Table 3.18 Comparison between the performance of the single membrane process with PBI 24xDBX membrane and the closed-loop membrane process with PBI 24xDBX and PBI 26xDBB membranes 96

Table 4.1 Rejections after 2h of operation at 10 bar and 25 °C for the different membranes tested against model mixture D2. 103

Table 4.2 Performance data for the purification of the product crude using PI2341 membrane at 21 °C. 104

Table 4.3 Overall rejections, $R_{cascade,i}$, of the separation stage as a function of the number of membrane units used for purification. 107

ABREVIATIONS

API(s)	Active pharmaceutical Ingredient(s)
BBR	Brilliant Blue R
BPR	Back pressure regulator
DBB	Dibromobutane
DBX	Dibroxylene
DMAc	*N,N*-dimetylacetamide (DMAc)
DMF	*N,N*-dimethylformamide
GHGs	Green house gases
HDA	1,6-Hexanediamine
HPLC	High pressure liquid chromatography
IPA	Isopropanol
MeCN	Acetonitrile
MeOH	Methanol
MF	Microfiltration
MPD	m-phenylene diamine
MW	Molecular weight ($g.mol^{-1}$)
MWCO	Molecular weight cut-off
MY	Martius Yellow
NF	Nanofiltration
OSN	Organic solvent nanofiltration
PA	Polyamide
PBI	Polybenzimidazole
PEEK	Poly(ether ether ketone)
PEG	Polyethylene glycol
PI	Polyimide
PP	Polypropylene
PRV	Pressure relief valve
PS	Polystyrene
RO	Reverse Osmosis
SRNF	Solvent resistant nanofiltration
SY7	Solven Yellow 7
TFC	Thin-film composite
THF	Tetrahudrofuran
UF	Ultrafiltration
UV	Ultraviolet
VOCs	Volatile organic compounds

NOMENCLATURE

x	Fraction in the retentate (dimensionless)
y	Fraction in the permeate (dimensionless)
R	Rejection of solute (%)
C	Concentration ($g.L^{-1}$)
P	Pressure (bar)
T	Temperature (℃)
J_s	Solute flux ($g.m^{-2}.h^{-1}$)
J_v	Solvent flux ($L.m^{-2}.h^{-1}$)
L_p	Hydrodynamic permeability ($L.m^{-2}.h^{-1}.bar^{-1}$)
$\bar{C}_s$	Logarithmic average of solute concentration across the membrane ($g.L^{-1}$)
r	Radius (m)
K_c	Solute hindrance factor for convection (dimensionless)
v	Solvent velocity ($m.s^{-1}$)
F	Faraday constant (96487 $C.mol^{-1}$)
R	Gas constant (8.341 $J.mol^{-1}.K^{-1}$)
D^*	Corrected diffusive coefficient according to (Bowen & Welfoot, 2002) ($m^2.s^{-1}$)
z	Valence (dimensionless)
D	Fick's law diffusive coefficient ($m^2.s^{-1}$)
K^L	Sorption coefficient (dimensionless)
l	Membrane thickness (m)
$C_{s,0}$	Concentration of the solute in the feed side ($mol.m^{-3}$)
$C_{s,l}$	Concentration of solute in the permeate side ($mol.m^{-3}$)
A	Membrane area (m^2)
B	Solvent permeability (($L.m^{-2}.h^{-1}.bar^{-1}$)
V	Volume (L)
t	Time (h)
N	Number of diafiltration volumes (dimensionless)
m	Mass (g)
Y_P	Yield of product (%)
P_P	Purity of product (%)
n	Number of membrane units in the cascade (dimensionless)
Q	Volumetric flow rate ($L.h^{-1}$)

GREEK SYMBOLS

α	Separation factor (dimensionless)
σ	Reflection coefficient (dimensionless)
π	Osmotic pressure (bar)
ω	Osmotic permeability ($g.m^{-2}.h^{-1}.bar^{-1}$)
ε	Surface porosity (dimensionless)
τ	Pore tortuosity (dimensionless)
η	Solvent viscosity ($kg.m^{-1}.s^{-1}$)
υ	Partial molar volume ($m^3.mol^{-1}$)
Ψ	Electrical potential (V)
δ	Boundary layer thickness (m)
λ_{max}	Maximum absorbance wavelength (nm)

SUBSCRIPTS

i	Species/Ion
v	Volume
s	Solute
m	Membrane surface
b	Bulk
P	Permeate side
R	Retentate side
F	Feed side
∞	Limiting
T	Total

Chapter 1

Literature Review

1.1. MEMBRANE TECHNOLOGY

1.1.1. The Membrane

There are many membrane processes based on different separation principles or mechanisms. However, in spite of these various differences, all membrane processes have one thing in common: the membrane. A membrane can be considered as a selective barrier between two phases, allowing only some components to pass through (Mulder, 1996).

A schematic representation of a two-phase system separated by a membrane is presented in Figure 1.1. The separation is achieved because the membrane has the ability to transport one component from the feed to the permeate side more readily than any other component. The transport trough the membrane takes place as a result of a driving force, i.e. a chemical or electrical potential difference, acting on the components in the feed. Either pressure (ΔP), concentration (ΔC) or temperature (ΔT) differences contribute to the chemical potential difference of a component (Mulder, 1996).

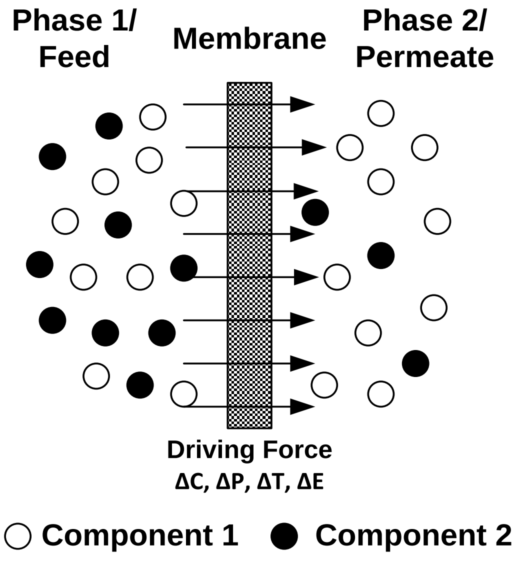

Figure 1.1 Schematic representation of a membrane separation: component 1 selectively passes through the membrane, driven by a chemical or electrical potential gradient. Adapted from (Mulder, 1996)**.**

1.1.2. Membrane types

Synthetic membranes can be organic (polymeric or liquid) or inorganic (ceramic, metal or zeolite) (Mulder, 1996).

Polymeric membranes are commonly classified according to its structure as symmetric or asymmetric. These two classes can be subdivided as shown in Figure 1.2.

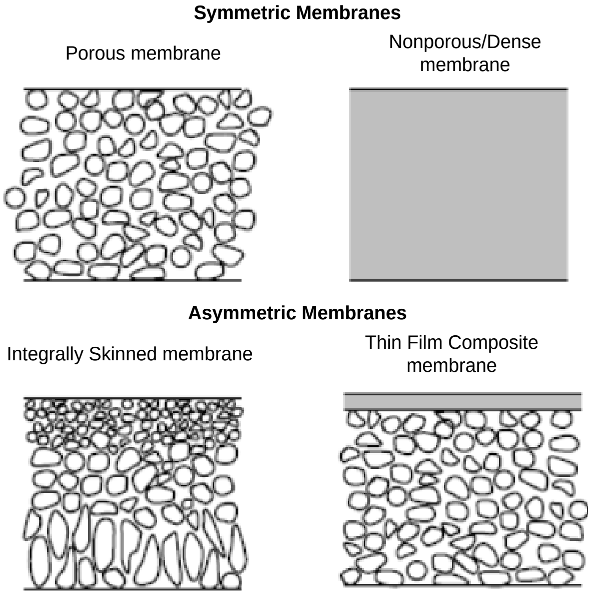

Figure 1.2 Principal types of membranes. Adapted from (Baker, 2004, Mulder, 1996)**.**

Symmetric membranes consist of a porous or dense (nonporous) polymer layer with a thickness ranging roughly from 10 to 200 μm. The resistance to mass transfer is determined by the total membrane thickness, whether the membrane is porous or dense (Mulder, 1996). However, in the first case the separation is mainly a function of molecular size and pore distribution, whereas in the second case it is a function of the diffusivity and solubility of the molecules in the membrane material. When these membranes are charged, they mostly separate by exclusion of ions of the same charge as the fixed ions of the membrane structure (Baker, 2004).

The development of novel membrane fabrication techniques to produce asymmetric membrane structures was one of the major breakthroughs of membrane technology during the past 30 years (Baker, 2004). These consist of a very thin toplayer with a thickness of 0.1 to 0.5 μm supported by a porous sublayer with a thickness of about 50 to 150 μm (Mulder, 1996). In this case only the toplayer determines the resistance to mass transfer and the separation properties whereas the porous sublayer functions only as a mechanical support. The toplayer and its porous sublayer may be formed in a single operation, with the formation of integrally skinned asymmetric membranes, or separately, with the formation of thin-film composite (TFC) membranes. The advantage of the composite ones is that both support and separation layers can be separately optimized (Baker, 2004, Mulder, 1996). The most used methods for asymmetric membrane preparation will be explained in greater detail in section 1.1.3.

The interest in membranes formed from less conventional materials has increased. Ceramic membranes, the main class of inorganic membranes, are being fairly applied in microfiltration and ultrafiltration fields, since these membranes possess superior chemical, thermal and structural stability relative to polymeric membranes. They do not deform under pressure, do not swell and are cleaned easily, since all kinds of cleaning agents, such as strong acids and alkali, can be used. Furthermore, they have a greater lifetime than that of organic polymeric membranes. However, they tend to be more expensive and brittle than polymeric membranes and are also less versatile in applications. In addition, their large-scale synthesis and module construction is not as easy as for polymeric membranes(Vandezande, Gevers & Vankelecom, 2008). That is why the majority of membranes used commercially are still polymer-based (Vandezande, Gevers & Vankelecom, 2008, Baker, 2004, Mulder, 1996).

1.1.3. Membrane preparation techniques

There are a number of membrane preparation techniques. The kind of technique employed depends mainly on the material used, despite some techniques can be used to prepare both polymeric and inorganic membranes, and on the desired membrane structure, which in turn is dependent on the separation problem. The most important techniques are sintering, stretching, track-etching, phase inversion, sol-gel process, vapour deposition and solution coating. With the first three techniques only porous membranes are obtained. These membranes can also be used as sublayer for composite membranes. Through the use of phase inversion techniques it is possible to obtain open as well as dense structures (Mulder, 1996).

The basic support material for a composite membrane is often an asymmetric membrane obtained by phase inversion. The separating layer can be prepared via dip-coating, spray coating, spin coating, interfacial polymerisation, in-situ polymerisation, plasma polymerisation and grafting. Except for the first three methods, all the techniques involve polymerisation reactions which generate new polymers as a very thin layer (Mulder, 1996).

Preparation techniques for both phase inversion membranes and for composite membranes by interfacial polymerisation will be described hereafter.

1.1.3.1. Phase inversion

Most commercially membranes are obtained by phase inversion since this represents one of the most versatile, economical and reproducible formation mechanisms for polymeric asymmetric membranes (Vandezande, Gevers & Vankelecom, 2008) (Mulder, 1996).

“Phase inversion” refers to the controlled transformation of a cast polymer film from a liquid to a solid state. During this process, a thermodynamically stable polymer solution is mostly subjected to a controlled liquid-liquid demixing during which the cast polymer film “phaseseparates” into a polymer-rich and a polymer lean-phase, ultimately forming the matrix and the pores of the membrane, respectively. This phase separation can be induced by immersing the film in a non-solvent bath (“immersion precipitation”), by lowering the temperature (“thermal precipitation”), by evaporating the volatile solvent from the polymer film (“controlled evaporation”) or by placing the cast polymer film in a non-solvent vapour phase (“precipitation from the vapour phase”). The most common phase inversion method is phase inversion. In this case the phase separation occurs because of the exchange of solvent and nonsolvent. When the demixing starts directly (“instantaneous demixing”) and the membrane forms immediately after immersion in the nonsolvent bath, a porous membrane structure will develop. On the other hand, when the demixing takes some time before the membrane is formed (“delayed demixing”), a membrane with a relatively dense top layer is obtained. A phenomenon often associated with immersion-precipitation, mostly with instantaneous precipitation, is the formation of macrovoids. These are enlongated, finger- or tear-like pores that can extent over the entire membrane thickness. They are generally considered undesirable as they cause mechanically weak spots in the membrane and thus severely limit the compaction resistance. Conditions favouring delayed demixing however can reduce or even suppress macrovoid formation, e.g. by adding a volatile co-solvent to the casting solution, by increasing the polymer concentration in the casting solution, by selecting a non-solvent with limited miscibility with the solvent in the casting solution, or by introducing an evaporation step before immersion of the cast film into the coagulation bath (Vandezande, Gevers & Vankelecom, 2008, Mulder, 1996).

In order to increase the separation performance of asymmetric membranes and to increase their long-term stability, several post-treatment or conditioning procedures can be used, such as annealing (wet or dry), crosslinking (chemical, plasma or photo-induced), drying by solvent exchange and treatment with conditioning agents, such as lube oils, glycerol or long chain hydrocarbons (Vandezande, Gevers & Vankelecom, 2008).

1.1.3.2. Interfacial polymerization

Interfacial polymerization has become a well-established and useful technique to prepare the dense, active top-layer of TFC membranes. The technique entails the application of an ultra-thin film upon an asymmetric, porous support-layer (normally prepared by phase inversion), via an *in-situ* polymerization reaction occurring at the interface between two immiscible solvents containing reactive monomers (Vandezande, Gevers & Vankelecom, 2008).

First, the support is impregnated, typically with an aqueous diamine solution. Then, and after remove the excess water, the saturated support is contacted with an organic phase containing acyl halides. Both monomers then react with each other and quickly form a thin selective polyamide layer that remains attached to the substrate. As soon as the top-layer is formed, it acts as a barrier for further monomer transport thus controlling the top layer thickness (Vandezande, Gevers & Vankelecom, 2008).

The composition, morphology and performance of interfacially polymerized membranes depends on several parameters, including the concentration of the reactants as well as their partition coefficients and reactivities, possible additives, solubility of the nascent polymer in the solvent phase, overall kinetics and diffusion rates of the reactants, presence of by products, competitive side reactions, crosslinking reactions and post reaction treatment. Higher monomer concentrations, higher reaction rates and longer polymerization times generally improve the efficiency of film formation. This results in thicker and denser barrier-layers with increased rejections but decreased fluxes (Vandezande, Gevers & Vankelecom, 2008).

The performance of TFC membranes can be further enhanced by applying an adequate post-polymerization treatment. Different techniques have been described including grafting, curing, plasma, UV and chemical treatment (Vandezande, Gevers & Vankelecom, 2008).

1.1.4. Membrane processes

Membrane processes can be classified according to their driving forces - Table 1.1

Table 1.1 Classification of membrane processes according to their driving forces (Mulder, 1996)**.**

Pressure difference	Concentration difference	Temperature difference	Electrical potential difference
Microfiltration	Pervaporation	Thermo-osmosis	Electrodialysis
Ultrafiltration	Gas separation	Membrane distillation	Electro-osmosis
Nanofiltration	Vapour permeation		Membrane electrolysis
Reverse Osmosis	Dialysis		
Piezodialysis	Diffusion dialysis		
	Carrier-mediated transport		

The most important pressure driven membrane processes are microfiltration (MF), ultrafiltration (UF), nanofiltration (NF) and reverse osmosis (RO). All of them are used to concentrate or purify a dilute (aqueous or non-aqueous) solution. What differs between them is basically the size of the solutes to be separated. As we go from microfiltration trough ultrafiltration and nanofiltration to reverse osmosis, the size (or molecular weight) of the particles or molecules separated diminishes and consequently the pore size in the membrane become smaller. This also implies that the resistance of the membranes to mass transfer increases. That is why higher pressures are applied when we go from microfiltration to reverse osmosis (Mulder, 1996). A comparison of the various pressure driven processes is given in

Table 1.2.

Commercial NF membranes were initially developed from RO membranes, and so at the beginning they were only made of hydrophilic polymeric materials such as polyethersulphone, polyamides and cellulose derivatives. There are now available a lot of membranes, both polymeric and ceramic, that can function in organic solvents. With those membranes a new technology, commonly designated by organic solvent nanofiltration (OSN) or solvent resistant nanofiltration (SRNF), has born, opening new opportunities in the chemical and refining industries (Boam & Nozari, 2006, White, 2006). Processes involving OSN membranes were already proposed for edible oil deacidification (Rama, Cheryan & Rajagopalan, 1996), lube oil dewaxing (White & Nitsch, 2000), solvent exchange (eg. exchanging a high boiling point solvent, such as toluene, for a low boiling point solvent, like methanol (Lin & Livingston, 2007), solvent recovery (see section 1.2.3), homogeneous (Luthra et al., 2002) and phase transfer catalysts (Luthra et al., 2001) reuse or recycling, product purification (e.g separation of amino acids (Reddy et al., 1996) or antibiotics from organic solvents (Shi et al., 2006)) and enantiomer separation (Ghazali et al., 2006).

Table 1.2 Comparison of various pressure driven membrane processes. Adapted from (Mulder, 1996)**.**

Microfiltration	Ultrafiltration	Nanofiltration/ Reverse Osmosis
Separation of particles	Separation of macromolecules (bacteria, yeasts)	Separation of low MW solutes (salts, glucose, lactose, micropollutents)
Pore sizes ≈ 0,05-10 µm	Pore sizes ≈ 1-100 nm	Pore sizes < 2nm
Applied pressure low (< 2 bar)	Applied pressure low (1-10 bar)	Applied pressure high (≈ 10-60 bar)
Separation based on the particle size	Separation based on the particle size	Separation based on differences on solubility and diffusivity

Gas separation and pervaporation are two important concentration driven membrane processes. The first one is actually the only concentration driven process for which was reported the utilization of both porous and dense membranes. All the other require the utilization of a dense membrane (asymmetric and/or composite membrane). It is a process used, not only for the separation of different gaseous mixtures (e.g. H2/He, CH4/CO2, O2/N2), including isotopic mixtures, but also for the dehydration (drying) of gases, and for the separation of organic vapours from non-condensable gases. Pervaporation, by its turn, is the only membrane process where phase transition occurs, with the feed being a liquid and the permeate a vapour. This process is generally used to separate a small amount of liquid from a liquid mixture and it is particularly attractive when the liquid mixture exhibits an azeotropic composition (Mulder, 1996).

Despite most of the membrane processes are non-thermal, there are still some which are thermally driven. Membrane distillation is an example. In this process two liquids or solutions at different temperatures are separated by a porous membrane, due to a vapour pressure difference between feed and permeate. This process is mainly applied to the production of pure water and removal of volatile organic compounds (Mulder, 1996).

Membrane processes such as electrodialysis, in which the driving force is supplied by an electrical potential difference, can only be employed when charged molecules are present using ionic or charged membranes. This process is used on the desalination of water, production of salt and separation of amino acids (Mulder, 1996).

1.1.5. Membrane characterization

Membranes can be characterized in terms of its performance or morphology. The most important performance related parameters are flux, permeability, rejection, diffusion coefficients and separation factors. Morphological parameters include both physical (e.g. pore shape, pore size, pore distribution, membrane/top layer thickness), and chemical parameters (e.g. charge, hydrophobicity). Performance parameters are derived from one or more morphological parameters. However, and despite the importance of characterize and better understand physical-chemical parameters, it is the functional parameters that, from a practical perspective, determine the usefulness of the membrane (Mulherkar & van Reis, 2004, Cuperus & Smolders, 1991).

Normally membrane selection is often based upon two performance parameters which are flux and selectivity. The flux, J (L.m^{-2}.h^{-1}), also denoted by permeate rate, is defined as the volume of liquid permeating through the membrane per unit area and per unit time. Many parameters like temperature, pressure and solute concentration affect the flux of OSN membranes. The permeate rate tend to increase with increasing temperature, because of reduction in solvent viscosity and increased polymer chain mobility (Van der Bruggen, Geens & Vandecasteele, 2002). An increase in pressure also led to an increase in flux. Solute concentration has an adverse effect on flux because of osmotic pressure and concentration polarisation. The effect of these last two parameters on the flux can be better understood by reading through sections 1.1.6 and 1.1.7.

In turn, the selectivity can be expressed using rejections or separation factors. The rejection towards a solute i, R_i (%), is more conveniently used to express the selectivity for mixtures consisting of a solvent and one or more solutes, and is given by

$$R_i=\frac{C_{F,i}-C_{P,i}}{C_{F,i}}\times 100=\left(1-\frac{C_{P,i}}{C_{F,i}}\right)\times 100 \qquad \textbf{1-1}$$

where $C_{P,i}$ and $C_{F,i}$ denotes the concentration of solute i at the permeate an feed-side, respectively. If a component has 100% rejection, none of it goes through the membrane, if a component has 0% rejection, all of it goes through the membrane.

By plotting the rejection for different solutes against its molecular weights (rejection or cut-off curve) it is possible to derive the ‘molecular weight cut-off’ (MWCO) of the membrane, which represents the molecular weight (MW) of a reference compound that is typically 90% rejected by the membrane. NF and OSN membranes are characterised by a sigmoidal rejection curve, as the ones depicted in Figure 1.3, and a MWCO between 200-1000 (Vandezande, Gevers & Vankelecom, 2008, Mulder, 1996).

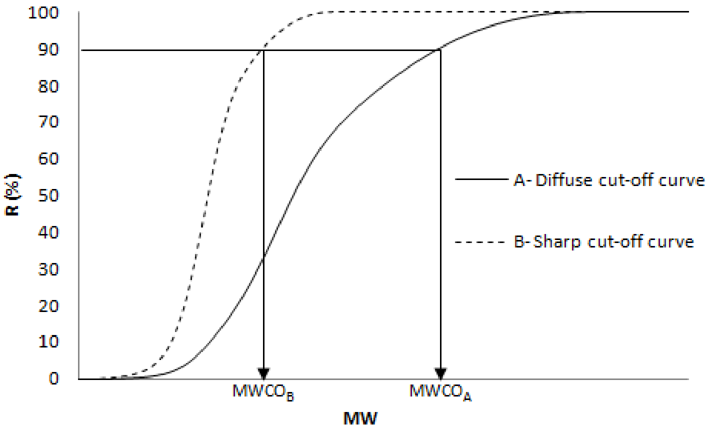

Figure 1.3 Typical rejection curves for membranes with a A) sharp cut-off and a B) diffuse cut-off. Adapted from (Mulder, 1996)**.**

The MWCO is particular useful when the mixture to be separated contains more than one component and all of different sizes. It should be noted, however, that MWCO itself can be a poor estimation of membrane performance, as the pore size distribution, solvent environment, molecular shape, charge, functional groups, occurrence of polarisation phenomena, temperature and the applied pressure also affect rejection. Nevertheless, the MWCO is still a good starting point when screening for suitable membranes (Kim, 2011, Vandezande, Gevers & Vankelecom, 2008, See Toh et al., 2007, Yang, Livingston & Freitas dos Santos, 2001, Mulder, 1996).

For gas mixtures and mixtures of organic solvents the selectivity is usually expressed in terms of the separation factor, α. For a mixture consisting of two components A and B the separation factor $\alpha_{A/B}$ is given by

$$\alpha_{A/B}=\frac{y_A/y_B}{x_A/x_B} \qquad \text{1-2}$$

where y_A and y_B are the concentrations of components A and B in the permeate and x_A and x_B are the concentrations of the components in the feed (Mulder, 1996).

1.1.6. Transport in membranes

It is possible to distinguish three groups of mathematical models that describe transport through membranes. One group of models originates from irreversible thermodynamics, treating the membrane as a black-box; the other two, the pore-flow and the solution diffusion models, take into account membrane properties (Vandezande, Gevers & Vankelecom, 2008).

One of the models based on irreversible thermodynamics was derived by Kedem & Katchalsky (1958). They proposed the following equations for the volume flux, J_v, and the solute flux, J_s, through a membrane:

$$J_v=L_p(\Delta P-\sigma.\Delta\pi) \tag{1-3}$$

$$J_s=\bar{C}_s(1-\sigma)J_v+\omega.\Delta\pi \tag{1-4}$$

where L_p is the hydrodynamic permeability, ΔP is the hydrodynamic pressure difference across the membrane, σ is the reflection coefficient ($0\leq\sigma\leq1$), which can be interpreted as the fraction of solute reflected by the membrane in convective flow (Vandezande, Gevers & Vankelecom, 2008), $\Delta\pi$ is the osmotic pressure difference across the membrane, $\bar{C}_s$ is the logarithmic average of solute concentration across the membrane and ω is the osmotic (solute) permeability. This kind of mathematical models have some limitations, since they do not take into account any information related to the nature or structure of the membrane. However, they not only allow for a very clearly description of the fluxes but also predict the existence of coupling of driving forces: equation 1-3 shows that even if there is no difference in hydrodynamic pressure across the membrane ($\Delta P = 0$) there is still a volume flux; on the other hand, equation 1-4 indicate that if the solute concentration on both sides of the membrane is the same ($\Delta\pi=0$) there is still a solute flux when $\Delta P\neq0$ (Mulder, 1996).

The most reliable transport models are the pore-flow and the solution-diffusion models. They are used to describe, respectively, the transport through porous (e.g. micro and ultrafiltration membranes) and dense membranes (e.g. reverse osmosis, gas separation and pervaporation membranes).

According to the pore-flow model, there is no solute or solvent concentration gradients over the membrane and the permeants are transported by pressure-driven convective flow through tiny pores. Separation occurs because one of the permeants is excluded (filtered) from some of the pores in the membrane through which other permeants move (see Figure 1.4-a). Like this, the volume flux through the pores may be described by the Hagen-Poiseuille equation:

$$J_v=\frac{\varepsilon.r_p}{8\eta.\tau}\frac{dP}{dx} \tag{1-5}$$

where ε is the surface porosity, r_p is the pore radius, τ is the pore tortuosity, η is the solvent viscosity, and dP/dx is the pressure gradient over the membrane (Vandezande, Gevers & Vankelecom, 2008, Baker, 2004).

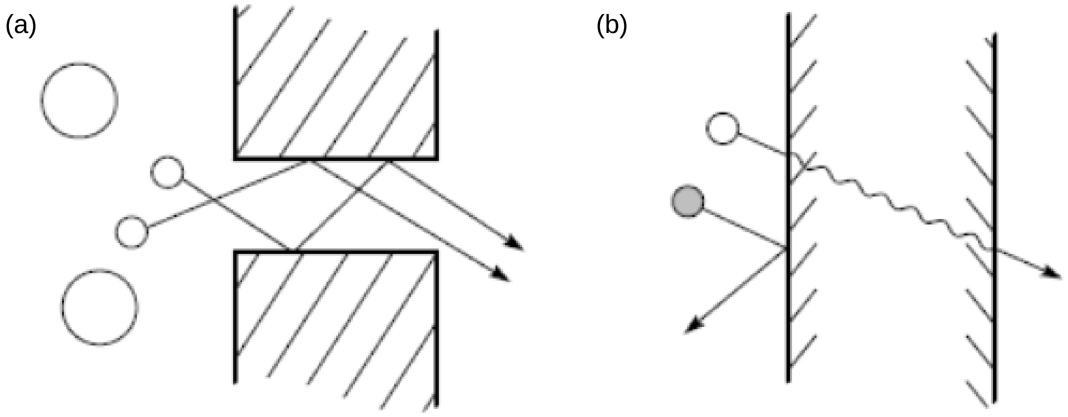

Figure 1.4 Schematic representation of the most important transport mechanisms through membranes: (a) the pore-flow model and (b) the solution-diffusion model (Baker, 2004).

For the solute flux, several empirical pore-flow models have been developed. Bowen et al. proposed a model based on the hydrodynamic model proposed by Ferry (1936), to describe the transport of uncharged solutes, and another one, based on the extended Nernst-Plank equation, to describe the transport of charged solutes (Bowen & Welfoot, 2002). Both models were modified to include the hindered convection and diffusion within the pores as proposed by Deen (1987):

$$J_s = K_c . C_S . V - D_p^* \frac{dC_s}{dx} - \frac{C_s . D_p^*}{R.T} \upsilon_s \frac{dP}{dx} \qquad \textbf{1-6}$$

$$J_i = K_{i,c} . C_i . V - D_{i,p}^* \frac{dC_i}{dx} - \frac{C_i . D_{i,p}^*}{R.T} \upsilon_i \frac{dP}{dx} - \frac{z_i . C_i . D_{i,p}^*}{R.T} F \frac{d\Psi}{dx} \qquad \textbf{1-7}$$

where K_c and $K_{i,c}$ are the solute and ionic hindrance factors for convection, υ_s and υ_i are the partial molar volume of the solute and ion, z_i is the valence of the ion, C_s and C_i are the solute and ion concentrations within pore, V is the solvent velocity, dc_s/dx and dc_i/dx are the concentration gradient of the solute and ion over the membrane, $d\Psi/dx$ is the electrical potential gradient over the membrane, T is the absolute temperature, F is the Faraday constant and R is the gas constant, and D_p^* and $D_{i,p}^*$ are the solute and ion pore diffusion coefficients, corrected for the diffusive hindrance and for the change in solvent viscosity with pore radius.

In keeping with the solution-diffusion model, the permeants dissolve in the membrane material and then diffuse through the membrane down a concentration gradient, while the pressure within the membrane is constant at the highest level (see Figure 1.4-b). The permeants are separated because of the differences in the solubilities of the materials in the membrane and the differences in the rates at which the materials diffuse through the membrane

(Baker, 2004). Following the assumptions made, two simple equations could be derived for volume and solute flux:

$$J_v=\frac{D.K^L.C.\upsilon}{l.R.T}(\Delta P\text{-}\Delta\pi)=A(\Delta P\text{-}\Delta\pi) \quad \text{1-8}$$

$$J_s=\frac{D_s.K_s^L}{l}\left(C_{s,0}\text{-}C_{s,\ell}\right)=\omega\left(C_{s,0}\text{-}C_{s,\ell}\right) \quad \text{1-9}$$

where D and D_s are the Fick's law diffusion coefficients, K^L and K_s^L are the solvent sorption and the solute distribution, respectively, C is the solvent concentration, υ is the solvent molar flux, l is the membrane thickness, $C_{s,0}$ is the solute concentration in the feed side and $C_{s,l}$ is the solute concentration in the permeate side; the constants A and ω are known as the solvent and solute permeability, respectively. According to equation 1-8 the solvent flux through a membrane remains small up to the osmotic pressure of the solute solution and then increases with applied pressure, whereas according to equation 1-9 the solute flux is essentially independent of the pressure. This explains why the rejection may increase with applied pressure for RO processes (Baker, 2004).

OSN membranes are intermediate between truly porous and truly solution-diffusion membranes, and so they are best described by transient mechanisms that take into account the changing contributions of the diffusive and convective mechanisms, like the irreversible thermodynamics and the pore-flow models presented, or the solution-diffusion with imperfections model (Bhanushali, Kloos & Bhattacharyya, 2002, Mason & Lonsdale, 1990), that accounts for the occurrence of convective flow and for the partial flux coupling effect. Plus, and since OSN membranes are applied to non-aqueous systems, special considerations regarding the various interactions between the system components and membrane swelling are also needed (Boam & Nozari, 2006, Dijkstra, Bach & Ebert, 2006, Robinson et al., 2004, Bhanushali, Kloos & Bhattacharyya, 2002).

1.1.7. Strengths and limitations of membrane processes

Membrane processes are generally considered cost-effective and environmentally sustainable processes: they consume low energy, comparing with other unit operations like distillation and crystallization, they are typically non-thermal and, with exception of pervaporation, do not involve phase changes. Furthermore, they can be easily installed as continuous processes and readily combined with existing processes into a hybrid process. The latter fact can be attributed to their modular set-up, which also renders upscaling relatively simple (Vandezande, Gevers & Vankelecom, 2008). Membrane processes are also extremely versatile, as membranes can be tailored to fit the most diverse applications like water purification, carbon capture and even organic solvent exchange.

In spite of all these advantages, and after all the progress in this area, membrane processes still have some limitations, that particularly slow down large-scale applications (Van der Bruggen, Mänttäri & Nyström, 2008, Baker, 2006). The most relevant limitations are discussed in the following sub-sections. A special attention was given to problems related to pressure driven membrane processes, like NF and OSN.

1.1.7.1. Concentration polarization and membrane fouling

Concentration polarization is basically the formation of concentration gradients due to differences in the permeate rates of the feed mixture components. By convention, concentration polarization effects are described by considering the concentration gradient(s) of the minor component(s), which can be the more or the less retained component(s), depending on the process. Plus, since in most membrane processes there is a bulk flow of a liquid or a gas through the membrane, only concentration gradients formed on the feed side are considered (Baker, 2004).

Pressure driven processes, like MF, UF, NF and RO, are usually applied to solutions consisting of a solvent, that can permeate through the membrane more or less freely, and one or more solutes, that are retained to different extents by the membrane. The retained solute(s) can accumulate at the membrane surface where their concentration will gradually increase. This causes not only a reduction in the driving force for the solvent, that translates in a flux decline, but also an increase in the driving force for the solute(s), reducing membrane selectivity. The increase in solute concentration at the membrane surface can also lead to a diffusive back flow towards the bulk of the feed, resulting in a concentration gradient between the bulk ($C_{s,b}$) and the membrane surface (C_m) – boundary layer-, like the one depicted in Figure 1.5, which increases the resistance to mass transfer (Mulder, 1996).

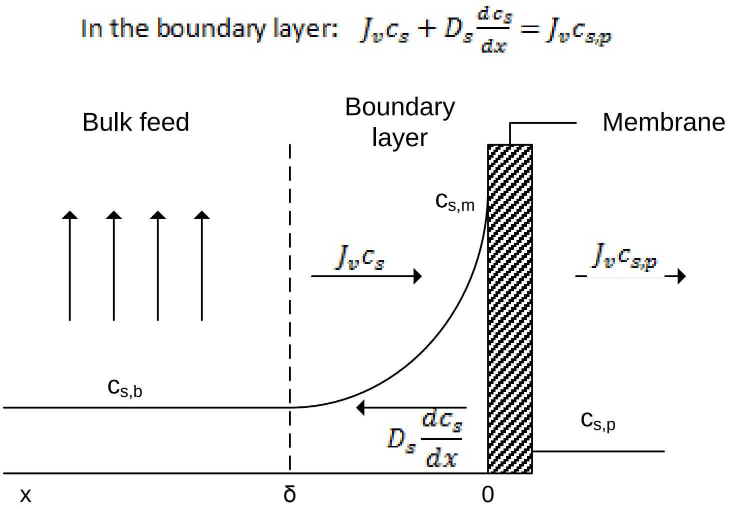

Figure 1.5 Concentration polarization: concentration profile under steady-state conditions.

It is possible to minimize the concentration polarization effect by decreasing the boundary layer thickness, δ. This can be achieved by increasing the fluid flow velocity past the membrane surface, by using membrane spacers, or by using pulsating flow, as all these options increase turbulent mixing at the membrane surface. However, the energy consumption of the pumps required and the pressure drops produced imposes a practical limit to the turbulence that can be obtained in a membrane module (Baker, 2004, Mulder, 1996).

It is known that concentration polarization increases exponentially with the volume flux, J_v. That is why after a certain pressure, the flux does not increase further on increasing the pressure and the so called limiting flux, J_∞, is achieved (see Figure 1.6). Thus, there is no point in having super-high-flux membranes, since the maximum flux will always be limited by osmotic pressure and concentration polarization. The only advantage of these membranes would be a reduction in energy costs, since they would allow for the same flux at lower applied pressure, minimize the overall processing time and limit the required membrane area (Baker, 2004).

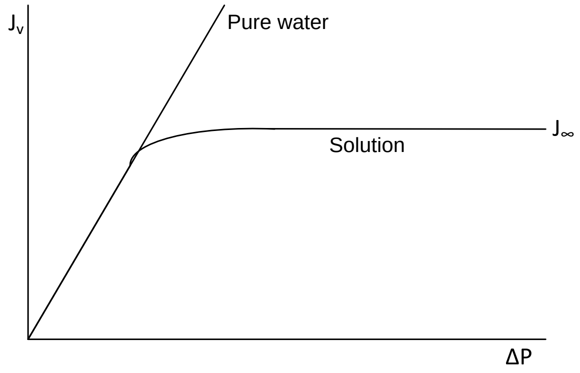

Figure 1.6 Flux as a function of the applied pressure both for pure water and for a solution: the flux of pure water increases lineary with applied pressure, considering that no compaction occurs; however when solutes are added to water the flux starts platteauing after a certain applied pressure (Mulder, 1996)**.**

In the worst case scenario concentration polarisation can result in membrane fouling, which is the deposition of retained solutes in the membrane, by adsorption, pore blocking, precipitation or cake formation. The type of separation problem and the type of membrane used in MF and UF make these processes the most susceptible to concentration polarization and fouling of all pressure driven membrane processes (Mulder, 1996). Fouling problems are, however, much more complex for NF processes, since the interactions leading to fouling take place at nanoscale, and are therefore difficult to understand (Van der Bruggen, Mänttäri & Nyström, 2008).

One of the main consequences of membrane fouling (and concentration polarization) is the decrease of flux. This has a negative impact on the operational costs of the process, since the permeate production gets lower and/or higher transmembrane pressures are required (Mulder, 1996).

Classical solutions to fouling are the pre-treatment of the feed and cleaning of membranes. Membrane design and process conditions can also be optimized to minimize fouling phenomena. Although, membrane modification is potentially the most sustainable solution, as it would allow to virtually abolish the problem (Van der Bruggen, Mänttäri & Nyström, 2008, Mulder, 1996).

1.1.7.2. Insufficient separation

The incompleteness of the separation is a major impediment for a wide application of membrane processes, including NF (Van der Bruggen, Mänttäri & Nyström, 2008).

As described in sub-section 1.1.5, NF membranes are characterized by a sigmoidal rejection curve, which is never completely sharp. This results in an insufficient separation between different compounds on the basis of molecular size. Since the separation depends also on other physical and chemical properties of the compounds/membrane, like charge (Bellona & Drewes, 2005), and since the pores of NF membranes follow a distribution of sizes (Richard Bowen & Doneva, 2000), permeate usually contains molecules with variable sizes, both below and above the claimed average pore size of the membrane. The separation can be even more challenging for OSN processes, since solvents can change membrane characteristics, like pore size and hydrophobicity (Van der Bruggen, Geens & Vandecasteele, 2002), and even solute characteristics, like solute effective diameter (Geens et al., 2005). Therefore, a single membrane separation is often insufficient to obtain the desired separation (Van der Bruggen, Mänttäri & Nyström, 2008).

There are different process strategies to overcome this problem, like multiple membrane passages, diafiltration or membrane cascades. As will be seen in section 1.3, membrane cascades offer further benefits, and begin to be considered for NF and OSN processes (Van der Bruggen, Mänttäri & Nyström, 2008).

1.1.7.3. Membrane compaction

Compaction is the mechanical deformation of a polymeric membrane matrix, due to the sealing and collapse of the pores at elevated pressures. Thus, this is a phenomenon which occurs specially with porous membranes used in pressure driven membrane operations, where the applied pressures are relatively high, like NF and RO (See Toh, Silva & Livingston, 2008, Mulder, 1996). However, dense membranes tend also to suffer some compaction when exposed to swelling conditions (Vankelecom et al., 2004). This is never a problem for ceramic membranes due to their superior mechanical stability.

During compaction the flux declines until the membrane reaches a steady state in which no further permeate flux reduction occur. On the other hand, the rejection tends to increase, eventually stabilizes after a critical volume of solvent permeates through the membranes. After relaxation the flux and rejection can return or not to its original value, depending on the reversibility of the membrane deformation (Gibbins et al., 2002, Whu, Baltzis & Sirkar, 2000, Mulder, 1996). In order to avoid this time dependent behavior, polymeric membranes should be pre-conditioned with pure solvent until a steady flux is obtained (Gibbins et al., 2002).

1.1.7.4. Low membrane stability and lifetime

In the case of NF and OSN processes, membrane stability and lifetime is related to the occurrence of fouling (and therefore, the need for cleaning), and the application of membranes in demanding circumstances, such as the ones created by organic solvents (Van der Bruggen, Mänttäri & Nyström, 2008).

For aqueous applications, membrane lifetime depends on the overall strategy against membrane fouling. Applications where fouling requires frequent cleaning often face a faster membrane deteoration, because even the mildest cleaning agents damage the membrane to some extent (Van der Bruggen, Mänttäri & Nyström, 2008).

In the case of OSN, membrane lifetime depends mostly on the compatibility between the membrane and the solvents. Recurrent problems resulting from the interaction between polymeric membranes and organic solvents are swelling, deformation or (ultimately) dissolution of the membrane (Van der Bruggen, Mänttäri & Nyström, 2008).

Membranes can be made more stable to overcome these problems by, e.g. crosslinking (See Toh, Lim & Livingston, 2007) or increasing the degree of crosslinking of the polymeric top layer (Schmidt et al., 1999), by improving common materials (Musale & Kumar, 2000), or by using alternative membrane materials (Florian, Modesti & Ulbricht, 2007, Gevers, Vankelecom & Jacobs, 2006, Golemme & Drioli, 1996). Ceramic membranes, for instance, can solve the problems of swelling, changes in performance, and limited lifetime, due to their superior chemical resistance (Van der Bruggen, Mänttäri & Nyström, 2008).

1.2. SOLVENT USE IN THE PHARMACEUTICAL INDUSTRY

1.2.1. Solvent utilization

The manufacturing of a drug product involves two phases: 1) the production of the active pharmaceutical product (API) and 2) the formulation process, in which the API is combined with one or more excipients to produce the final product. During all the manufacturing process, solvents are inevitably used for cleaning process equipment and for analytical instruments employed for process control and quality assurance. However, during the batch-wise API synthesis phase solvents are used for many other purposes (Dunn, Wells & Williams, 2010).

Most APIs are produced using liquid phase organic reactions which often require large quantities of different solvents. Between each reaction step, there are a series of operations required to separate, purify and isolate APIs intermediates (work-up phase), that frequently require more solvents and/or generate solvent wastes. Because of the considerable number of steps and the large amount of solvents required per each step, solvent use can account for as much as 80-90% of the total mass in an API production process (Dunn, Wells & Williams, 2010). A scheme of the different steps involved in a typical API synthesis process, including solvent waste streams generated in each step is shown on Figure 1.7.

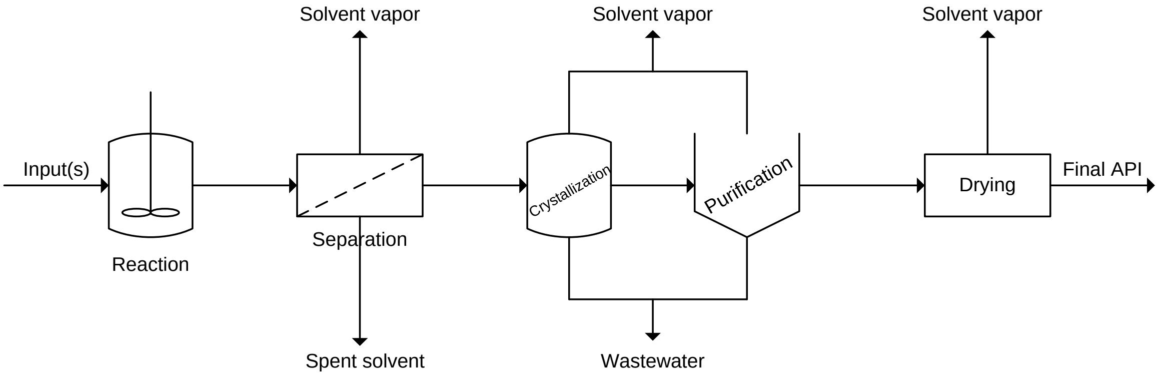

Figure 1.7 Typical pharmaceutical batch operation. Adapted from (Dunn, Wells & Williams, 2010)**.**

A very broad spectrum (an average of 0.9 types of solvents per production stage) of solvents is used in the pharmaceutical industry (Seyler et al., 2006). As an example of solvent use within a large pharmaceutical company, Table 1.3 shows the top 10 most frequently used solvents for highly developed chemical processes from 1990-2000 and again from all pilot-plant processes carried out in 2005 at GlaxoSmithKline. Most of them are volatile organic compounds (VOCs) that can easily disperse in the environment. Furthermore, they can show both acute and chronic toxicities (Reichardt, 2010). Although, this data suggest that there is a trend towards decreasing highly hazardous solvents use, such as tetrahydrofuran, toluene, and dicloromethane (Constable, Jimenez-Gonzalez & Henderson, 2007).

Table 1.3 Comparison of solvent use at GSK based on overall manufacturing operations (1995-2000) and more recent pilot plant operations (2005) (Constable, Jimenez-Gonzalez & Henderson, 2007)**.**

Chemical	GSK pilot plant processes (2005 rank)	GSK manufacturing processes (1995-2000 rank)
2-Propanol	1	5
Ethyl acetate	2	4
Methanol	3	6
Denaturated ethanol	4	8
n-Heptane	5	12
Tetrahydrofuran	6	2
Toluene	7	1
Dichloromethane	8	3
Acetic acid	9	11
Acetonitrile	10	14

Besides all the environmental, health and safety impacts, there are also economical issues that should drive pharmaceutical companies to reduce solvent waste and usage, like the price of purchasing and the price of waste treatment. Purchasing excessive solvent increases raw material costs as well as waste treatment costs for the disposal of these solvents. The cost to purchase fresh solvents varies on the method of transport, the quantity purchased, and the cost of manufacture (Dunn, Wells & Williams, 2010). On the other hand, it is known that 10-35% of the total plant investment can be consumed during the handling, storage and treatment of waste streams (Mulholland & Dyer, 2001).

It is peremptory: if pharmaceutical companies want to contribute to the reduction of the overall environmental footprint, produce efficient and robust processes, and be competitive they will need to minimize solvent utilization and waste generation (Dunn, Wells & Williams, 2010).

1.2.2. Waste minimization and solvent recovery

There are several ways to reduce or eliminate the amount of solvent used in a pharmaceutical process, such as the use of continuous processes, biosynthetic processes, solid-state chemistry and the reduction of the number of chemical bond-forming steps and unit operations within a process, also known as telescoping. However, there are still a lot of situations where the use of solvents is unavoidable and where normally they have to be used in excess. In these situations the only way to avoid or minimize the costs and environmental burden related to solvents usage is by reusing them (Dunn, Wells & Williams, 2010).

Pharmaceutical companies already do their recovery since decades, but they are still seeking ways for enhance the feasibility of solvent recovery processes (Thomas, 2012), by minimizing the input of energy required and/or the waste produced by their own (Dunn, Wells & Williams, 2010).

The capital investment for solvent recovery typically includes piping, tank farms and recovery equipment, which is easy to justify for large volumes and expensive solvents, but not so easy with smaller streams, that can't necessarily be pooled with other solvents. Thus, there is also a need to find new and integrated ways for solvent recovery (Thomas, 2012).

Currently, distillation is used for approximately 95% of all solvent separation processes. However it leads to waste generation, such as the release of green house gases (GHGs), high energy requirements and the inadequate condensing of distillate products (Dunn, Wells & Williams, 2010).

Membrane processes can be easily installed as a continuous process, and due to its modular set up, they can be combined readily with existing processes into hybrid processes. All these factors make membrane technology an attractive alternative for the solvent recovery in solvent intensive processes such as the pharmaceutical ones (Vandezande, Gevers & Vankelecom, 2008).

1.2.3. Use of membrane technology for solvent recovery

The use of membrane technology for the solvent recovery was not only proposed for the separation of liquid mixtures, or for the use in the pharmaceutical industry. Some membranes/membrane processes were also suggested for the solvent recovery on other situations, such as the recovery of solvents from air resulting from drying, glueing, and coating, the extraction of vegetable oils, dewaxing of lube oils, and the production of reactive dyes.

The first time a membrane process was proposed for solvent recovery was by Kimmerle et al. (1988), who set up a pilot plant with a module of composite hollow fibres for the recovery of acetone from air. The idea was to show the economic feasibility of this separation process for the less permeable solvent within the solvents tested and then extend it to the recovery of solvents from air streams resulting from some industrial processes such as drying, glueing, and coating.

Rama, Cheryan & Rajagopalan (1996) proposed the utilization of two NF membrane units in series for the solvent recovery from vegetable oil extraction, to not only reduce the amount of solvent needed to be evaporated by distillation and allow the reutilization of the permeating solvent in the following extractions, but also to maximize oil recovery. Other authors like Köseoglu & Engelgau (1990) and Snape & Nakajima (1996) also proposed the use of hybrid membrane systems for this application.

There is a process, trademarked by Mobil Oil Corporation as MAX-DEWAX®, that combines a conventional solvent lube dewaxing process with a polyimide membrane system for recovery of chilled solvent from the lube filtrates. Significant increases in energy efficiency and solvent recovery capacity were realized by doing this combination (White & Nitsch, 2000). This process, running at the Exxon Mobile refinery in Beaumont (Texas) since 1998, is the largest OSN-plant running for years at industrial scale (Vandezande, Gevers & Vankelecom, 2008).

To solve the shortcomings of the conventional processes for the production of reactive dyes, He et al. (2010) proposed a two stage UF membrane separation process, in which the first stage is used for diafiltration and concentration of dye solution, and the second is essentially to recover the salt water and circulate it back to synthesis processes.

Pervaporation is a membrane-based process already used by some pharmaceutical companies to separate aqueous azeotropic solvent mixtures. The use of this technology in hybrid processes for the solvent recovery in pharmaceutical manufacture was evaluated in several studies (Dunn, Wells & Williams, 2010). A process that integrated a pervaporation unit with a batch constant volume distillation, for instance, was proposed to dehydrate a tetrahydrofuran (THF)/water azeotropic mixture during the synthesis of a Bristol-Myers Squibb oncology drug. In this case the pervaporation membrane was used to dehydrate the distillation vapour at azeotropic conditions, allowing to reduce the waste disposal cost by 93%, the cost of purchase of THF by 56% and a reduction of 95% in greenhouse gas emissions (Slater et al., 2007). Another hybrid process was proposed for the recovery of isopropanol (IPA) from a waste stream composed by equal amounts of IPA and water, with small amounts of methanol, ethanol, and other dissolved solids. The proposed process provided a 72% overall operating cost saving and a 92% reduction in emissions (Savelski et al., 2008).

OSN is now emerging as an alternative technique for solvent recovery in the pharmaceutical industry. Wong et al. (2006) proposed the utilization of OSN to separate a ionic liquid, that was working as a solvent, and a palladium catalyst from the product resultant from a Suzuki reaction (a type of coupling reaction widely used in the synthesis of APIs (Carey et al., 2006) and reutilize them in the subsequent consecutive reactions. The product was recovered in the nanofiltration permeate, while the ionic liquid and palladium catalyst were retained by the membrane. After a few cycles the mass of palladium per unit mass of product started to increase in the permeate stream, probably due to the degradation of the catalyst into nanoparticles. Like this, product purity remains unacceptable for pharmaceutical applications, and so further improvements have to be made in order to apply this process in the pharamaceutical industry.

Sereewatthanawut et al. (2010) proposed the utilization of a dual OSN membrane process for the recovery of THF during the diafiltration of an organic synthesis solution containing an API intermediate from Janssen Pharmaceutica, its isomer, and a series of oligomeric impurities based on the API intermediate (i.e., dimers, trimers, tetramers and pentamers). Using this process they were able to recover 99,2% of the product while reducing the overall content of impurities from 6,8% to 2,4%. They also claim that the integration of the solvent recovery stage allowed to reduce the fresh solvent requirement by up to 90%. Like this, they proved that membrane technology can contribute to have a solvent-efficient process, which does not generate large volumes of waste and/or does not provide a dilute product solution that would require further processing.

Rundquist, Pink & Livingston (2012) investigated the feasibility of using OSN as an alternative to distillation for solvent recovery from crystallization mother liquors. They proved that, despite less solvent is recovered by OSN, this technique is capable of recovering organic solvent with a purity suitable for re-use in subsequent API crystallizations and it uses 25 times less energy per liter of recovered solvent when compared to distillation. They also demonstrated that equivalent recovery volumes can be obtained by using a OSN hybrid process with the energy consumption remaining 9 times lower than when distillation is used alone.

Despite very few studies have been done in this field, it is indisputable the potential of using OSN for solvent recovery. The key to the success of this technique is clearly the membrane itself. The membrane needs to be (highly) permeable to the solvent to be recovered and also be stable on all the solvents present in the initial mixture. Furthermore, in the case of being mixed with some solutes, it needs to have a low MWCO so it can retain even the lowest MW compounds present in solution.

1.3. MEMBRANE CASCADES

1.3.1. Module configurations and mode of operation

A module is the smallest unit into which a membrane can be packed. The module is the central part of a membrane installation and is often referred to as the separation unit. Here the feeding material is fractionated into two streams, i.e. the permeate that is the fraction of the feed stream which passes through the membrane and the retentate which is in turn the fraction retained by the membrane (Mulder, 1996).

There are two basic module configurations which are flat and tubular. The choice of the configuration should be based both on economic considerations and on the type of application (Mulder, 1996).

A module can also operate in two basic ways: a) dead-end and b) crossflow. In dead-end modules (see Figure 1.8-a), the feed is forced through the membrane by a pressure perpendicular on the membrane surface. This implies that the concentration of the rejected components in the feed increases. On the other hand, in a cross-flow module the feed flows parallel to the membrane surface (see Figure 1.8-b), which implies a feed composition change along the module. Consequently, cross-flow operation has lower fouling tendency relative to the dead-end mode and so is less prone to cake formation or to concentration polarization problems. That is why industrial membrane applications generally run in cross-flow mode (Vandezande, Gevers & Vankelecom, 2008, Mulder, 1996).

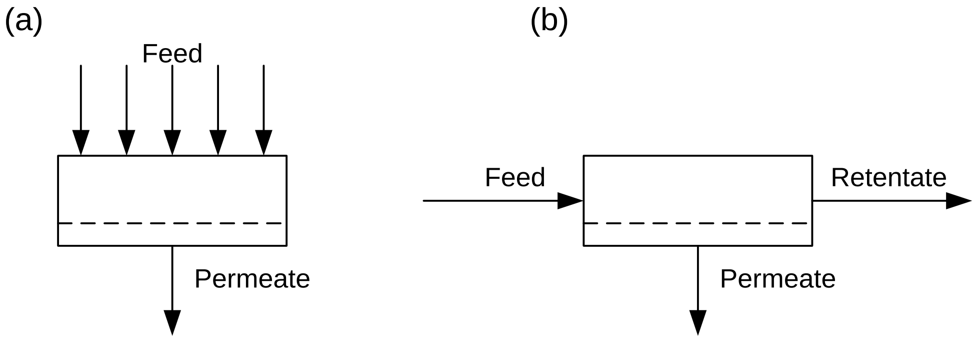

Figure 1.8 The two basic module operations: (a) Dead-end and (b) Cross-flow (Mulder, 1996)**.**

There are other cross-flow operation modes in addition to the one depicted in the Figure 1.8-b, where the feed and the permeate streams are parallel to each other, namely the co-current and counter-current operation modes. It can be demonstrated by process calculations that the counter-flow gives the best results followed by the cross-flow and co-current flow, respectively (Mulder, 1996).

The simplest membrane process design is one in which a single module is used. However, the single-module design does not often result in the desired separation, since membranes are not always sufficient selective. A multiple membrane passage, by using a recirculation system, may improve the overall rejection but not the separation between the different compounds (Van der Bruggen, Mänttäri & Nyström, 2008). Another solution, especially for pressure driven processes, could be operate the module in diafiltration mode (Mulder, 1996). However, during diafiltration processes there could be a significant product loss to permeate and, normally, a lot of fresh solvent is consumed to achieve the target purity and product yield (Sereewatthanawut et al., 2010, Krstić et al., 2004).

In the next sections it will be demonstrated that membrane cascades, which are nothing but combinations of modules in series that allow to retreat the retentate and/or the permeate as many times as necessary (Mulder, 1996), may actually improve the separation between individual compounds by playing around with their configuration and mode of operation.

1.3.2. Membrane cascades configurations and modes of operation.

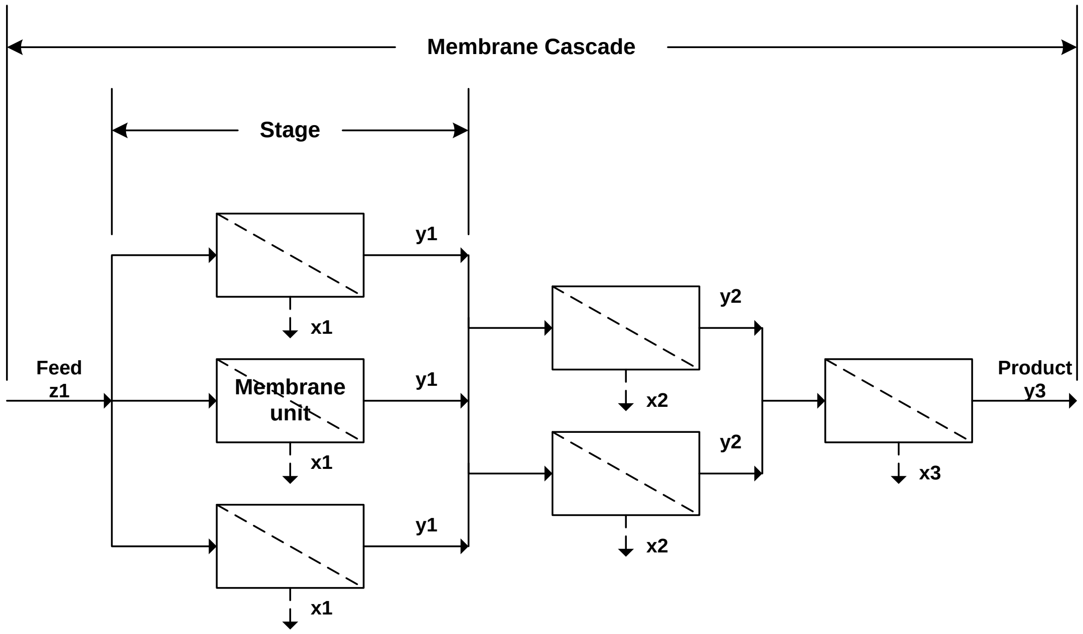

Figure 1.9 The arrangement of membrane units and stages in a cascade. Adapted from (Benedict, Pigford & Levi, 1981)**.**

The basic concept of a cascade is illustrated in Figure 1.9, which shows an array of membrane units organized in stages. The membrane units within a stage are said to be connected in parallel, that is, they all receive identical inputs and produce identical outputs which are fed into other stages. On the other hand, the various stages are connected to each other in series, that is, each stage receives input from the previous one and passes its output on to the next stage. Often a single unit serves as a stage. However, when units have low capacity, it is necessary to use many units in parallel so large amounts of material can be processed (Krass, 1983, Benedict, Pigford & Levi, 1981, Villani & Becker, 1979)

In simple cascades, the stream that follows to the next cell is always a fraction of the feed. Consequently the final product stream amount decrease as the number of cells in the cascade increase. To overcome this problem one can use either cells of different size, as shown in Figure 1.10-a, or a tapered-cascade arrangement. A disadvantage of simple schemes is that these ones involve the discharge and no utilization of considerable material in discarded streams, so one should use such schemes only when relatively few stages are involved and if the disposed components are not fairly valuable (Villani & Becker, 1979, Hwang & Kammermeyer, 1975).

Almost all cascades recycle because it greatly increases the recovery of the product. A recycling cascade has two sections, the enriching section, consisting of the stages above the point at which the feed enters the cascade and the stripping section below the feed point. The stripping section increase the recovery of the material, whereas the enriching section produces material of increased concentration. There are many possible recycle cascade configurations but a very effective and common cascade design is the symmetric countercurrent recycle cascade, which in some ways is very similar to a continuous distillation column (Benedict, Pigford & Levi, 1981). In the case of the countercurrent recycle cascade schematized in the Figure 1.10-b the permeate of a stage feeds the next upper stage, while its retentate stream is recycled back to the immediately preceding stage (Villani & Becker, 1979).

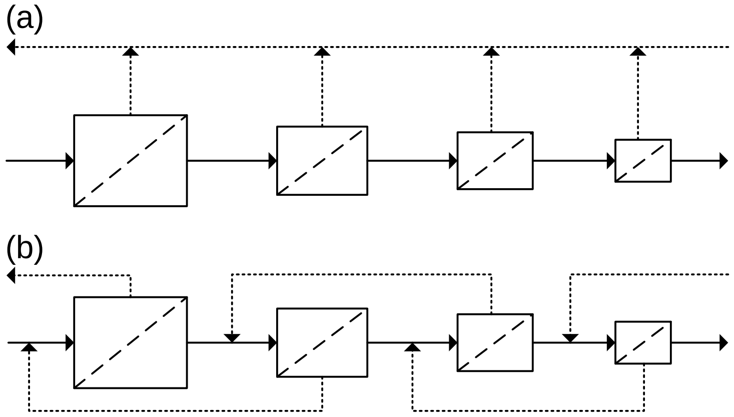

Figure 1.10 Modes of cascade operation: (a) simple cascade and (b) countercurrent recycle cascade. Adapted from (Villani & Becker, 1979)**.**

One of the possible variations of that basic design, introduced by Hwang & Kammermeyer (1965), is the ideal cascade. In this case, the compositions of permeate and retentate streams that make up the feed to interior stages have the same composition, which means that there is no mixing of streams of different compositions between stages, and so there are no losses of separative work. To meet the no-mix criteria the flow rate between stages and the size of each stage must vary, which means that each stage will has to be of different size. In addition, the feed is introduced within the cascade where the retentate composition is the same as the feed.

Thus, in spite of the fact that ideal cascades minimize the energy consumptions and the global size of the plant, its realization is complicated in terms of design, fabrication, operation and maintenance (McCandless & Herbst, 1990, McCandless, 1990). The solution to this problem in practical cascade design is to approximate the ideal cascade by a small number of squared cascade segments connected in series, in what is called a squared-off cascade. Like this, all of the stages can be made identical and so a large reduction in the cost of separative units can be achieved (McCandless & Herbst, 1990).

Many membrane cascades, with these and other configurations, were already proposed to solve separation problems encountered in different membrane processes and many different areas of application. These are reviewed in the next sections.

1.3.3. Membrane cascades applications

1.3.3.1. Gas separation

Cascade theory was highly developed during the 1940s in connection with the gaseous diffusion process for uranium-235 (^{235}U) enrichment using porous membranes (Halle & Shacter, 2000, Mulder, 1996, Hwang & Kammermeyer, 1975). Natural uranium exists in the gas form and consists mostly of ^{238}U and 0.711 wt % ^{235}U plus a little amount of ^{234}U (Halle & Shacter, 2000). Due to the similar physical and chemical properties of these isotope molecules it was hard or even impossible to recover enough ^{235}U isotope using a single membrane module. In order to achieve higher separations a large number (thousands) of membrane units were connected and the result was a ^{235}U product stream 90% pure (Agrawal & Xu, 1996b).

After this successful event, and since membrane selectivities were too limited for many gas-separation applications (Robeson, 1991), a lot of authors started proposing different cascade schemes, derived from the countercurrent recycle cascade, for the separation of binary systems (Agrawal & Xu, 1996a, McCandless & Herbst, 1990, Yan & Kao, 1989, McCandless, 1985, Ohno et al., 1978b) and even mixtures with three or more gaseous components (Agrawal, 1996, Kothe et al., 1989, Sengupta & Sirkar, 1987, Hwang & Ghalchi, 1982, de la Garza, 1963).

Each time a stream enters a gas separation unit, it needs to be pressurized, so a lot of compressors (about the same as membrane units) were necessary per cascade. This was acceptable for an expensive product like uranium, but impractical for other gas-separation applications. That is why a lot of the studies propose cascades with lower number of stages and/or less recycle streams (Pathare & Agrawal, 2010, Agrawal & Xu, 1996a, Agrawal & Xu, 1996b, Agrawal, 1996, Xu & Agrawal, 1996, Laguntsov et al., 1992, Ohno et al., 1978a, Ohno et al., 1978a). Agrawal (1997) developed a stepwise procedure for design of membrane cascades using a limit number of recycle compressors. Nowadays, most commercial gas separation membrane cascades use one or two compressors.

Another big contribution to cascade theory was given by Hwang & Kammermeyer (1975), which proposed to use the McCabe-Thiele method, originally developed for distillation, to design countercurrent recycle membrane cascades for the separation of binary gas mixtures. Since then that this method has been widely used to design cascades, not only for gas separation but also for liquid separation (Keurentjes et al., 1992) and solid fractionation (Vanneste et al., 2011).

1.3.3.2. Liquid solutions/Liquid separation

Most of the studies on membrane cascades for the purification of liquid solutions are related to wastewater treatment.

Several authors, like Evangelista (1987) and Maskan et al. (2000) developed design methodologies to optimize RO network configurations and operating conditions.

Many dual membrane systems, where normally a MF/UF module precedes a NF/RO module, were proposed for wastewater treatment (and recovery) (Luo et al., 2011, Peng & Tremblay, 2008, Peng, Tremblay & Veinot, 2005, Gryta, Karakulski & Morawski, 2001). Peng & Tremblay (2008) designed and tested a pilot scale membrane cascade system using MF, UF and NF membranes to remove oil and grease from bilge water accumulated in ships. The authors concluded that it is possible to reduce the oil and grease content of water to the allowable discharge limit through the proper design of the membrane system, selection of appropriate membranes, determination of optimal operating parameters, and assessment membrane performance.

Caus et al. (2009) compared simple and recycling cascades with two and three stages for removal of pesticide in drinking water. Through modeling based on transport equations and mass balances they showed that is possible to achieve an adequate pesticide rejection, meeting the European standard for potable water, using a three-stage NF cascade with recycle.

Kale, Katikaneni & Cheryan (1999) suggested a NF membrane cascade for the removal of free fatty acids from methanol, after its extraction from crude rice bran oil. Design estimates indicate that a two-stage NF membrane system can recover 97.8% of the free fatty acids and result in a methanol stream with only 0.13% of free fatty acids that can be recycled for extractions.

Keurentjes et al. (1992) theoretically compared the performance of two different cascades (one made with only one type of RO membranes and another one made with RO membranes of opposite selectivities but equal permeabilities), for the separation of water-1,3-butanediol mixtures. It was concluded that the total membrane area can be reduced by 25% when two membranes of opposite selectivity are available. Pervaporation cascades were also considered for the separation of azeotropic mixtures (Rautenbach & Albrecht, 1985, Hoover & Hwang, 1982).

After Livingston et al. (2003) and Sheth et al. (2003) proposed a OSN diafiltration process for organic solvent exchange, Lin & Livingston (2007) came up with a countercurrent OSN membrane cascade for the same purpose. Despite the feasibility of the process has been theoretically and experimentally proved, it was concluded that with the countercurrent recycle configuration it would be required an infinite number of stages to achieve a complete exchange between the two solvents.

1.3.3.3. Solute fractionation

UF membrane cascades were largely considered to improve fractionation efficiency of heat-labile macromolecules (Mohanty & Ghosh, 2008, Ghosh, 2003, Muller, Daufin & Chaufer, 1999, Barker & Till, 1992, Ward et al., 1987). Although it was unsuccessful, UF membrane cascades were also suggested for the separation of racemic mixtures (Higuchi et al., 2003, Overdevest et al., 2002).

The increasing need for a continuous, high-throughput, economical and easily scalable separation process for downstream processing of biological substrates, like proteins, carbohydrates, plasmids, viruses, organelles, and even whole cells, led Lightfoot (2005) to propose membrane countercurrent cascades as an alternative for chromatography and simulated moving bed chromatography. He and his co-workers (Lightfoot, Root & L. O'Dell, 2008) also proposed an extended version of the binary ideal cascade theory for modeling diafiltration membrane cascades for fractionation of binary systems of two solutes in a single solvent. Each stage of a diafiltration membrane cascade consists of a UF module combined with a RO module to remove excess solvent from the permeate stream.

Caus et al. (2009) assessed the potential of countercurrent NF cascades with recycle of retentate for separation of individual organic compounds in aqueous solution by means of single-stage filtration experiments using xylose and maltose and cascade simulations. They found that, in order to obtain high product purity with a limit number of stages, there has to be a sufficiently high rejection difference between the components. They also concluded that the optimal number of modules depends on the trade-off between selectivity and recovery.

More recently, Vanneste et al. (2011) adapted the Mc-Thiele method, for solute membrane cascades without diafiltration and applied it on three different sugar separations for which the state of the art is simulated moving bed chromatography: raffinose-sucrose, fructose-glucose and xylose-glucose. After comparing membrane cascades performance with simulated moving bed chromatography performance, membrane cascades seemed more promising for large scale continuous production of a product with medium purity.

Lin, Peeva & Livingston (2006) were the first to propose membrane cascades for solute separation in an organic solvent environment. In their study they compared the performance of a three-stage OSN membrane cascade with recycle with the performance of a single OSN membrane module operating in diafiltration mode for API purification. Two dyes, Martius Yellow and Brilliant Blue R, were respectively used as API product and color impurity. Both systems allowed to control the impurity level in the final product. However, the single-stage configuration showed better performance in terms of product productivity than the three-stage cascade.

1.4. IMPLICATION OF THE LITERATURE REVIEW AND RESEARCH MOTIVATION

The purification of APIs is a critical issue for pharmaceutical companies, as the production of pharmaceuticals follows very strict regulation. APIs and the intermediate products are generally thermally labile and need to be separated from smaller or higher molecular weight byproducts, residual reactants, catalysts or even residual solvents. The currently preferred purification technologies are crystallization and column chromatography, which are in general expensive, solvent intensive, and difficult to control and scale-up.

Another important issue for pharmaceutical companies is solvent use that can account for as much as 80-90% of the total mass in an API synthesis process. This has a negative impact, not only over the environment and people’s health, but also over the economics of pharmaceutical companies. Despite most of them already do their recovery since decades, there is still a need to find more efficient, economic and integrated ways to minimize solvent requirements.

OSN is an emerging membrane-based separation technique with a lot of potential to improve the current API synthesis processes: it is a non-thermal technique that only requires a pressure gradient, can withstand harsh organic solvents, and discriminate compounds ranging between 100-1000 g mol^{-1}. However, conventional membrane processes still require large volumes of solvent to achieve the target purity and yield of desired product. Plus, they do not allow for a sharp separation between compounds.

Recently, a solvent efficient OSN process emerged as a competitive alternative to purify APIs (Sereewatthanawut et al., 2010). However, this process still requires a delicate control system and a considerable investment in equipment, such as buffer tanks and pumps.

Here we propose a simple closed-loop membrane process for the purification of API that operates in a self-regulating manner without any additional solvent or extra equipment. The system is pressurized with liquid using only a single pump and combines two OSN membranes, one for purification and another for solvent recovery.

It is known that it is possible to improve the separation between individual compounds by cascading. Thus, it should be possible to increase the yield and purity of the recovered product by increasing the number of membrane units for separation in the closed-loop membrane process. The potential of integrating a membrane cascade on the closed-loop membrane process to improve its separation performance will be assessed through simulations.

Chapter 2

Materials & Methods

2.1. MODEL MIXTURES

Three model mixtures of dyes with MW in the OSN range were used in this study. The first one was a mixture of Solvent Yellow 7 (SY7) and Brilliant Blue R (BBR) in N,N-dimethylformamide (DMF) - model mixture A . The second was a mixture of Martius Yellow (MY) and BBR in DMF – model mixture B. The last one was a mixture of MY and BBR in methanol (MeOH) – model mixture C. The three dyes were purchased from Sigma-Aldrich. The organic solvents were HPLC grade and purchased from VWR. The solubility of the dyes in the selected solvents was verified before running the experiments.

These mixtures were used as typical pharmaceutical production challenges where the API to be purified has a lower MW than the impurities, so SY7 and MY were used as APIs while BBR was always used as impurity.

It was decided to use dyes with different colors as model product and impurity because they can be visually detected when pure or mixed with each other, and easily analyzed by UV/Vis spectroscopy: SY7 and MY are yellow and absorb at 353 and 432 nm, respectively, while BBR is dark blue and absorbs at 600 nm; a mixture of SY7 and BBR or of MY and BBR is green. The structure, molecular weight and the maximum absorbance wavelengths (λ_{max}) of these compounds are summarized in Table 2.1.

The cascade simulations were based on a single membrane diafiltration carried on a mixture from an actual oligonucleotide synthesis step. This was a mixture of an oligonucleotide intermediate (MW=6900g.mol^{-1}) and excess succinate nucleotides (MW=700g.mol^{-1}) in acetonitrile (MeCN). Before this diafiltration membranes were screened using two other model mixtures, one of polyethylene glycol 400 (PEG400), polyethylene glycol 2000 (PEG2000) and polyethylene glycol 8000 (PEG8000) (1 g.L^{-1} each) in MeCN – model mixture D1 - and a similar one to which the succinate monomer (0.2 g.L^{-1}) was added– model mixture D2.

Table 2.1 Properties of the dyes used as model compounds.

Compound	Structure	λ_{max} (nm)
Solvent Yellow 7 (MW=198.2g.mol^{-1})	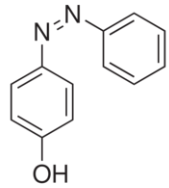	353
Martius Yellow (MW=274.16 g.mol^{-1})	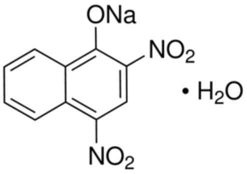	432
Brilliant Blue R (MW=826.0g.mol^{-1})	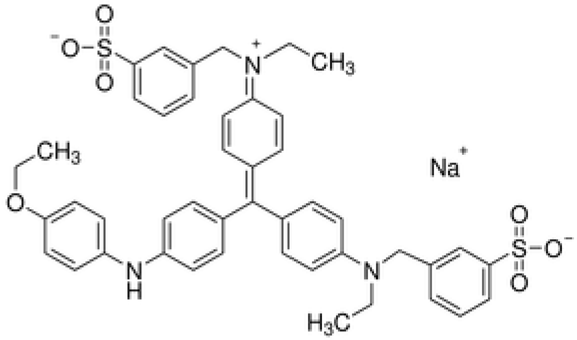	600

2.2. MEMBRANES

Different solvent resistant membranes were prepared for this work: polyimide (PI) and polybenzimidazole (PBI) integrally skinned membranes were prepared by phase inversion; polyamide (PA) thin film composite membranes were prepared by interfacial polymerization upon PI asymmetric support layers.

Some commercial membranes and a poly(ether ether ketone) (PEEK) membrane prepared by a colleague in the lab were also used in this work. A description of these membranes is presented in Table 2.2.

Table 2.2 Summary of the membranes not prepared but used in this work

Membrane Code	Description	MWCO
DM150	DuraMem® 150 (Evonik) – P84® polyimide membrane[a]	150
TFNF-DK	Thin Film Nanofiltration membrane DK (GE Osmonics) - Polyamide layer on top of a microporous polysulfone support[b](Vandezande, Gevers & Vankelecom, 2008)(Vandezande, Gevers & Vankelecom, 2008)	0[c]
TFRO-SE	Thin Film Reverse Osmosis membrane SE (GE Osmonics)	0[d]
TFRO-SG	Thin Film Reverse Osmosis membrane SG (GE Osmonics)	0[e]
4P1231	Poly(ether ether ketone), 12%, 3:1 (Methane Sulphonic: Sulphuric Acid)	N/A

[a] (Evonik Industries, 2012); [b] (Vandezande, Gevers & Vankelecom, 2008) [c] 98% rejection for $MgSO_4$ (Sterlitech Corporation, 2012); [d] 98.9% rejection for NaCl (Sterlitech Corporation, 2012); [e] 98.2 rejection for NaCl (Sterlitech Corporation, 2012).

2.2.1. Integrally Skinned Membranes

2.2.1.1. Polyimide membranes

Chemicals

Lenzing P84® polyimide was purchased from HP polymer GmbH. Maleic Acid (HPLC grade) was purchased from Fluka and used as a pore forming additive. *N,N*-dimethyl formamide (DMF) was purchased from VWR, and 1,4-dioxane from Rathburn Chemicals both HPLC grade. Isopropanolamine (IPA) was purchased from VWR. 1,6-Hexanediamine (HDA), used as crosslinker, was purchased from ACROS Organics, (99,5+%). Polyethylene glycol 400 (PEG400) was purchased from Merck and used as a conditioning agent.

Membrane preparation

The commercial polymer and, in some cases, the maleic acid were dissolved in DMF and 1,4-dioxane and stirred continuously at room temperature for approximately 16 h to obtain an homogenous dope solution. The polymer solution was allowed to stand for a couple of hours at room temperature to remove air bubbles. The membrane was cast on a bench top laboratory caster. The dope solution was used to cast 300 μm-thick film on a polypropylene (PP) non-woven backing (Freudenberg Nonwovens), placed over a glass plate, using an adjustable casting knife on an automatic film applicator (Braive Instruments, UK). The plate was immersed on the precipitation water bath at room temperature by making an angle of $\sim 30°$ with the water surface. The membrane was allowed to stand in this bath for approximately 30 min. Then it was immersed into a cylinder filled with IPA and allowed to stand there for further 24 h, so all the water has removed from the membrane. For the crosslinking, the membrane was immersed into a solution of HDA in IPA (100g.L^{-1}) for 16 h at room temperature. The membrane was then removed from the crosslinking solution and washed three times with fresh IPA to remove any traces of HDA. To prevent its drying out, the membrane was impregnated with PEG400 by immersion in a solution of PEG400/IPA (60/40, v/v%). The membrane was allowed to stand there for about 16h at room temperature. Finally, the membrane was air dried to remove excess solvent. The PI membranes prepared for this work are listed in Table 2.3.

Table 2.3 Summary of the integrally skinned PI membranes prepared.

Membrane Code	Description	MWCO
PI2411	PI, 24 wt%, 1:1 (DMF:Dioxane), Cross-linked with HDA for 16 h	200[a]
PI2321	PI, 23 wt%, 2wt% maleic acid, 2:1 (DMF:Dioxane), Cross-linked with HDA for 16 h	N/A
PI2341	PI, 23 wt%, 2wt% maleic acid, 4:1 (DMF:Dioxane), Cross-linked with HDA for 16 h	N/A
PI2211	PI, 22 wt%, 1:1 (DMF:Dioxane), Cross-linked with HDA for 16 h	300[a]
PI2210	PI, 22 wt%, 2wt% maleic acid, 1:0 (DMF:Dioxane), Cross-linked with HDA for 16 h	N/A

[a] MWCO determined in DMF using crossflow filtration at 30 bar (See Toh, Silva & Livingston, 2008)

2.2.1.2. Polybenzimidazole membranes

Chemicals

Celazole® 26 wt%, a commercially available 26% dope solution of PBI in *NN*-dimetylacetamide (DMAc), was purchased from PBI Performance Products Inc. DMAc and acetonitrile (MeCN) were purchased from VWR. Dibromobutane (DBB) and Dibroxylene (DBX), used for the crosslinking reaction, were purchased from Sigma Aldrich.

Membrane preparation

When required, Celazole® 26 wt% was diluted with DMAc to a different polymer concentration and stirred continuously at room temperature for 4 h in order to obtain homogeneous dope solutions. Otherwise the solution was used as received. Membranes were cast using the prepared dope solutions on a bench top laboratory casting machine with adjustable knife set at 250 µm. The polymer film was applied on non-woven PP material used for mechanical support. Following this, the membranes were immersed in a water precipitation bath at room temperature for 24 h. The obtained membranes were washed with IPA to remove residual solvent and water. To crosslink the polymer the membranes were immersed in a 10 wt% DBB or 3 wt% DBX in MeCN solution and the reaction was carried out at 80 °C for 24 h. After the crosslinking reaction the membranes were first washed with IPA to remove residual crosslinking agent and later on immersed in a PEG400/IPA (1:1) bath for 4 h to preserve the pore structure. A summary of the PBI membranes prepared for this work is presented in Table 2.4.

Table 2.4 Summary of the integrally skinned PBI membranes prepared.

Membrane Code	Description	MWCO
PBI 17xDBX	PBI, 17wt%, Cross-linked with DBX for 24 hrs	N/A
PBI 24xDBB	PBI, 24wt%, Cross-linked with DBB for 24 hrs	N/A
PBI 26xDBB	PBI, 26wt%, Cross-linked with DBB for 24 hrs	N/A

2.2.2. Thin Film Composite Membranes

Chemicals

Hexane was purchased from VWR. The monomers, m-phenylene diamine (MPD), hexamethylenediamine (HDA) and trimesoylchloride (TMC) were both purchased from Sigma-Aldrich.

Membrane preparation

Two PA-based thin film composite membranes were prepared by interfacial polymerization. Both resulted from the reaction between an amine (MPD or HDA) and TMC on a P84$^{®}$ (24% in DMSO) crosslinked polyimide support. For each membrane two solutions were prepared: an organic solution of 0.1% (w/v) TMC in hexane and an aqueous solution of 2% (w/v) amine (MPD or HDA) in water. After fix the support on a glass plate, to prevent the polymerization from taking place at its back side, it was immersed in the aqueous solution for 2 minutes. Then, and after the aqueous solution excess was removed from the support top surface, the plate was immersed in the organic solution for 1 minute. After this time, it was taken out of the solution, let dry and rinsed with distilled water. The membranes were stored in the cold room immersed in distilled water. A list of the TFC membranes prepared is presented in Table 2.5.

Table 2.5 Summary of the TFC membranes prepared.

Membrane Code	Description	MWCO
TFC-MPD	TMC and MPD on PI crosslinked support	N/A
TFC-MPD24	TMC and MPD on PI crosslinked support, annealed for 24h at 85°C	N/A
TFC-HDA	TMC and HDA on PI crosslinked support	N/A

2.2.3. Membrane performance

In this work only flux and rejection were used to evaluate the performance of the membranes tested. Flux was obtained by measuring the volume permeated, V_p, per unit area, A, per unit time, t, using the following equation:

$$J=\frac{V_p}{A.t} \qquad \textbf{2-1}$$

The rejection of species i, R_i, was calculated from its concentrations in the permeate, $C_{P,i}$, and retentate, $Q_{R,i}$, using the following equation:

$$R_i=\left(1-\frac{C_{P,i}}{C_{R,i}}\right)\times 100 \qquad \textbf{2-2}$$

2.3. MEMBRANE FILTRATION

2.3.1. Cross-flow Filtration

A liquid pressurized cross-flow cell rig, like the one schematized in Figure 2.1, was used for membrane screening tests. The cross-flow unit consists of a glass reservoir vessel, with a capacity of up to 5L, and four or eight cross-flow cells connected in series holding a membrane with effective separation area of 14 cm^2 each. A flow-meter is used to measure the flow rate, provided by a diaphragm pump. The pressure within the system is measured by a pressure gauge and adjusted using a back-pressure regulator. Temperature control is provided by a temperature controller connected to a solenoid valve that controls the flow of cooling/heating water through a heat exchanger. Permeate samples are collected from the individual sampling ports located in the permeate line of each cross-flow cell and feed samples can be collected from the drainage valve situated before the pump.

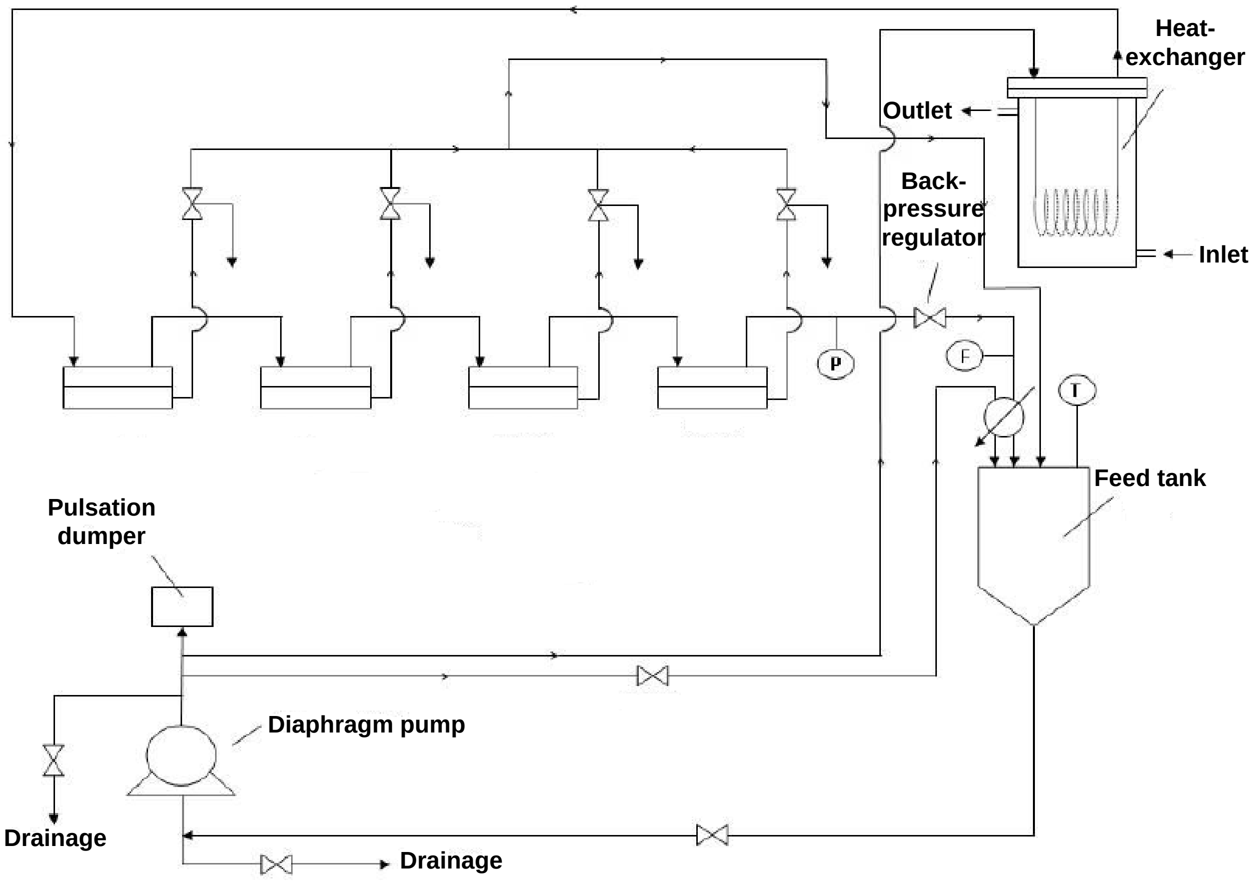

Figure 2.1 Process diagram of the cross-flow cell rig used for membrane screening tests (F: Flow meter; P: Pressure gauge; T: Temperature thermocouple).

2.3.2. Experimental set-ups

2.3.2.1. Membrane cells

All the systems used in this work were set up using membrane cells like the one schematized in Figure 2.2. Each custom made cell, made of stainless steel, have a liquid capacity of 92 mL, and hold circular flat sheet membranes with an effective area of 51 cm^2. These cells operate in a bottom-to-top permeation mode, and contain a magnetic stirrer in the feed/retentate chamber (see Figure 2.2-a). Six ports surround the bottom section of the cells (see Figure 2.2-b). These were used as inlet (feed) and outlet (retentate and permeate) ports and to connect a pressure gauge for pressure monitoring. The retentate port was also connected to a pressure release valve that allowed to control the pressure within the system. A safety pressure relief valve was also connected to one of the ports. In the case of the closed-loop process, only the first cell was equipped with this safety valve. All the ports not in use were maintained tapped.

The two cells used were individually tested for leaks by filtrating a solution of three different styere oligomers (PS580 (MW=580 g mol^{-1}), PS1300 (MW=1300 g mol^{-1}) and α-methylstyrene dimer (MW=236 g mol^{-1})) in MeCN using DM150 (MWCO=150). Permeate samples were analyzed by HPLC and showed no traces of PS, confirming that the cells were well sealed and ready to be used.

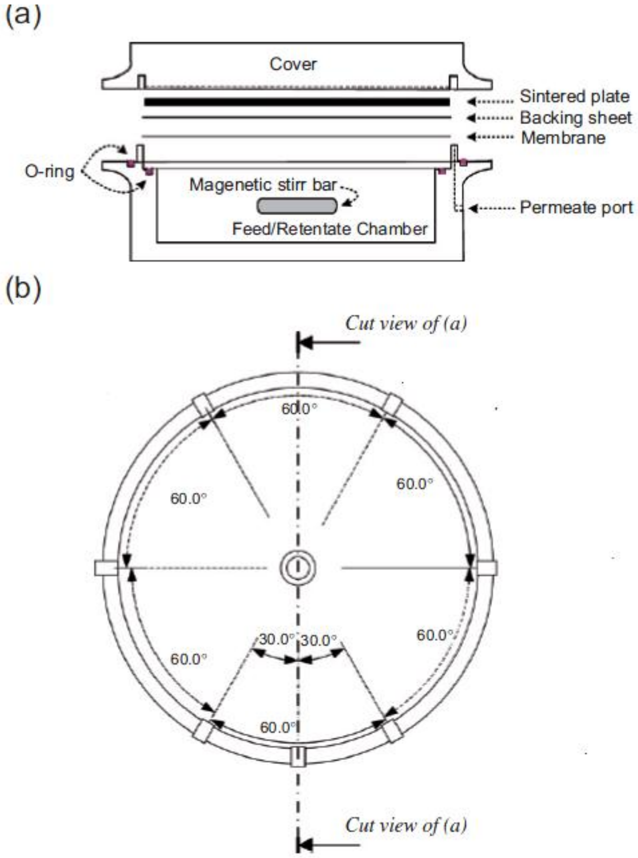
(a)
Cover
Sintered plate
Backing sheet
Membrane
O-ring
Magenetic stirr bar
Feed/Retentate Chamber
Permeate port
(b)
Cut view of (a)
60.0°
60.0°
60.0°
60.0°
60.0°
30.0°
30.0°
60.0°
Cut view of (a)

Figure 2.2 Schematics of the (a) front and (b) top views of the custom-made membrane cells used for the experimental set-ups of this work. Adapted from (Lin & Livingston, 2007)**.**

2.3.2.2. Single membrane system

Single membrane purifications were performed using a system like the one illustrated in Figure 2.3. This system consists of a feed tank and a single membrane cell. It operates in continuous or constant volume diafiltration mode: fresh solvent is added to the feed tank at the same rate as permeate comes out the membrane cell, so the system volume is always constant. Both feed tank and membrane cell are stirred using magnetic stirrers to maintain homogeneity along the system and avoid osmotic pressure build up and concentration polarization effects in the membrane unit. The temperature in the feed tank is monitored using a temperature controller EKT Hein-Con (Heidolph). Circulation is provided by a Gilson 305 HPLC pump able to provide feed flow rates up to 50 mL/min. To have control over the transmebrane pressure within a certain range, the pump flow rate must be higher than the permeate flow rate at the maximum pressure of the chosen range.

Before each new diafiltration the system was always washed with pure solvent to wash away membrane preservatives and any remaining impurities from the previous filtrations. During washing both permeate and retentate were collected in a separated tank and then discarded.

During experiments, samples were taken from feed (F), retentate (R) and permeate (P). Samples were analyzed by UV-Vis Spectroscopy or HPLC.

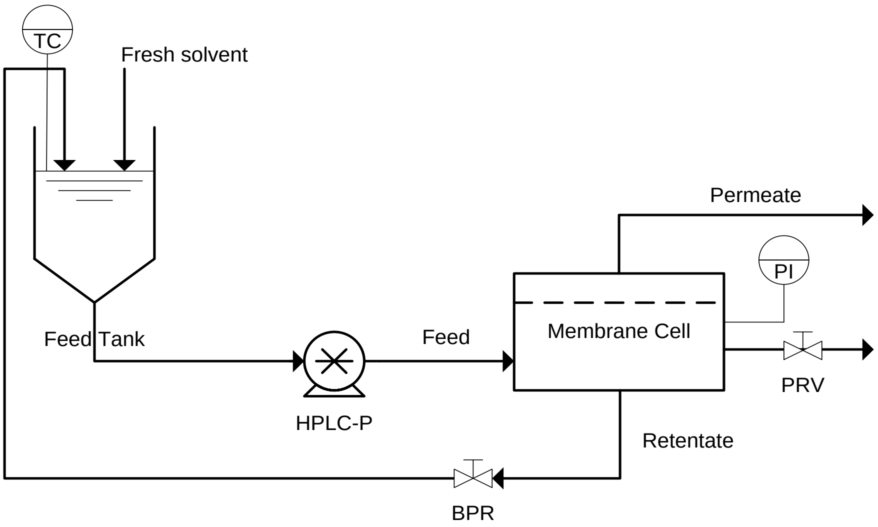

Figure 2.3 Process diagram of the single membrane system (HPLC-P: HPLC pump; BPR: Back pressure regulator; PRV: Pressure relief valve; PI: Pressure gauge; TC: Temperature controller).

2.3.2.3. Closed-loop membrane system

The process diagram of the closed-loop system is presented in Figure 2.3. It consists of a feed tank and two membrane cells connected in series. It also operates in continuous diafiltration mode but since BPR2 is closed (only opened for collecting samples) and permeate 2 is re-circulated back to the feed tank, no addition of fresh solvent is required to maintain the system volume constant. Feed tank and both membrane cells are stirred using magnetic stirrers to maintain homogeneity along the system and avoid osmotic pressure build up and concentration polarization effects in the membrane units. The temperature in the feed tank is monitored using a temperature controller EKT Hein-Con (Heidolph). Circulation is provided by a Gilson 305 HPLC pump able to provide feed flow rates up to 50 mL/min.

When two membrane cells are connected in series, the transmembrane pressure across each membrane is set by itself so the flux out the second membrane equals the flux out the first membrane.

Before each new filtration the system was always washed to remove membrane preservatives and any remaining impurities from the previous filtrations. During washing retentate 1, retentate 2 and permeate 2 were collected in a separated tank and then discarded.

During experiments, samples were taken from feed, retentate 1, retentate 2 and permeate 2. Due to the configuration of the system it was not possible to collected samples from permeate 1. Samples were analyzed by UV-Vis Spectroscopy or HPLC.

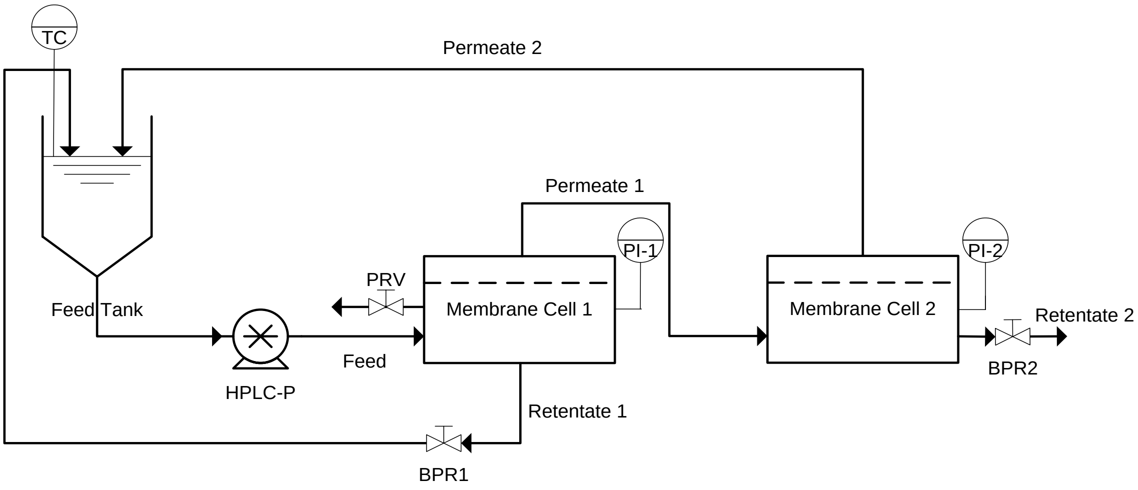

Figure 2.4 Process diagram of the closed loop system. (HPLC-P: HPLC pump; BPR: Back pressure regulator; PRV: Pressure relief valve; PI: Pressure gauge; TC: Temperature controller).

Since it was not possible to analyze permeate 1, the rejections of the first membrane were calculated from another equation, derived from the mass balance over the membrane cell 2 (see Appendix C):

$$R_{i,1}=1-\frac{V_{R2}\frac{dC_{R2,i}}{dt}+J.A.C_{R2,i}.(1-R_{i,2})}{J.A.C_{R1,i}} \qquad \text{2-3}$$

where $R_{i,1}$ and $R_{i,2}$ are the rejections of species i for membrane 1 and 2, respectively, V_{R2} is the volume of membrane cell 2, and $C_{R1,i}$ and $C_{R2,i}$ are, respectively, the concentrations of species i in the retentate of membrane cells 1 and 2.

2.4. ANALYTICAL METHODS

2.4.1. UV/Vis Spectroscopy

Model mixtures A and B were analyzed using a 1800 Shimadzu UV spectrophotometer. Experimental rejections and mass/yield and purity profiles were determined based on the absorbance at λ_{max} of the product (SY7/MY) and impurity (BBR). Samples were diluted so the absorbances were always between 0 and 2.

2.4.2. High Pressure Liquid Chromatography (HPLC)

Model mixtures C and D and the mixture from the oligonucleotide synthesis step were analyzed by Agilent 1100 Series HPLC system coupled to an UV detector at 260 nm and an ELSD (Evaporative Light Scatering Detector, Varian 385-LC). The column used was a reversed-ACE C18 RP column, which temperature was set at 30°C. Two different solvents were used as mobile phase: solvent A was MeOH and solvent B was a 0.1 M ammonium acetate aqueous solution (pH =6.5). The initial mobile phase was 50% of solvent B over 2 minutes and a linear gradient changed the mobile phase to 5% solvent B over 23 minutes. The 5% solvent B mobile phase was held for 15 minutes before returning to the initial 50% solvent. The 50% solvent B was held for more 2 minutes. Calibration curves were obtained for each compound of Model mixture C using the UV signal, as the UV detector was more sensitive to BBR (see Appendix A).

It was decided to analyze model mixture C using HPLC because it was found that the absorbance of MY and BBR was dependent on the temperature (see Appendix B) and it was not possible to have control over the temperature at which samples were analyzed by using the UV/Vis spectrophotometer.

2.5. PROCESS MODELING

Mathematical models were developed and implemented into MATLAB® to calculate the concentration profiles of each solute in the system, and help understanding the process. The models are based on mass balances at steady state. See Appendix C for more details.

The mass profiles for each species were obtained from the concentration profiles predicted by the models and normalized for the initial mass in the feed, $m_{F0,i}$. The normalized mass profiles $(m_i/m_{F0,i})$ were then plotted as a function of the number of diafiltration volumes, N, which is defined as

$$N=\frac{V_p}{V_T}=\frac{J.A.t}{V_T} \qquad 2\text{-}4$$

where V_T is the total volume of solvent in the system.

Chapter 3

Closed-loop membrane process

The process proposed in this work is illustrated in Figure 3.1. This process combines two membrane stages, one for purification and another for solvent recovery. In the first stage the higher MW compound is separated from the lower MW compound using membrane 1. In the second stage the lower MW compound is retained using membrane 2, while the permeating solvent is recycled back to the purification stage. Like this there is no need of adding fresh solvent to the system.

The flow is supplied using only a single pump and the pressure is regulated using a back pressure regulator in the downstream of the purification stage. The retentate from the first membrane cell is also recycled and each component of the system is stirred vigorously to guarantee that the compounds are well mixed and minimize any adverse concentration polarization effects inside the membrane cells. Furthermore, this system operates in a self-regulating manner, so no external control is required once the process starts.

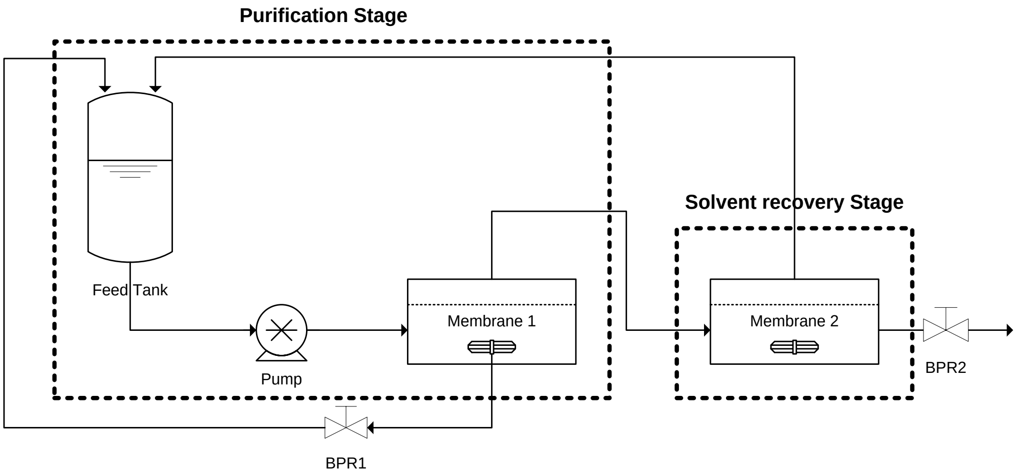

Figure 3.1 Schematic diagram of the closed-loop membrane process.

The feasibility of the closed-loop membrane process for the purification of APIs will be demonstrated in this chapter, which is divided in three sections, each one dedicated to the presentation and discussion of the results obtained with a different model mixture of dyes, used to mimic actual API synthesis separation challenges.

3.1. MODEL MIXTURE A

3.1.1. Experimental

3.1.1.1. Membrane screening

To identify a suitable membrane for the solvent recovery stage, four types of tight membranes were tested: DM150, PBI24xDBB, TFC-MPD and 4P123. Two discs of each membrane were loaded onto a 8-cross-flow cell rig like the one described in sub-section 2.3.1. The system was first washed with 1.5 L of DMF at 20 bar and 25 °C for 1h. After washing, the system was drained and reloaded with 1.5 L of a solution containing 5 g.L-^{1} of SY7 and 0.5 g.L^{-1} of BBR. The screening test was carried out at 30 bar and 25 °C for 2 h. Samples were taken from the feed and each permeate line after 30 min and 2 h of operation and then analyzed by UV-Vis spectroscopy.

3.1.1.2. Purification using the single membrane system

The system described in sub-section 2.3.2.2 was used to diafilter model mixture A. A disc of PI2411, the membrane selected for purification, was loaded onto the cell and washed with pure DMF at 10 bar for 2h. During washing the pump flow rate was set at 2 mL.min^{-1}. After washing the system the solvent feed tank was replaced by a flask containing 250 mL of a SY7 (10 g.L^{-1}) and BBR (1 g.L^{-1}) solution. The aim was to recover more than 90% of SY7 with purity higher than 99%. For this the diafiltration was carried out at 30 bar and 22 °C for 8 diafiltration volumes. During diafiltration the pump flow rate was maintained at 5 mL.min^{-1}.

The yield of product, $\mathrm{Y_p}$, and purity of product, $\mathrm{P_p}$, were calculated from equations 3-1 and 3-2 and plotted as a function of N.

$$\mathrm{Y_p=\frac{m_{F0,SY7}\text{-}(m_{F,SY7}+m_{R,SY7})}{m_{F0,SY7}}\times 100} \tag{3-1}$$

$$\mathrm{P_p=\frac{m_{P,SY7}}{m_{P,SY7}+m_{P,BBR}}\times 100} \tag{3-2}$$

A trapezoidal rule was used to estimate the mass of solute that permeated through the membrane, $\mathrm{m_{P,i}}$, in a time interval, $\Delta\mathrm{t}$:

$$\mathrm{m_{P,i}=J.A.(C_{P,i,t\text{-}1}+C_{P,i,t}).\frac{\Delta t}{2}} \tag{3-3}$$

3.1.1.3. Purification using the closed-loop membrane system

Two diafiltrations were performed over model mixture A using the system described in sub-section 2.3.2.3. A PI2411 disc was used for purification in both diafiltrations. A different membrane for solvent recovery was used in each diafiltration. A TFC-MPD disc was used first.

Then, in a second try, this disc was replaced by a DM150 disc. Between diafiltrations the PI2411 membrane was washed using pure solvent.

After loading the membranes, the system was washed with pure DMF at 10 bar and 22 °C for 2h. During washing the pump flow rate was set at 5 mL.min^{-1}. After washing the system the solvent feed tank was replaced by a flask containing 100 mL of a SY7 (5 g.L^{-1}) and BBR (0.5 g.L^{-1}) solution. The first diafiltration (using the PI2411/TFC-MPD membrane set) ran for 13 diafiltration volumes while the second (using the PI2411/DM150 membrane set) ran for 10 volumes. During these diafiltrations the pump flow rate was always maintained at 5 mL.min^{-1}.

The yield of product, $\mathrm{Y_p}$, and purity of product, $\mathrm{P_p}$, were calculated from equations 3-4 and 3-5 and plotted as a function of N.

$$\mathrm{Y_p}=\frac{\mathrm{m_{F0,SY7}}-(\mathrm{m_{F,SY7}}+\mathrm{m_{R1,SY7}})}{\mathrm{m_{F0,SY7}}}\times 100 \qquad \mathbf{3\text{-}4}$$

$$\mathrm{P_p}=\frac{\mathrm{m_{R2,SY7}}}{\mathrm{m_{R2,SY7}}+\mathrm{m_{R2,BBR}}}\times 100 \qquad \mathbf{3\text{-}5}$$

To achieve the desired yield with the PI2411/TFC-MPD and PI2411/DM150 sets it was necessary to disconnect the cells after 13 and 10 volumes, respectively, and continue the diafiltrations using only the first membrane unit. From this point the systems were operated like described in sub-section 2.3.2.2 for further 9 and 12 volumes, respectively. The yield and purity were calculated considering the yield and purity achieved while the cells were still connected and using equations 3-1 and 3-2.

3.1.2. Results & Discussion

3.1.2.1. Membrane screening

Before applying the proposed process it was necessary to find a pair of membranes: one for purification and another for solvent recovery. Since the aim of the purification stage is to separate the high MW impurity (BBR), from the product (SY7) the ideal membrane should completely retain the impurity ($\mathrm{R_{BBR}}=100\%$) whilst allowing product to freely pass through ($\mathrm{R_{SY7}}=0\%$). On the other hand, in order to recover the process solvent from the permeate coming out the purification stage and reuse this solvent for further purification, the ideal is to find a really tight membrane, able to completely retain the product ($\mathrm{R_{SY7}}=100\%$). In addition to the rejection requirements, a high permeability is desirable in both situations, as this allow to speed up the process and operate at lower transmembrane pressures.

From the literature it was known that PI2411 had a MWCO around 200 (See Toh, Silva & Livingston, 2008), so it was decided to use this membrane for the purification of model mixture A without screening any membranes.

The screening results performed in order to find a membrane for the solvent recovery stage of the closed-loop membrane process are all presented in Table 3.1.

Table 3.1 Summary of the screening results for 14 cm^2 membrane discs using model mixture A (Mix A).

	J (L.m^{-2}.h^{-1}) [B (L.m^{-2}.h^{-1}.bar^{-1})]			R_i (%)			
Membrane	**DMF 1h**[a]	**Mix A 30 min**[b]	**Mix A 2h**[b]	**BBR 30 min**	**SY7 30 min**	**BBR 2h**	**SY7 2h**
DM150-A	4.0 [0.40]	9.3 [0.31]	8.6 [0.29]	98.7	93.4	97.9	94.2
DM150-B	3.4 [0.34]	7.9 [0.26]	7.4 [0.25]	99.0	94.1	99.3	93.1
PBI24xDBB-A	4.3 [0.43]	2.3 [0.08]	2.0 [0.07]	100.0	84.7	100.0	36.5
PBI24xDBB-B	3.7 [0.37]	2.1 [0.07]	1.8 [0.06]	100.0	88.8	100.0	97.8
TFCMPD-A	64.3 [6.43]	96.4 [3.21]	87.9 [2.93]	98.6	87.2	99.3	85.7
TFCMPD-B	51.4 [5.14]	72.9 [2.43]	68.6 [2.29]	100.0	89.1	99.0	82.1
4P1231-A	2.8 [0.28]	3.7 [0.12]	3.7 [0.12]	99.0	95.6	93.1	68.9
4P1231-B	3.1 [0.31]	4.3 [0.14]	4.3 [0.14]	98.8	91.1	97.3	57.8

[a] Fluxes and permeabilities measured at 20 bar and 25°C
[b] Fluxes and permeabilities measured at 30 bar and 25°C

As it can be seen from Table 3.1, PEEK membrane (4P1231) seemed to be the most promising membrane in the beginning, since it presented the highest rejection for SY7 after 30 minutes of operation. However, after 2 h the SY7 rejection of both membrane discs were already too little for the solvent recovery purpose.

One of the PBI discs (PBI 24xDBB-A) also suffered a huge drop in SY7 rejection. In a recent conference, I.B. Valtcheva (Valtcheva et al., 2012) attributed the loss of rejection of DBB crosslinked PBI membranes in DMF to interactions between the crosslinker and the solvent, which may also explain the observed drop in the rejection.

DM150 membrane presented the highest rejections and the most consistent performance over time. However, TFC-MPD presented the highest flux of all the membranes tested and at the same time a relative high rejection for SY7 (80-90%). Therefore it was decided to try both membranes on the solvent recovery stage.

The main purpose of the process proposed in this work is to minimize the amount of solvent required by a continuous diafiltration process to achieve a certain product yield and purity. To quantify the amount of solvent saved by using the closed-loop process, model mixture A was first diafiltered in the conventional way by using the single membrane process. This diafiltration was performed using the membrane selected for the purification stage, the PI2411 membrane. The results for this diafiltration will be presented and discussed in the next sub-section.

3.1.2.2. Purification using the single membrane process with PI2411 membrane

Table 3.2 Summary of the data recorded during the diafiltration of model mixture A using the single membrane process with a PI2411 membrane disc.

N	ΔP (bar)	J ($L.m^{-2}.h^{-1}$)[a] [B ($L.m^{-2}.h^{-1}.bar^{-1}$)]	R_{SY7} (%)	R_{BBR} (%)
DMF	31	24.71 [0.79]	-	-
0	30	8.2 [0.27]	-	-
1	30	7.9	32	100
2	30	7.6	45	100
3	30	6.3	34	100
4	30	5.2	53	100
5	30	6.4	53	100
6	30	4.2	41	100
7	30	4.0	24	100
8	30	3.7 [0.12]	35	100
			40 ± 10	100

[a] Fluxes and permeabilities measured at 22 °C.

[b] Permeability determined by plotting J_{DMF} vs. ΔP: $J_{DMF}=0.79.\Delta P$, $R^2=0.9998$

The permeate fluxes and rejections of SY7 and BBR are summarized in Table 3.2. It can be seen that the permeate permeability was, from the beginning, smaller than the pure solvent permeability. This difference was already observed by many authors for different solute-solvent systems (Peeva et al., 2004, Gibbins et al., 2002, Yang, Livingston & Freitas dos Santos, 2001, Whu, Baltzis & Sirkar, 2000), and can have several causes, such as osmotic pressure, concentration polarization or hindered diffusion within the pores. Another fact is that the permeate flux dropped along the diafiltration process. This could be attributed to membrane compaction. However, membrane compaction is normally accompanied by an increase in the rejection which was not observed. Thus, it is more likely that the flux continued to drop due to fouling effects, like membrane adsorption or pore blocking (Whu, Baltzis & Sirkar, 2000).

As it can be seen from Figure 3.2, the color of permeate varied only from dark yellow to light yellow, which confirms that no BBR permeated through the membrane and consequently that the rejection of PI2411 for BBR maintained constant and equal to 100% during this diafiltration.

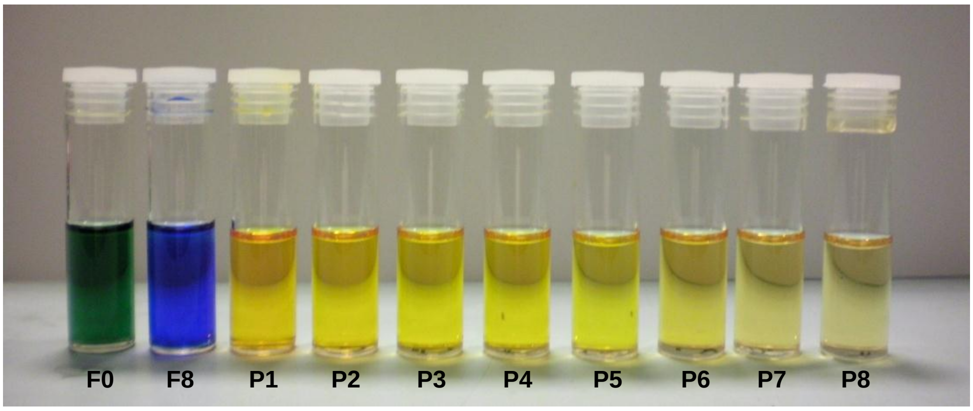

Figure 3.2 Photograph of the feed solution at the beginning (F0, 40 times diluted) and after 8 diafiltration volumes (F8, 8 times diluted) and of the permeate samples at each diafiltration volume (P1-P8, without dilution).

Figure 3.3 presents the experimental and calculated mass profiles for SY7. The calculated mass profiles for BBR are also shown but not the experimental data. What happened was that some of the samples from the feed and retentate, which when collected were green or blue, became orange or yellow after being left in the benchtop for a weekend. Other samples turned reddish when were being diluted for UV/Vis spectroscopy analysis. After this, the expected peak at 600 nm in the absorption spectra was either vanished or shifted to the blue region of the visible spectrum with loss of intensity. Thus it was not possible to have a reliable measurement of BBR concentrations in the feed and membrane cell and that is why no experimental mass profiles are shown for this compound.

It was also observed that samples of BBR in DMF turned reddish and then colorless, even if capped, when left in the benchtop for one or two days. It is known that the color of BBR depends on the acidity of the solution, being red or green under extremely acidic conditions, blue when the medium is slightly acidic or neutral, or pink under alkaline conditions (Carl Roth, 2012). However, this does not explain the complete loss of color or loss of absorbance intensity. It was then hypothesized that BBR was being degraded by air and/or light. However, the literature only reported the degradation/discoloration of BBR and some azo dyes by UV light in the presence of hydrogen peroxide (H_2O_2) (Rauf, Ashraf & Alhadrami, 2005, Malik & Sanyal, 2004). It was then found that H_2O_2 could be generated during the degradation of DMF under aerobic conditions and that the amount of H_2O_2 could be enhanced by exposure to solar light.

The flask used to keep DMF was sometimes negligently left opened on the benchtop. This could have contributed to DMF degradation and consequently to BBR discoloration. However, further studies would be necessary to understand what was actually promoting this phenomenon.

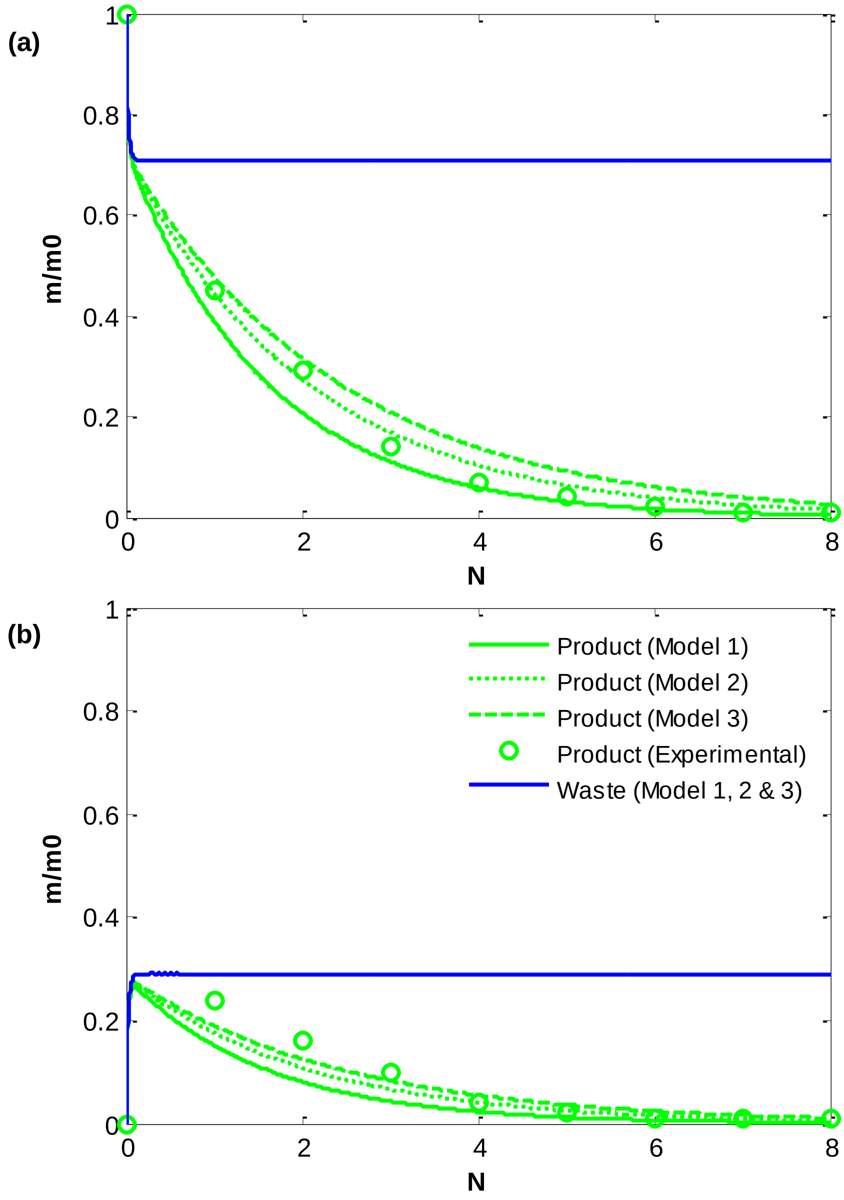

Figure 3.3 Calculated and experimental mass profiles of product (SY7) and waste (BBR) in (a) feed tank and (b) membrane cell for the purification of model mixture A using single membrane process with a PI2411 membrane disc at 30 bar and 22 °C. Curve fitting was done by assigning different values to R_{SY7}: Model 1-R_{SY7}=40.0%/R_{BBR}=100.0%, Model 2-R_{SY7}=52.0% /R_{BBR}=100.0%; Model 3- R_{SY7}=61.0%/R_{BBR}=100.0%.

As it can be seen from Figure 3.3, the experimental mass profiles for SY7 follow the trend predicted by the models. They are even in good agreement with Model 1 for the last 5 volumes. However this model, that considers an average of the calculated rejections (40 ± 10 %), seems to somehow underestimate the mass profiles, which means that the rejection for SY7 was underestimated. This fact has two possible explanations, one based on the concentration polarization effect on the membrane surface and the other based on the relative affinity of the mixture components to the membrane. Because of concentration polarization the solute concentration increases at the membrane surface. Thus the observed rejections can be underestimated since they are calculated from the bulk retentate concentrations (Mulder, 1996). On the other hand, when the solute has a higher affinity for the membrane material than the solvent, the observed rejections can also be considerably lower (Bhanushali, Kloos & Bhattacharyya, 2002). This is a limitation of the rejection calculation, since it is referenced against a certain solvent background (White, 2002). The intense yellow (almost orange) color exhibited by the permeate samples in the beginning of the diafiltration process (see Figure 3.2), supports this last argument.

Due to the referred inconsistencies, an attempt was made to completely fit the predicted curves to the experimental results by adjusting the SY7 rejection value (Model 2 and Model 3). To have a better fitting it was necessary to assume a rejection higher than the average of the measured values. This fact is in accordance with what was stated before. However, it was not possible to find a rejection value that gave simultaneously a good fitting in the feed and membrane cell profiles.

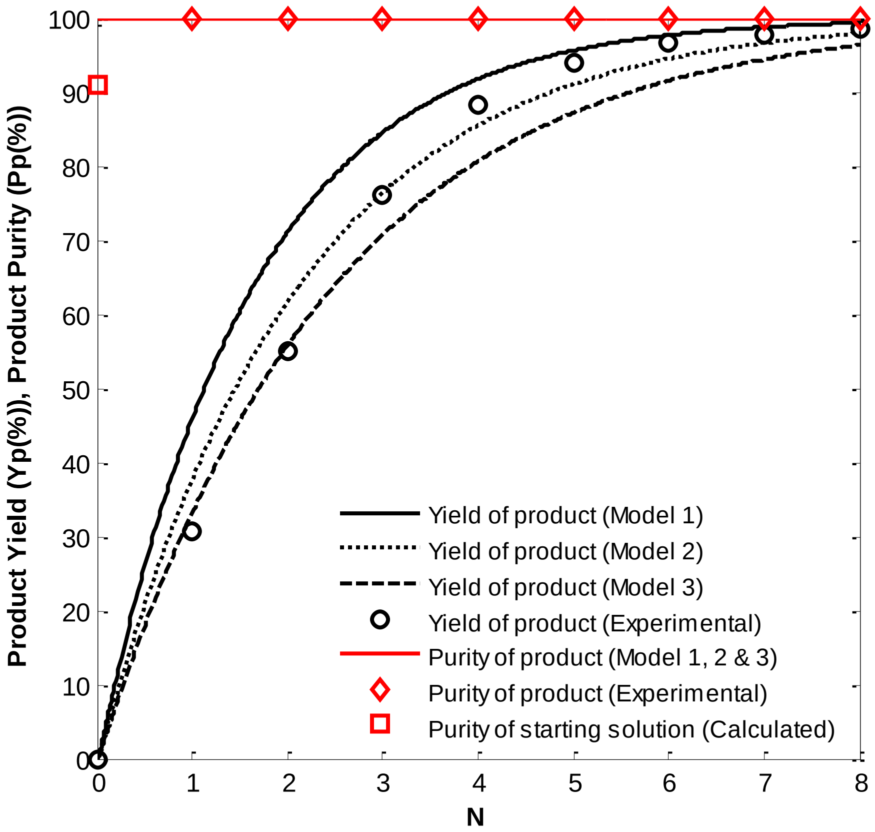

Figure 3.4 Yield and purity profiles for the purification of model mixture A using single membrane process with a PI2411 membrane disc at 30 bar and 22 °C. Curve fitting was done by assigning different values to R_{SY7}: Model 1-R_{SY7}=40.0%/R_{BBR}=100.0%, Model 2-R_{SY7}=52.0%/R_{BBR}=100.0%; Model 3- R_{SY7}=61.0%/R_{BBR}=100.0%.

The yield and purity profiles are presented in Figure 3.4. As for the mass profiles, the experimental data for the yield follows the predicted trend but is not in complete agreement with the calculated curve (Model 1). It can be observed that the model that better fits the experimental yield is the model that best describes the mass profile in the feed tank – Model 2.

The experimental yield and purity profiles show that 98% of the product, with a purity of 100%, was recovered after 8 volumes from a starting solution with a purity of 91%. PI2411 membrane allowed to surpass the target yield and purity, but at the expense of using 2.7 L of pure DMF. In the next sub-sections it will be shown how much solvent it is possible to save by using he closed-loop membrane process. The first results to be presented are the ones obtained for the system that combines PI2411 and DM150 membranes.

3.1.2.3. Purification using the closed-loop membrane process with PI2411 membrane for purification and DM150 membrane for solvent recovery

After starting the process and waiting for the pressure to build up in the cells, no permeate was coming out of the second membrane unit. In order to understand what was happening, the pump was stopped and the second cell opened. It was then realized that the outer O-ring was damaged and allowing the permeate to leak around the cell. To prevent further leaks and continue on with the process, the outer O-ring was replaced, the cell was closed and the pump restarted.

The permeate fluxes and rejection of both membranes for SY7 and BBR are summarized in Table 3.3. As it can be seen the flux was very slow. This was due to the low permeability of DM150 membrane. It was necessary to have a transmebrane pressure higher than 30 bar in the second membrane unit and only of 2 bar in the first cell to have a flux of about 4 $L.m^{-2}.h^{-1}$.

The average rejection of PI2411 for SY7 (Table 3.3: 83 ± 3% at 2 bar) is very different from the average rejection obtained for the diafiltration using the single membrane process with the same membrane (Table 3.2: 40 ± 10% at 30 bar). Rejection is commonly a big function of pressure, and usually higher rejections are obtained at higher pressures (Bhanushali, Kloos & Bhattacharyya, 2002, Gibbins et al., 2002, Whu, Baltzis & Sirkar, 2000). However, this time a higher rejection was obtained at a lower pressure. Thus, these differences could be due to the lack of uniformity of this self-prepared membrane. On the other hand, and as expected from the previous experiments, BBR continued to be completely rejected by the PI2411 membrane. DM150 revealed a rejection for SY7 (Table 3.3: 95 ± 3%) pretty much consistent with the average rejection expected from the screening test (Table 3.1: 94 ± 1%), probably because this is a commercial membrane.

Table 3.3 Summary of the data recorded along the diafiltration of model mixture A using the closed-loop membrane process with a PI2411 membrane disc for purification and a DM150 membrane disc for solvent recovery.

				PI2411		DM150
N	**ΔP_1 (bar)**	**ΔP_2 (bar)**	**J ($L.m^{-2}.h^{-1}$)[a] [B ($L.m^{-2}.h^{-1}.bar^{-1}$)]**	**$R_{SY7,1}$ (%)**	**$R_{BBR,1}$ (%)**	**$R_{SY7,2}$ (%)**
DMF	11	-	27.65/- [2.43[b]/-]	-	-	-
0.07	2	33	3.76 [1.88/0.11]	-	100	-
1.21	2	33	4.35	-	100	89.3
1.29	2	31	4.12	84.0	100	94.6
1.36	2	32	4.00	84.4	100	95.4
1.44	2	31	4.00	87.6	100	96.9
1.52	2	32	5.41	82.6	100	96.3
1.60	2	32	4.24	84.8	100	96.9
1.75	2	32	4.24	78.6	100	95.9
1.95	2	34	4.41	80.4	100	96.4
2.08	3	33	4.24 [1.41/0.13]	-	100	-
				83 ± 3	100.0	95 ± 3

[a] Fluxes and permeabilities measured at 22°C
[b] Permeability determined by plotting J_{DMF} vs. ΔP: $J_{DMF}=2.43.\Delta P$, $R^2=0.9996$

The experimental and calculated mass profiles for SY7 are shown in Figure 3.5. The BBR profiles are not showed because samples from the feed and retentate of the first cell lost again the blue color. Samples were taken only after the O-ring was replaced, so it was assumed that the process only started from this point. At this point the compounds were already distributed in the system; this explains why the mass profile for the feed tank does not start at 1 or at 0 for the membrane cells.

As it can be seen, the data follows once again the trend predicted by the model in all situations. However, it was not possible to fit the curves to the experimental data considering an average of the calculated rejections (Model 1). It was also difficult to find a combination of rejections that allowed to simultaneously fit the curves to the experimental profiles in the feed tank, membrane cell 1 and membrane cell 2. That is why two more models were proposed.

Model 2, which was calculated considering a rejection of 42.5% for PI2411 membrane and 97% for DM150 membrane fits perfectly to the data obtained for the feed and first membrane unit. This might be an indicator that the rejections calculated from the experimental concentrations were overestimated for PI2411 membrane and underestimated for DM150 membrane.

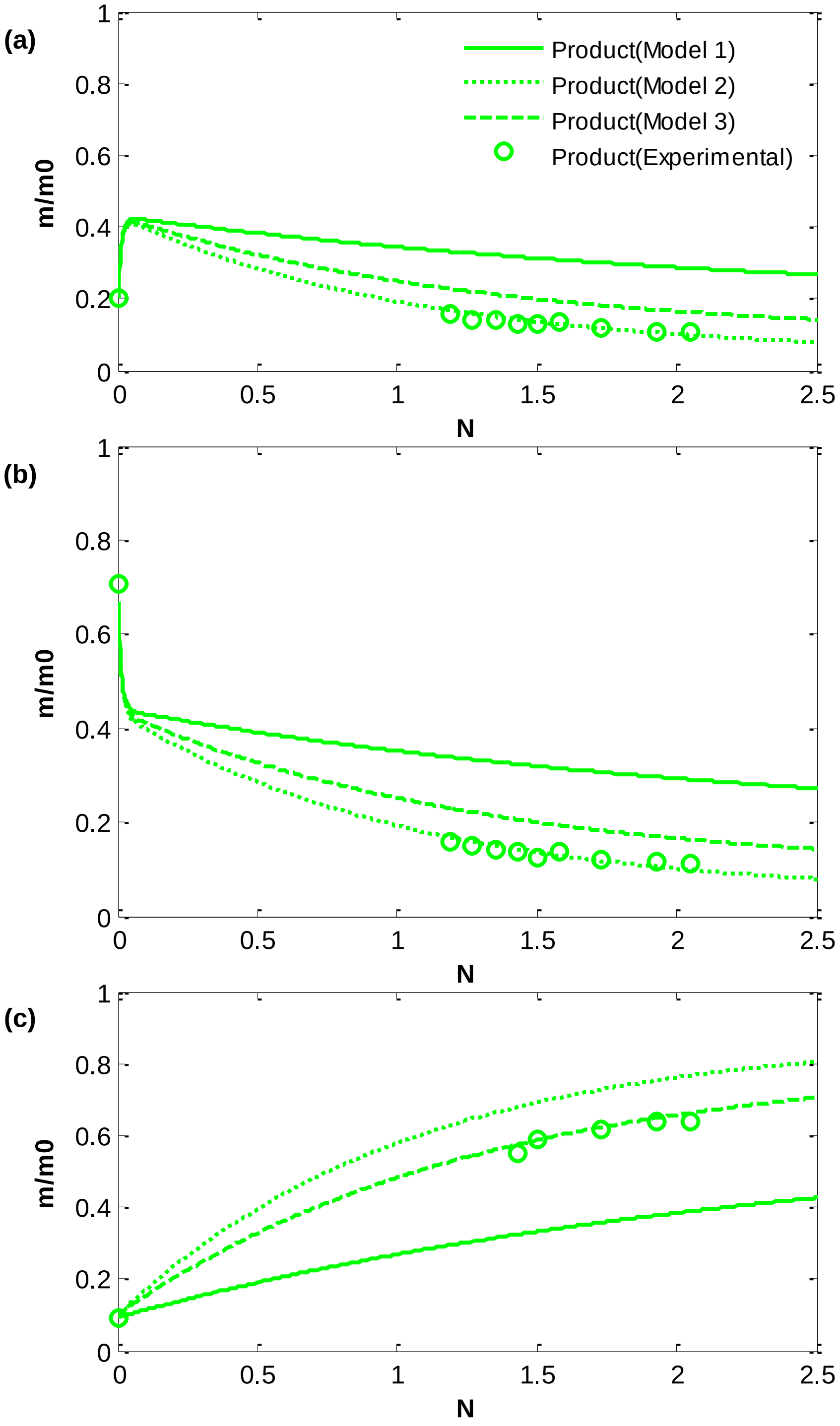

Figure 3.5 Calculated and experimental mass profiles of the product (SY7) and waste (BBR) in (a) feed tank, (b) membrane cell 1 and (c) membrane cell 2 for the purification of model mixture A using the closed-loop membrane process with a PI2411 and a DM150 membrane disc. Curve fitting was done by assigning different values to R_{SY7}: Model 1- $R_{SY7,1}$=83% and $R_{SY7,2}$=95%, Model 2- $R_{SY7,1}$=42.5% and $R_{SY7,2}$=97%, Model 3- $R_{SY7,1}$=59% and $R_{SY7,2}$=95%..

The observed rejections of DM150 membrane for SY7 ($R_{SY7,2}$) could have been underestimated because of concentration polarization effects and/or the different rates of transport of the components through the membrane, reasons already discussed in sub-section 3.1.2.2 However, there is another possible explanation for this particular system. Between the cell port and the back-pressure regulator outlet of the second membrane cell (BPR2), from where samples were taken, there is a dead volume. To be sure that the concentration of the liquid coming out this valve is equal to the concentration in the bulk of the cell it would be necessary to drain that dead volume first and only after collect the sample. This would require return the dead volume, containing purified product, to the system by pouring it into the feed tank, so samples were collected without draining de dead volume. This procedure could have led to an underestimation of SY7 concentrations in the second cell, and consequently to an underestimation of $R_{SY7,2}$.

The observed rejections of SY7 for PI2411 ($R_{SY7,1}$) were calculated using equation 2-3, which depends on $R_{SY7,2}$ and on the concentrations of SY7 in the first and second cells, $C_{R1,SY7}$ and $C_{R2,SY7}$ respectively. Thus, one of the reasons for the overestimation of $R_{SY7,1}$ could be the underestimation $C_{R2,SY7}$, already considered as a possibility.

Since Model 2 seems to overestimate the mass profile in the second membrane cell a third model was proposed: Model 3 was obtained considering that PI2411 and DM150 membranes have, respectively, rejections of 59 and 95% for SY7. However, Model 2 may not fit to the mass profile in membrane cell 2 just because of the underestimation of the concentrations inside this cell.

The same rejections were used in the determination of theoretical yield and purity profiles. From Figure 3.6 one can see that the measured rejections for SY7 (83 ± 3% for PI2411 membrane and 95 ± 3% for DM150 membrane) completely underestimate the yield profile (Model 1). On the other hand, Model 2, that considers that PI2411 membrane has actually a rejection of 42.5%, gives a good fitting to experimental values. This is also the model that best describes the mass profiles in the feed tank and in the first membrane cell.

The yield profile plateaued out before reaches the maximum yield (100%). This happened because DM150 membrane do not completely rejects SY7 allowing it to escape from the solvent recovery stage, where it should accumulate, to the purification stage. This leads the system to reach a kind of steady state, where it is not possible to recover more product than the percentage determined by the plateau. As can be seen, the diafiltration was stopped before the yield attained the plateau at 91% (Model 2). It was decided to stop the process after only 2 volumes because at that point a considerable amount of product had already been recovered and because the diafiltration was taking too long (each volume was taking about 13 h). It worth noting, however, that with this set of membranes it would be technically possible to achieve the desired yield and purity without adding more solvent.

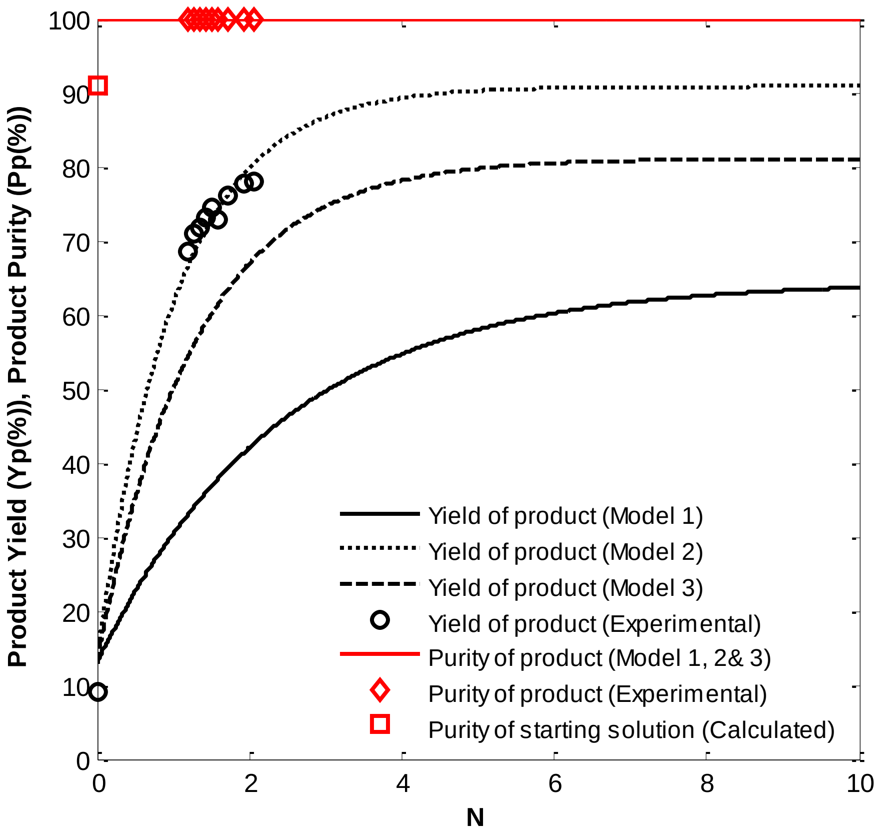

Figure 3.6 Yield and purity profiles for the purification of model mixture A using closed-loop membrane process with a PI2411 and a DM150 membrane discs. Curve fitting was done by assigning different values to R_{SY7}: Model 1- $R_{SY7,1}$=83%/$R_{BBR,1}$=100.0% and $R_{SY7,2}$=95%/$R_{BBR,2}$=100.0%, Model 2- $R_{SY7,1}$=42.5%/$R_{BBR,1}$=100.0% and $R_{SY7,2}$=97%/$R_{BBR,2}$=100.0%, Model 3- $R_{SY7,1}$=59%/$R_{BBR,1}$=100.0% and $R_{SY7,2}$=95%/$R_{BBR,2}$=100.0%..

In order to meet the target and have comparable results with the single membrane process, the second cell was disconnected and the diafiltration has continued using only the first cell. The data for the simple diafiltration using PI2411 membrane after disconnect the cells is shown in Table 3.4. The average rejection of PI2411 membrane for SY7 (Table 3.4: 87 ± 4%) is consistent with the rejections obtained for this membrane when the two cells were connected (Table 3.3: 83 ± 3%). The permeabilities are also in accordance with the last results. The only difference is that this time the permeability was slowly returning to its original value, the permeability of pure DMF (Table 3.3: 2.43 L.m^{-2}.h^{-1}.bar^{-1}), as SY7 was getting washed away.

Table 3.4 Summary of the data recorded along the diafiltration of model mixture A using the single membrane process with a PI2411 membrane disc after disconnected the cells.

N	ΔP_1 (bar)	J ($L.m^{-2}.h^{-1}$)[a] [B ($L.m^{-2}.h^{-1}.bar^{-1}$)]	$R_{SY7,1}$ (%)	$R_{BBR,1}$ (%)
0	30	58.82 [1.96]	-	-
1	30	57.65	82.0	100.0
2	30	55.29	83.8	100.0
3	28	55.29	83.9	100.0
4	28	55.29	86.2	100.0
5	28	55.29	86.5	100.0
6	28	55.29	88.3	100.0
7	27	54.12	88.8	100.0
8	27	54.12	81.1	100.0
9	27	54.12	87.4	100.0
10	28	57.65	89.8	100.0
11	30	61.18	91.9	100.0
12	30	61.18	91.6	100.0
13	28	57.65 [2.06]	92.1	100.0
			87 ± 4	100.0

[a] Fluxes measured at 21°C

The experimental and calculated mass profiles for SY7 are shown in Figure 3.7. The yield and purity profiles are shown in Figure 3.8. This time it was not required to consider other values for the rejection of SY7: the model completely fits the data by considering an average value of the measured rejections. This is not in accordance with the previous experiments where it was necessary to consider a rejection of 42.5% for PI2411 membrane to have a good fitting between the experimental and theoretical curves. However, it is noteworthy that this rejection is in the range of the rejections considered for the single membrane process with PI2411 membrane that were between 40 and 61 % (see Figure 3.3). One of the differences between these two experiments and the diafiltration performed after disconnect the second cell from the closed-loop system is the concentration of SY7 in the system, which is lower for the last case. These facts suggest that the SY7 rejection increased as its concentration in system decreased. This is something rather expected from the solution-diffusion model, since the driving force for the solute gets lower as it gets washed away from the system.

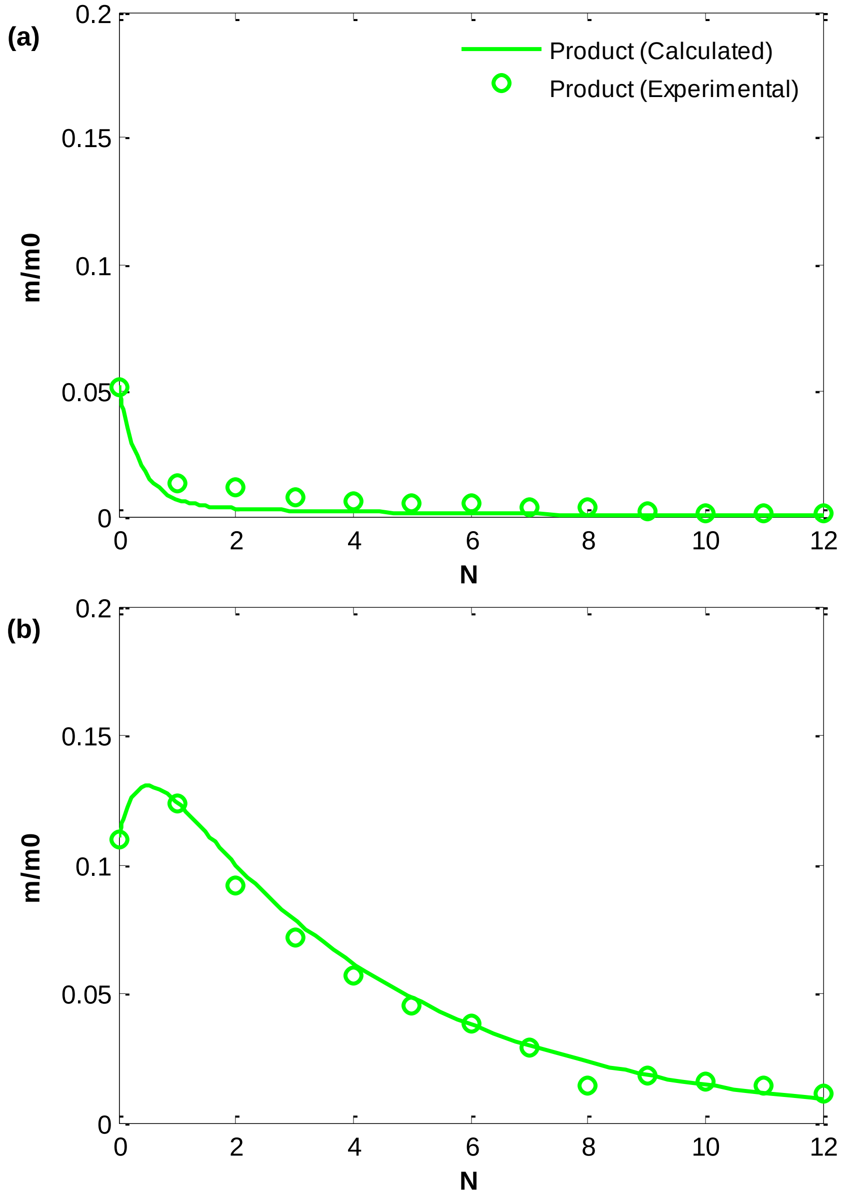

Figure 3.7 Calculated and experimental mass profiles of the product (SY7) and waste (BBR) in (a) feed tank and (b) membrane cell 1 after disconnecting the second cell from the system PI24411/DM150 (R_{SY7}=87%).

From Figure 3.8 one can see that after disconnecting the second cell 12 volumes were required to increase the yield up to 99% whilst the purity of the product maintained at 100%. This required, however, the use of 2.1 L of pure solvent.

To recover 98% of the SY7 initially present in the feed tank, about 9 volumes were required, which in this case was equivalent to 1.7 L of DMF. After comparing this value with the amount of solvent required by the single membrane process using PI2411 membrane to reach the same yield and purity (2.7 L), it can be concluded that 37% of the solvent was saved by applying the closed-loop membrane process to the purification of model mixture A. It should be mentioned, however, that it would be possible to save more solvent with the PI2411/DM150 system if the closed-loop process had run for a couple more volumes. It would actually be possible to achieve the target yield (90%) and purity (>99%) without additional solvent.

In the next sub-section it will be presented and discussed the results for the closed-loop process where the PI2411 membrane is used once again for purification and the TFC-MPD membrane is used on the solvent recovery stage.

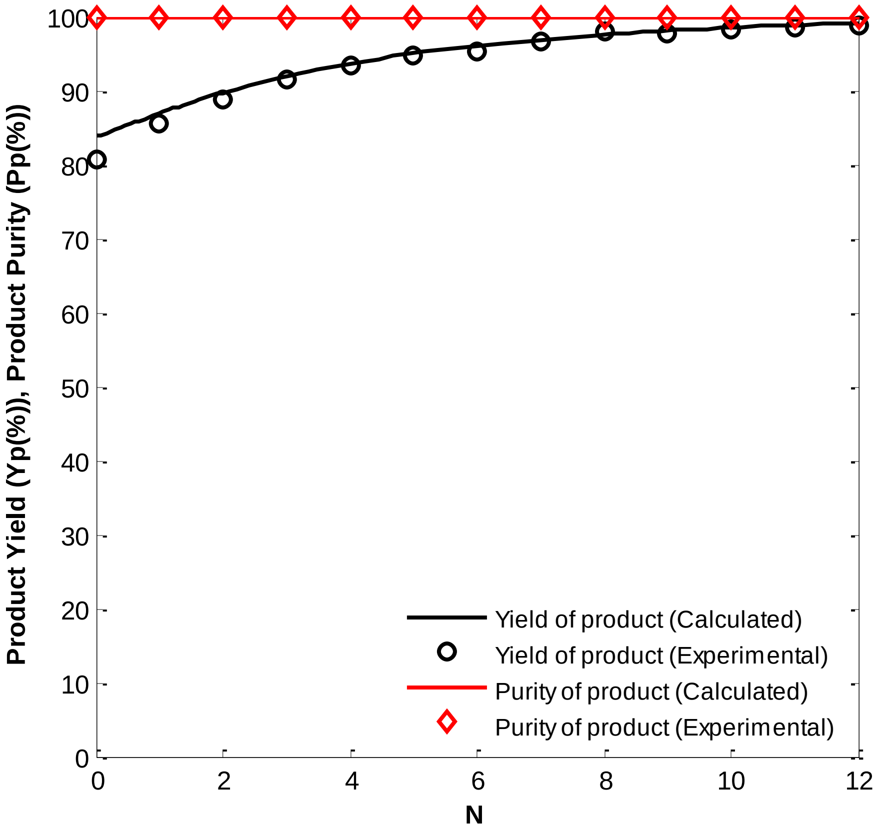

Figure 3.8 Yield and purity profiles for the purification of model mixture A after disconnecting the second cell from the system PI24411/DM150 (R_{SY7}=87%).

3.1.2.4. Purification using the closed-loop membrane process with PI2411 membrane for purification and TFC-MPD membrane for solvent recovery

The permeate fluxes and rejection of both membranes for SY7 and BBR are summarized in Table 3.5. Once again, a big difference between the flux of pure DMF and model mixture A was observed. This time the transmembrane pressure in the first membrane cell (ΔP_1) was higher than the transmembrane pressure in the second cell (ΔP_2) because the PI2411 membrane was less permeable than the TFC-MPD membrane.

Table 3.5 Summary of the data recorded along the diafiltration of model mixture A using the closed-loop process with a PI2411 membrane disc for purification and a TFC-MPD membrane disc for solvent recovery.

N	ΔP_1 (bar)	ΔP_2 (bar)	J ($L.m^{-2}.h^{-1}$)[a] [B ($L.m^{-2}.h^{-1}.bar^{-1}$)]	PI2411		TFC-MPD
				$R_{SY7,1}$ (%)	$R_{BBR,1}$ (%)	$R_{SY7,2}$(%)
DMF	22	20	52.94/62.35 [2.43[b]/2.95[c]]	-	-	-
0.1	17	12	24.71 [1.45/2.06]	-	-	-
0.3	17	12	31.76	97	100	44
0.4	17	12	31.76	95	100	66
0.6	17	12	31.76	94	100	43
0.9	17	12	32.94	88	100	42
1.4	16	13	31.76	80	100	49
2.6	16	13	31.76	78	100	62
3.1	16	13	31.76	76	100	68
4.0	15	12	28.24	76	100	73
4.6	16	13	29.41	81	100	79
5.8	16	13	29.41	77	100	76
12.2	16	13	25.06	79	100	80
15.3	16	13	27.06 [1.69/2.08]	82	100	82
				83 ± 8	100 ± 0	64 ± 15

[a] Fluxes measured at 22°C
[b] Permeability determined by plotting J_{DMF} vs. ΔP: $J_{DMF}=2.43.\Delta P$, $R^2=0.9996$
[c] Permeability determined by plotting J_{DMF} vs. ΔP: $J_{DMF}=2.95.\Delta P$, $R^2=0.9883$

The calculated rejections for SY7 varied considerably during the diafiltration process. Despite this fact the average rejections of PI2411 for this compound (Table 3.5: 83 ± 8%) and for BBR (Table 3.5: 100 ± 0%) are consistent with the values obtained previously (see Table 3.3 and Table 3.4). This result was expected since the same PI2411 membrane disc was used in the previous process. On the other hand, the average rejection of TFC-MPD membrane for SY7 (64 ± 15%) is not in accordance with the screening results, which predicted a rejection between 80 and 90% for this compound. Some differences may be from the variation between the two different discs tested in different systems (crossflow cell rig and closed-loop membrane process).

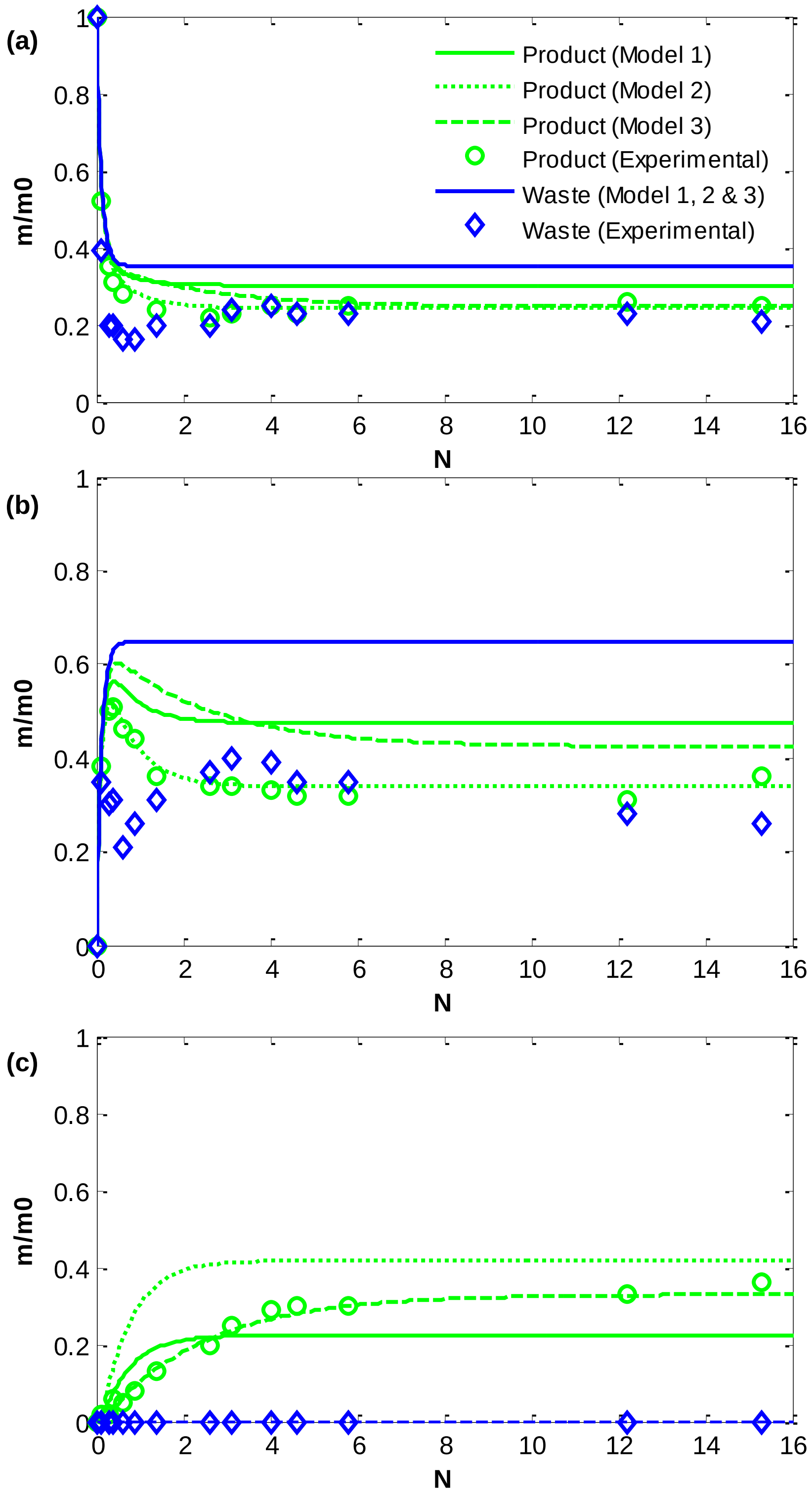

Figure 3.9 **Calculated and experimental mass profiles of the product (SY7) and waste (BBR) in (a) feed tank, (b) membrane cell 1 and (c) membrane cell 2 for the purification of model mixture A using closed-loop membrane process with a PI2411 and a TFC-MPD discs. Curve fitting was done by assigning different values to R_{SY7}: Model 1- $R_{SY7,1}$=83%/$R_{BBR,1}$=100% and $R_{SY7,2}$=64%/$R_{BBR,2}$=100%, Model 2- $R_{SY7,1}$=68%/$R_{BBR,1}$=100% and $R_{SY7,2}$=74%/$R_{BBR,2}$=100%, Model 3- $R_{SY7,1}$=93%/$R_{BBR,1}$=100% and $R_{SY7,2}$=91%/$R_{BBR,2}$=100%..**

The experimental and calculated mass profiles for both SY7 and BBR are shown in Figure 3.9. As it can be seen, the data follows the trend predicted by the model in all situations. However, the same inconsistencies between the experimental and calculated profiles of SY7 for the closed-loop with PI2411 and DM150 were also found for this system. In one hand, it was not possible to fit the curves to the experimental data considering the average of the calculated rejections (Model 1). On the other hand, it was also difficult to find a combination of rejections that allowed to simultaneously fit the curves to the experimental profiles in the feed tank, membrane cell 1 and membrane cell 2. That is why two more models are presented: Model 2, which was calculated considering a rejection of 68% for PI2411 membrane and 74% for TFC-MPD membrane fits perfectly to the data obtained for the feed and first membrane unit; on the other hand, Model 3, which was obtained considering that PI2411 and TFC-MPD membranes have, respectively, rejections of 93 and 91%, fits only to the mass profile on the second membrane unit. As explained before, it is possible that the concentrations in the second membrane unit were underestimated. If so, the experimental mass profile was also underestimated and maybe that is why Model 2 does not fit to this data.

This time all the samples taken during the purification process were maintained capped and were kept in a dark place in order to minimize the contact of the samples with air and light. However, from Figure 3.9 we can see that the experimental data for BBR was underestimated. In effect, BBR maximum absorbance was between 588-599 nm, but never at 600 nm. Plus, the color of the samples from the feed and the retentate of the first cell changed over time to orange or yellow. The precautions taken only helped delaying the loss of blue color and were not sufficient to avoid this problem.

Since the beginning, no traces of BBR were found on the samples from the second membrane cell, which support the measured rejection of PI2411 membrane for this compound. That is why the rejection of BBR was not corrected and only one mass profile is shown for this compound.

From Figure 3.10 one can see that the SY7 average rejections (83 ± 8% for PI2411 membrane and 64 ± 15% for TFC-MPD) underestimate once again the yield profile (Model 1). On the other hand, Model 2 that considers rejections of 68% and 74% for PI2411 and TFC-MPD membranes, respectively, gives a good fitting to experimental values. This is also the model that best describes the mass profiles in the feed tank and in the membrane cell 1.

The experimental purity of the starting solution is a bit higher than the calculated value. This might have to do with the loss of blue color from samples. On the other hand, the experimental purity of product completely matches the calculated purity profile, since no BBR was detected in the second membrane cell.

As predicted by the model, the yield profile plateaued out after some volumes. This happened because, as DM150 membrane, the TFC did not complete rejected SY7. This impeded the system to recover more than ~43% of the product.

Despite the recovered product was 100% pure, the yield was very low and, once again, bellow the target value (90%). Thus, in order to meet the target and have comparable results with the single membrane process, the purification and solvent recovery stages were disconnected and the diafiltration has continued using only the first cell.

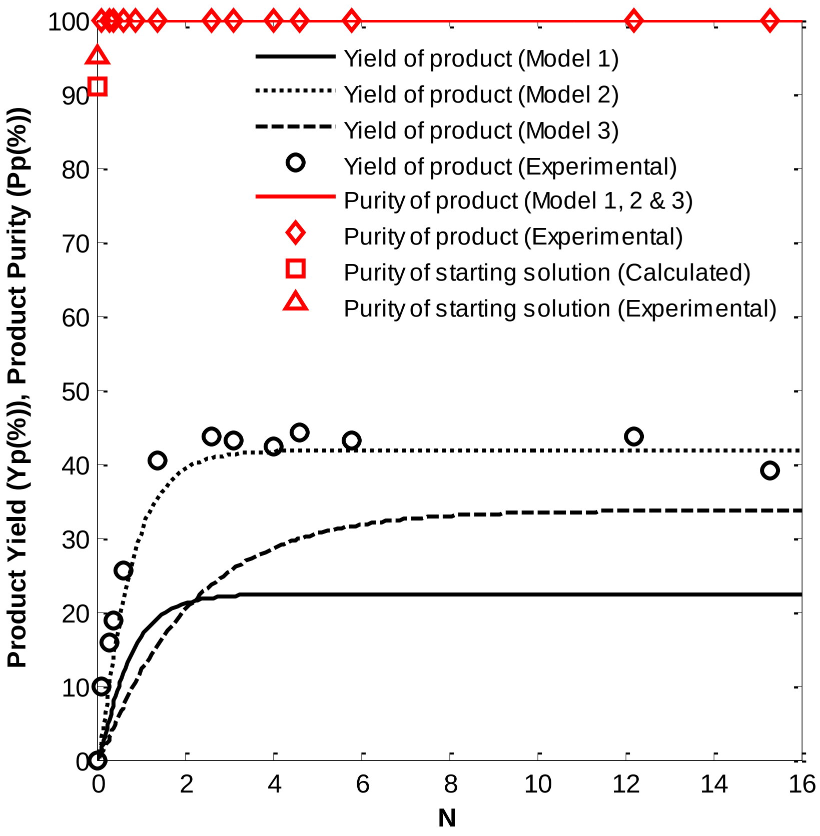

Figure 3.10 Yield and purity profiles for the purification of model mixture A using the closed-loop membrane process with a PI2411 and a TFC-MPD disc Curve fitting was done by assigning different values to R_{SY7}: Model 1- $R_{SY7,1}$=83%/$R_{BBR,1}$=100% and $R_{SY7,2}$=64%/$R_{BBR,2}$=100%, Model 2- $R_{SY7,1}$=68%/$R_{BBR,1}$=100% and $R_{SY7,2}$=74%/$R_{BBR,2}$=100%, Model 3- $R_{SY7,1}$=93%/$R_{BBR,1}$=100% and $R_{SY7,2}$=91%/$R_{BBR,2}$=100%..

The permeate fluxes and rejections of SY7 and BBR for PI2411 membrane after disconnecting the cells are summarized in Table 3.6. The measured flux and rejections are consistent with the values measured during the closed-loop process (compare Table 3.6 and Table 3.5).

Table 3.6 Summary of the data recorded along the diafiltration of model mixture A using the single membrane process with a PI2411 membrane disc after disconnected the cells.

N	ΔP_1 (bar)	J ($L.m^{-2}.h^{-1}$)[a] [B ($L.m^{-2}.h^{-1}.bar^{-1}$)]	$R_{SY7,1}$ (%)	$R_{BBR,1}$ (%)
1	19	37.65 [1.98]	80.6	100.0
2	19	37.65	83.4	100.0
3	19	40.00	83.9	100.0
4	19	40.00	84.4	100.0
5	21	36.47	66.9	100.0
6	20	40.00	86.4	100.0
7	20	40.00	85.0	100.0
8	21	41.18	84.9	100.0
9	21	41.18 [1.96]	83.9	100.0
			82 ± 6	100.0

[a] Fluxes measured at 21°C

Figure 3.11 presents the experimental and calculated mass profiles for SY7 after disconnect the cells. Model 1, that considers an average of the measured rejections, fits well to the experimental mass profiles. Nevertheless, and as for the closed-loop process it was necessary to consider a lower rejection for SY7 (72%) to have a reasonable fit between the calculated and experimental profiles for this compound. Although a little random, this time BBR data remained more or less constant as predicted by the models.

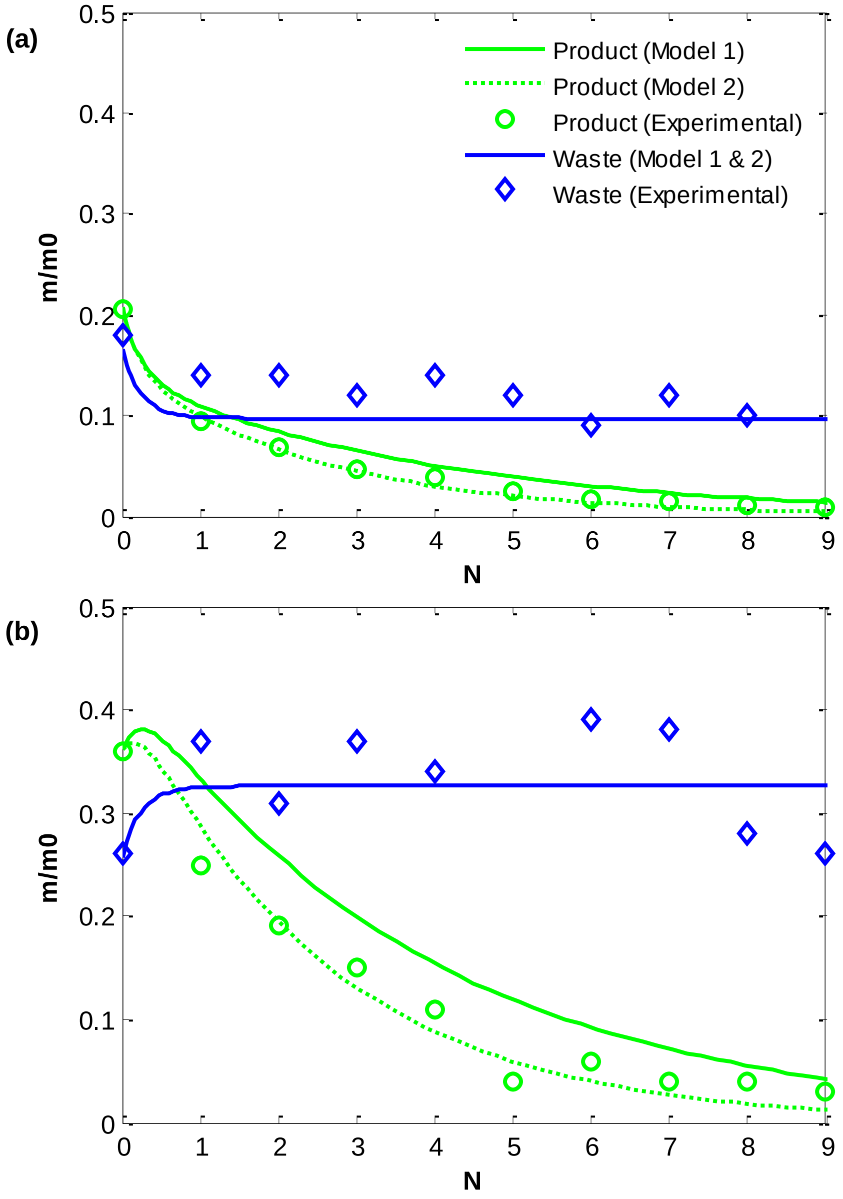

Figure 3.11 Calculated and experimental mass profiles of the product (SY7) and waste (BBR) in (a) feed tank and (b) membrane cell 1 after disconnecting the second cell from the system PI24411/TFC-MPD. Curve fitting was done by assigning different values to R_{SY7}: Model 1- R_{SY7}=82%/R_{BBR}=100%, Model 2- R_{SY7}=72.0% /R_{BBR}=100%.

From the yield and purity profiles of Figure 3.12 it can be seen that this diafiltration, performed right after a diafiltration using the closed-loop membrane process with PI24411 and TFC-MPD membranes, allowed to meet the objectives. By running 9 volumes through the purification membrane it was possible to go up to 96% yield while maintaining the product purity at 100%. However, this required the use of 1.7 L of pure solvent.

To achieve the same yield and purity by performing a simple diafiltration at constant volume, 2.1 L of solvent were required. Comparatively, the closed-loop membrane process with the PI2411/TFC-MPD membrane system allowed to save up 19% of the solvent.

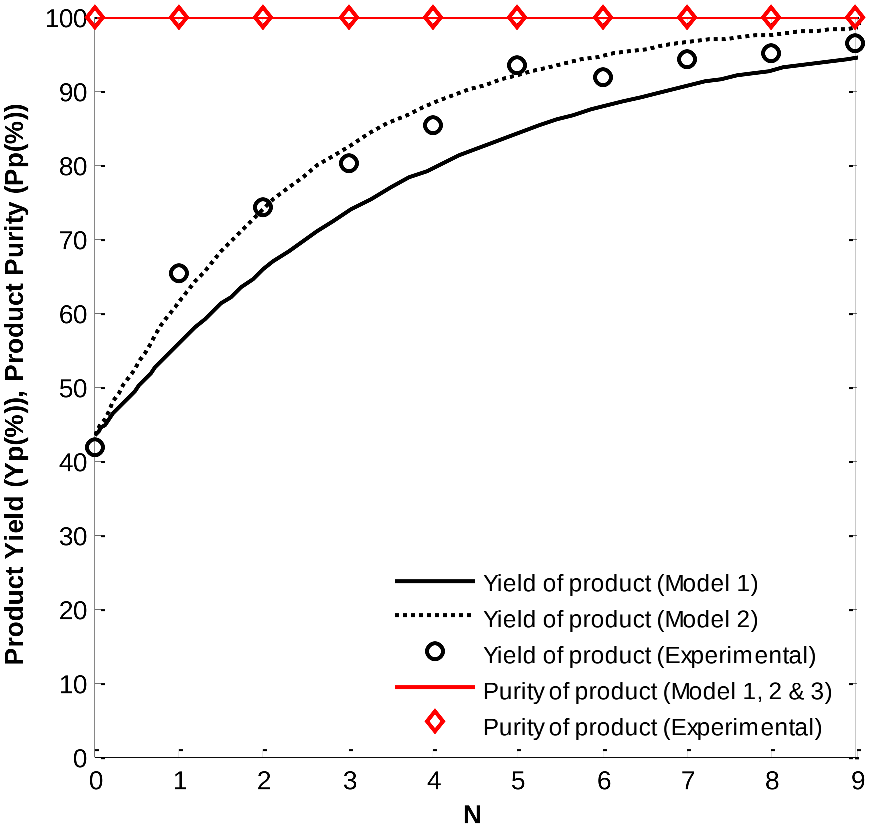

Figure 3.12 Yield and purity profiles for the purification of model mixture A after disconnecting the second cell from the system PI24411/TFC-MPD. Curve fitting was done by assigning different values to R_{SY7}: Model 1- R_{SY7}=82% and R_{BBR}=100%, Model 2- R_{SY7}=72.0% and R_{BBR}=100%.

The performance of the three processes used to purify model mixture A using PI2411 is summarized in Table 3.7.

Table 3.7 Comparison between the three processes used to purify model mixture A.

					Purification Stage		Solvent-recovery Stage	
Process[a]	Y_P (%)	P_P (%)	V_p (L)	Solvent saved (%)	$R_{SY7,1}$ (%)	$R_{BBR,1}$ (%)	$R_{SY7,2}$ (%)	$R_{BBR,2}$ (%)
SM-PI2411	96.7	100	2.1	-	40-61	100	-	-
CL-PI2411/DM150	96.8	100	1.2[b]	43	42.5/87[c]	100	97	NA[d]
CL-PI2411/TFC-MPD	96.3	100	1.7[b]	19	68/72[c]	100	74	NA[d]

[a] SM: single membrane; CL: closed-loop.
[b] Solvent only required after disconnect the second cell.
[c] Rejection before disconnect the cells/ Rejection after disconnect the cells.
[d] NA: not available.

Since only 96.3% of SY7 was recovered using the CL-PI2411/TFC-MPD process, all the processes are compared in terms of the solvent required to achieve a yield around 96%. As it can be seen, CL-PI2411/DM150 process allowed for the higher percentage of solvent savings comparing to the amount of solvent required by the SM-PI2411 process. Luckily it was found a membrane able to complete retain BBR. Because of that, all the processes allowed to obtain a product completely free of impurities.

The only thing that changed between the CL-PI2411/DM150 process and the CL-PI2411/TFC-MPD process was the membrane used for solvent recovery, which was tighter in first case. However, nothing is possible to conclude about their influence on the performance of the process because the first membrane, the PI2411 membrane, showed different rejections for SY7.

Figure 3.13 shows the influence of the product rejection in the solvent recovery stage on the product yield, assuming that the membrane used for purification has a rejection of 83% for SY7 and a rejection of 100% for BBR. As it can be seen, the higher the product rejection in the solvent recovery stage, $R_{SY7,2}$, the higher is the yield possible to attain with the closed-loop process. It can be concluded that a minimum product rejection of 98.9% is required to achieve the target product yield of 90%, and that only with a rejection of 100% for SY7 would be possible to complete remove the product from the purification stage without disconnect the second cell from the system.

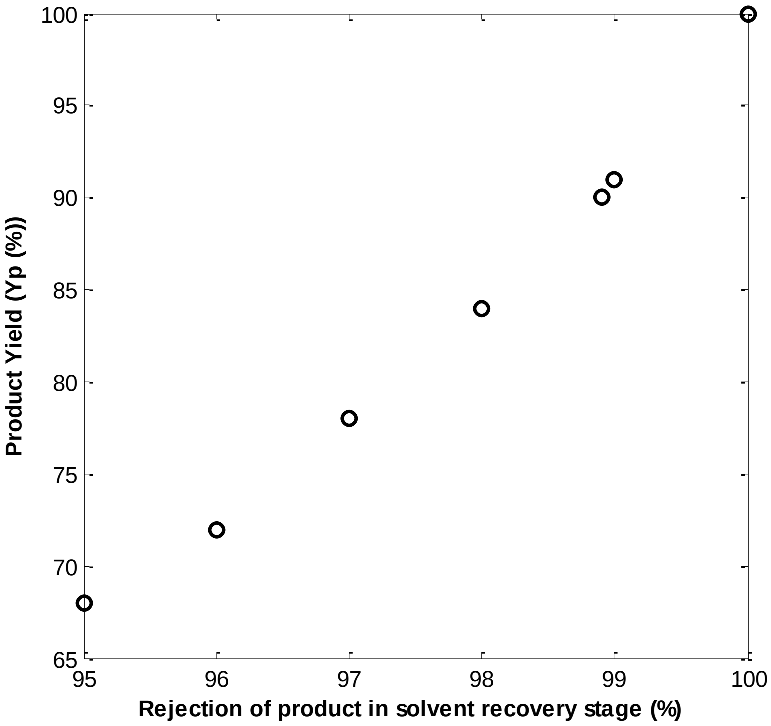

Figure 3.13 Effect of product rejection in the solvent recovery stage in a closed-loop membrane process to the product yield. Simulations were performed assuming that $R_{SY7,1}$=83% and $R_{BBR,1}$=100%.

3.1.3. Conclusions

By applying the closed-loop membrane process to the purification of model mixture A it was possible to generate a purified product with a purity of 100% and recover ~96% of the product, while reducing the fresh solvent consumption in up to 43%, comparing to the amount of solvent required by a conventional diafiltration process. However, much more solvent could have been saved if the membrane used for solvent recovery was able to completely retain the lower MW compound. Thus, it can be concluded that the feasibility of the closed-loop membrane process really depends on the performance of the membranes used in each stage, but in particularly on the performance of the membrane used for solvent recovery that should be tighter enough to allow only the solvent to pass.

Inconsistencies between the experimental results and the predictive model were recurrently encountered. These inconsistencies were mainly attributed to concentration polarisation, membrane fouling, and interactions between the membrane and mixture components, based on the similarity between what was observed in this study and the observations made by other authors. However, more experiments are required to understand the influence of those phenomena on the performance of the systems studied, as it depends on many factors such as the concentration of the solutes, the membrane-solvent-solute system, and also on the mode of operation.

Although the experiments presented in this section prove the feasibility of the closed-loop membrane process, we wanted to show that there is no need to use more solvent than the initially present in the system. For this it was needed a membrane with a rejection of ~100% for the lower MW compound, which is difficult to find, particularly for a compound with such a lower MW as SY7 (198.20 g.mol^{-1}). Hence, it was decided to use another compound to mimic the API.

The chosen compound was Martius Yellow (MY), which is also a yellow dye but with a MW of 274.16 g.mol^{-1}. The experiments performed using the new dye (model mixture B) are described hereafter.

3.2. MODEL MIXTURE B

3.2.1. Experimental

3.2.1.1. Membrane screening

Four different polyimide membranes, PI2411, PI2211, PI2321 and PI2341, were tested in order to find a suitable membrane for the purification stage. Only TFC-MPD and DM150 membranes were tested considering the solvent recovery stage.

This time, the membranes were tested one by one using the system described in sub-section 2.3.2.2. After loading the membrane, the system was washed with pure DMF for approximately 2h. The solvent was fed at 5 mL.min^{-1} and the pressure in the cell was set at 10 bar. After washing, the permeability for the pure solvent was determined by measuring the flow rate at three different transmembrane pressures (10, 20 and 30 bar). Then, a solution containing 5 g.L^{-1} of MY and 0.5 g.L^{-1} BBR was loaded to the system. At this point, the pump continued to be set at 5 mL/min but the transmembrane pressure was only maintained at 10 bar for PI2411; for all the other membranes the pressure was increased to 30 bar. Both feed tank and membrane cell were stirred at 250 rpm. Both permeate and retentate were recirculated back to the feed tank. After the time equivalent to one volume, samples were taken from the retentate and permeate and analyzed by UV/Vis spectroscopy. Only for DM150 membrane the samples were taken after 1 h, since 1 volume would take more than 10 h.

3.2.2. Results & Discussion

3.2.2.1. Membrane screening

The DMF permeability and rejections for MY and BBR of each membrane tested are summarized in Table 3.8.

It is known that the MWCO of integrally skinned asymmetric membranes made of PI can be tuned by varying the DMF:dioxane ratio or the polymer concentration in the dope solution: decreasing DMF:dioxane ratios lead to tighter membranes; although to a less extent, higher polymer concentrations lead normally to tighter membranes (See Toh, Silva & Livingston, 2008). It was then expected that the MWCO of the PI membranes tested increased in the order DM150 < PI2411 < PI2211 < PI2321 < PI2341. In fact, DM150 exhibited the lowest permeability. However, and unlike what was expected, the highest permeability was obtained for PI2411 membrane. This could be due to the temperature at which the permeability of this membrane was determined, which was slightly higher (27 °C) than the temperature at which the other permeabilities were measured (21-22 °C). However, the temperature may not affect the permeability in such a big extent since the value here obtained for the PI2411 permeability is similar to the permeability obtained in previous experiments for this same membrane at a lower temperature (Table 3.3 and Table 3.5: 2.43 L.m^{-2}.h^{-1}.bar^{-1} at 22 °C).

Table 3.8 Summary of the screening data.

Membrane	B_{DMF} (L/m^2.h.bar)	R_{MY}^{d} (%)	R_{BBR}^{d} (%)
PI2341	1.20[a]	21.2	72.7
PI2321	0.44[a]	45.8	88.9
PI2211	1.05[b]	74.6	100.0
PI2411	2.65[c]	86.9	100.0
DM150	0.11[b]	96.1[e]	98.1[e]
TFC-MPD	1.17[b]	96.5	99.7

[a] Permeability measured at 21°C. [b] Permeability measured at 22°C. [c] Permeability measured at 28°C. [d] Rejections determined after 1 volume have ran through the membrane. [e] Rejections determined after 1 h of operation.

In fact, the permeability and rejections obtained for PI2411, DM150 and TFC-MPD membranes with mixture B are pretty consistent with the data obtained for these membranes when using model mixture A, being the MY rejections (slightly) higher than the SY rejections. This was expected as MY has a higher MW than SY7. Only TFC-MPD membrane was expected to be a little more permeable to DMF.

As it can be seen from Table 3.8, it was estimated that PI2211 and PI2411 membranes, both looser membranes than DM150 membrane, have a rejection of 100% for BBR. This suggests that these rejections were probably overestimated and, once again, this could have happened because of the loss of blue color from the samples.

Despite these inconsistencies, PI2411 and PI2211 membranes seemed to be the best candidates for the purification of mixture B, as they rejected BBR completely and presented a relatively low rejection for MY. Even though PI2211 membrane presented a lower permeability, it shown to be slightly looser than PI2411 membrane and yet complete reject BBR, which makes this membrane the most suitable for the purification stage.

The two membranes tested for the solvent recovery stage, TFC-MPD and DM150, rejected MY to about the same extent. The rejection for BBR and the permeability were, however, relatively higher for TFC-MPD membrane, making this membrane the best choice for solvent recovery.

The developed mathematical model was used to simulate the performance of the closed-loop membrane process with PI2211 and TFC-MPD membranes. As confirmed by the yield profile shown in Figure 3.14, a rejection of 96% for MY in the solvent recovery stage is not enough to achieve the target product yield of 90% when using PI2211 membrane in the purification stage.

Hereupon, it was unlikely that better results would be obtained for the closed-loop process by using model mixture B. Plus, it needs to be mentioned that during the screening tests the back-pressure valve, used to regulate the pressure inside the membrane cell, started to fail on a regular basis, letting the liquid leak out of the cell and leading to losses of solution. This problem, which came with the prolonged use of DMF as solvent, required that the valve sealing parts were replaced before or even during each test. This was time consuming and would affect the results when running single or closed-loop membrane process. Hence, it was decided to buy new valves and apply the process to the same compounds, MY and BBR, but using another solvent widely used in the pharmaceutical industry – MeOH. The results for this new mixture, model mixture C, will be presented in the next section.

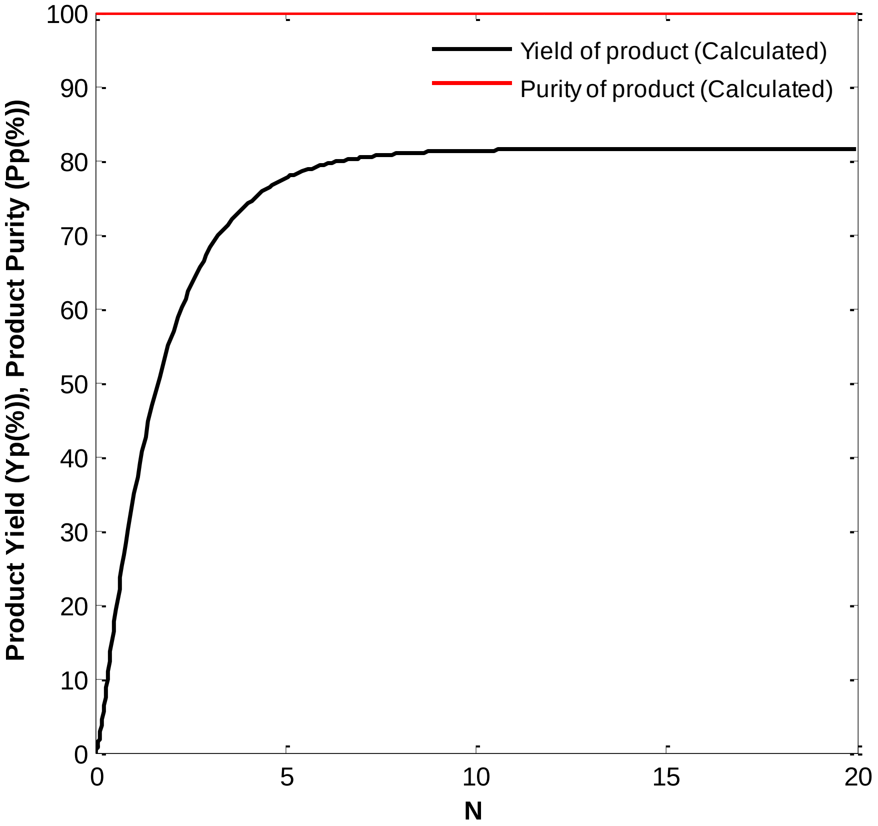

Figure 3.14 Calculated yield and purity profiles for the purification of model mixture B using the closed-loop membrane process with PI2211 membrane (R_{MY}=74.6%/R_{BBR}=100%) for purification and TFC-MPD membrane (R_{MY}=96.5%/R_{BBR}=99.7%) for solvent recovery.

3.2.3. Conclusions

To show the feasibility of the closed-loop membrane process without the need for using more solvent than the initial present in the system, another dye, MY, was chosen to be used instead of SY7 as a model product.

From the membranes tested using model mixture B, PI2211 and TFC-MPD membranes emerged as favorites for the purification and solvent recovery stage, respectively. However, simulations shown that they wouldn’t allow to recover more than about 80% of the product when combined in a closed-loop membrane process. Thus, MY proved to be as challenging as SY7, and a sufficiently tight membrane for the solvent recovery stage was not found.

Since no better results were envisaged by using this model mixture, and since DMF was giving rise to some technical problems, it was decided to not apply the closed-loop membrane process to the purification of model mixture B. Instead, the proposed process was applied to the separation of MY and BBR by using MeOH, another solvent widely used in the pharmaceutical industry. The results using this mixture, model mixture C, will be presented and discussed in the next section.

3.3. MODEL MIXTURE C

3.3.1. Experimental

3.3.1.1. Membrane screening

Two screening tests were made using a 4-crossflow cell rig like the one described in 2.3.1, using model mixture C. In the first screening only two membranes were screened: PI2211 and TFNF-DK. Two discs of each of these membranes were tested. In the second screening four different membranes were screened: DM150, TFC-MPD24, TFRO-SE and TFRO-SG. Only one disc of each of these membranes was tested. Before each screening test, the rig was washed two times with 1.5 L of MeOH at 10 bar for 2h. Then the membranes were loaded to the system and washed for 2h at 10 bar using MeOH. A solution of MY (5 g.L^{-1}) and BBR (0.5 g.L^{-1}) in MeOH was then loaded to the system. Samples were taken from the feed and each permeate line after 5 and 24 hours of operation and analyzed by HPLC.

3.3.1.2. Purification using the single membrane process with PI2211 membrane

The system described in sub-section 2.3.2.2 was used to diafilter model mixture C. A disc of PI2411, the membrane selected for purification, was loaded onto the cell and washed with pure MeOH at 10 bar for 2h. During washing the pump flow rate was set at 10 mL.min^{-1}. After washing the system the solvent feed tank was replaced by a tank containing 100 mL of a MY (5 g.L^{-1}) and BBR (0.5 g.L^{-1}) solution. The diafiltration was carried out at an average transmembrane pressure of 30 bar and 23 °C for 10 diafiltration volumes. During diafiltration the pump flow rate was maintained at 10 mL.min^{-1} and the feed and membrane cell were stirred at 250 rpm. This time, samples were taken from the feed only in the beginning and in the end of the diafiltration.

The yield of product, $\mathrm{Y_P}$, and purity of product, $\mathrm{P_P}$, were calculated from equations 3-6 and 3-7 and plotted as a function of N.

$$\mathrm{Y_P}=\frac{\mathrm{m_{P,MY}}}{m_{\mathrm{F0,MY}}}\times 100 \tag{3-6}$$

$$\mathrm{P_P}=\frac{\mathrm{m_{P,MY}}}{\mathrm{m_{P,MY}}+\mathrm{m_{P,BBR}}}\times 100 \tag{3-7}$$

where $\mathrm{m_{P,i}}$ is given by 3-3.

3.3.1.3. Purification using the closed-loop membrane process with PI2211 membrane for purification and TF-ROSG membrane for solvent recovery

The system described in sub-section 2.3.2.3 was used to diafilter model mixture C using PI2211 membrane for purification and TFRO-SG membrane for solvent recovery. The PI2211 membrane disc used in the single membrane process described before was used in this process. The cell containing this membrane was first washed with pure MeOH in order to remove the dyes from the previous diafiltration. Another cell, with a TFRO-SG disc loaded, was also washed with pure MeOH at 10 bar and 22 °C for 2h. During washing the pump flow rate was set at 10 mL.min^{-1}. After washing the cells were connected and a feed tank containing 100 mL of a MY (5 g.L^{-1}) and BBR (0.5 g.L^{-1}) solution was added to the system. The pump flow rate was maintained at 10 mL.min^{-1}, while the feed tank and membrane cells were stirred at 250 rpm. The diafiltration ran for 7 diafiltration volumes.

This time the yield of product, $\mathrm{Y_P}$, was calculated from the following equation:

$$\mathrm{Y_P} = \frac{\mathrm{m_{R2,MY}}}{m_{\mathrm{F0,MY}}} \times 100 \qquad \textbf{3-8}$$

The purity of product, $\mathrm{P_P}$, was calculated from equation 3-5. Both variables were then plotted as a function of N.

In order to have results comparable to those obtained using the single membrane process with PI2211, it was necessary to disconnect the cells after 7 volumes and continue the diafiltrations using only the first membrane unit. From this point the system was operated like described in sub-section 2.3.2.2 for further 8 volumes. This time, samples were taken from the feed only in the beginning and in the end of the diafiltration. The yield and purity were calculated using equations 3-6 and 3-7 and plotted as a function of N.

3.3.1.4. Purification using the single membrane process with PBI 24xDBX membrane

As a last attempt to find a membrane for the purification of model mixture C that complete rejected BBR, PBI 24xDBX membrane was applied on the purification of that mixture using the system described in sub-section 2.3.2.2, without screening this membrane previously. A disc of PBI 24xDBX was loaded onto the cell and washed with pure MeOH at 10 bar for 2h. During washing the pump flow rate was set at 10 mL.min^{-1}. After washing the system the solvent feed tank was replaced by a tank containing 100 mL of a MY (5 g.L^{-1}) and BBR (0.5 g.L^{-1}) solution. The diafiltration was carried out at an average transmebrane pressure of 21 bar and 23 °C for 14 diafiltration volumes. During diafiltration the pump flow rate was maintained at 5 mL.min^{-1} and the feed and membrane cell were stirred at 250 rpm. The yield of product, $\mathrm{Y_P}$, and purity of product, $\mathrm{P_P}$, were calculated from equations 3-6 and 3-7 and plotted as a function of N.

3.3.1.5. Purification using the closed-loop membrane process with PBI 24xDBX membrane for purification and PBI 26xDBB membrane for solvent recovery

PBI 26xDBB was considered to be used in combination with PBI 24xDBX, in the closed-loop process as it was expected that membrane was expected to be tighter than the later one. The system described in sub-section 2.3.2.3 was then used to diafilter model mixture C using PBI 24xDBX membrane for purification and PBI 26xDBX membrane for solvent recovery.

The PBI 24xDBX membrane disc used in the single membrane process described before was used in this process. The cell containing this membrane was first washed with pure MeOH in order to remove the dyes from the previous diafiltration. Another cell, with a PBI 26xDBB disc loaded, was also washed with pure MeOH at 10 bar and 27 °C for 2h. During washing the pump flow rate was set at 8 $mL.min^{-1}$. After washing the cells were connected and a feed tank containing 100 mL of a MY (5 $g.L^{-1}$) and BBR (0.5 $g.L^{-1}$) solution was added to the system. The pump flow rate was set at 15 $mL.min^{-1}$, while the feed tank and membrane cells were stirred at 250 rpm. The diafiltration ran for 29 diafiltration volumes. This time, samples were not taken from the second membrane unit. The yield of product, Y_P, and purity of product, P_P, were calculated from equations 3-8 and 3-5 respectively, and plotted as a function of N.

In order to have results comparable to those obtained using the single membrane process with PBI 24xDBX it was necessary to disconnect the cells after 29 volumes and continue the diafiltrations using only the first membrane unit. From this point the system was operated like described in sub-section 2.3.2.2 for further 6 volumes. The yield and purity were calculated using equations 3-6 and 3-7 and plotted as a function of N.

3.3.2. Results & Discussion

3.3.2.1. Membrane screening

The results of the screening tests performed using model mixture C are summarized in Figure 3.15 and Table 3.10.

The flux profiles presented in Figure 3.15 show that the permeate flux was lower than the flux of pure solvent for almost all of the membranes tested. It can be seen that the drop was significantly higher for PI2211 membrane, the loosest of all the membranes tested, and lower for most of the tighter membranes, suggesting that other factor in addition to all the possible factors already mentioned, like concentration polarization or membrane fouling, influenced the permeate flux reduction.

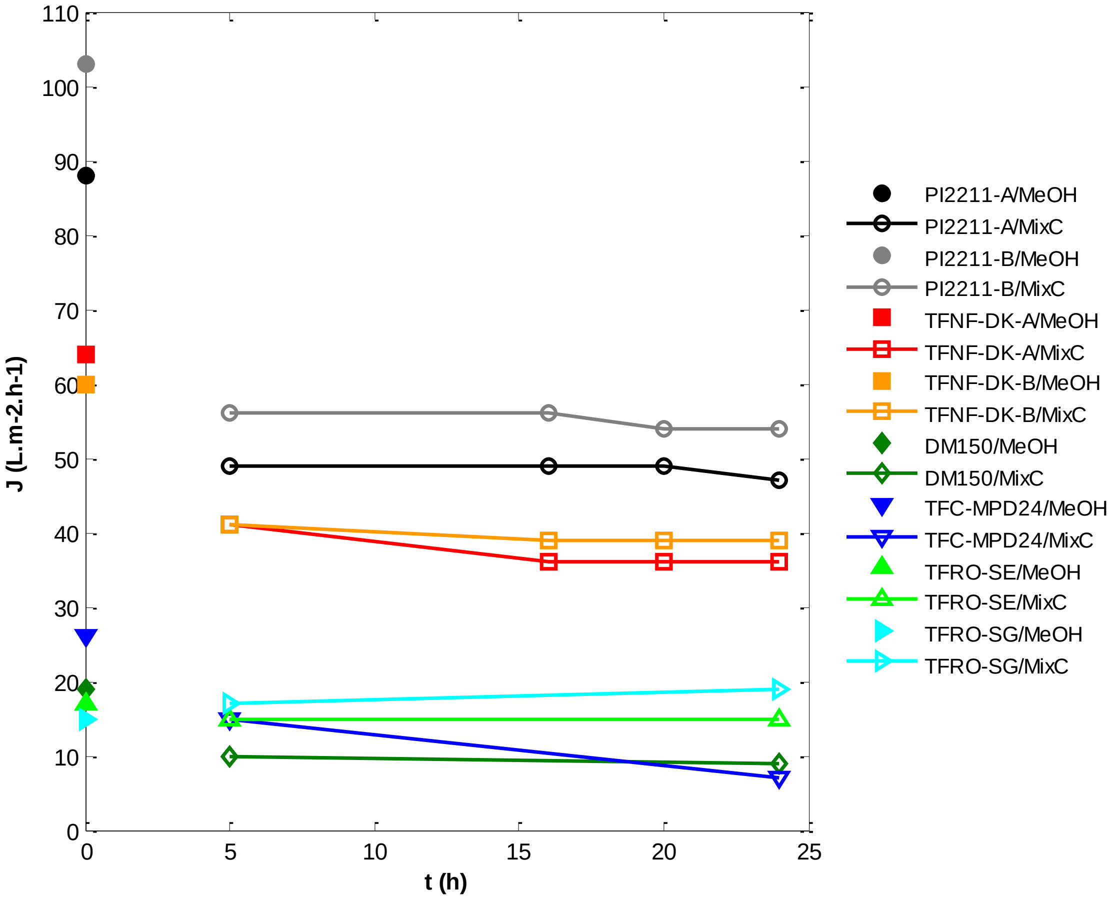

Figure 3.15 Flux profiles over time at 10 bar and 27 °C for the membranes screened using model mixture C. The flux at time 0 is the flux of pure MeOH.

In general, the major decrease in the flux was observed in the first 5 h. For some membranes flux continued to decrease in the following hours, though to a smaller extent, until a steady-state was reached. This behavior, also observed by other authors, is normally attributed to membrane compaction, and its effect was found to be more pronounced within micro porous membranes (See Toh, Silva & Livingston, 2008, Yang, Livingston & Freitas dos Santos, 2001, Whu, Baltzis & Sirkar, 2000) or for membranes with dense top layers prone to swell (Vankelecom et al., 2004). TFRO-SG was the only membrane for which the flux has increased over time and relatively to the flux of pure solvent. This is a membrane designed for aqueous systems that can lose their structural integrity and separation performance when exposed to organic solvents. Thus, the observed increase in the flux can also be attributed to membrane swelling and ultimately to membrane cracking (Yang, Livingston & Freitas dos Santos, 2001).

As expected, PI2211 membrane, presented the highest fluxes. However, one of the discs revealed to be more permeable than the other, which reflects the non-uniformity of the membrane. On the other hand, the flux profiles of the two discs of TFNF-DK tested are pretty consistent.

The flux of TFNF-DK, TFRO-SE and TFRO-SG membranes is consistent with their MWCO (see Table 2.2), which decreases in the order TFNF-DK > TFRO-SE > TFRO-SG. However, these fluxes are higher than the flux measured for DM150 membrane, which is supposed to be looser than those three membranes, and so, it was expected to present a higher flux. It is worth noting that any of those TFC membranes are made for organic solvent applications. Consequently, the high fluxes encountered could have to do, once again, with membrane swelling.

Table 3.9 Physical parameters of the solvents.

Solvent	Density[a] (g.cm^{-3})	MW (g.mol^{-1})	Viscosity[a] (mPa.s)	Dielectric constant[b]
DMF	0.949	73	0.82	36.7
MeOH	0.792	32	0.61	32.7

[a] Density and viscosity at 20 °C; [b] Dielectric constant at 25 °C

The permeabilities of PI2211 and DM150 membranes for MeOH at 27°C are 9.54 ± 1.06 L.m^{-2}.h^{-1}.bar^{-1} and 1.86 L.m^{-2}.h^{-1}.bar^{-1}, respectively, whereas the permeabilities for DMF were estimated in the previous experiments to be 1.05 L.m^{-2}.h^{-1}.bar^{-1} at 22 °C for PI2211 membrane and 0.11 L.m^{-2}.h^{-1}.bar^{-1} at 22 °C for DM150 membrane. Even though these permeabilities were measured at different temperatures it seems that the permeability of MeOH is always higher than the permeability of DMF. It can be seen from Table 3.9 that MeOH has a lower viscosity then DMF, so by the pore-flow model it was already expected to find a higher flux for MeOH. Due to the hydrophobicity of polyimide membranes, higher fluxes were also expected for MeOH as this solvent presents a lower dielectric constant comparing to DMF, and so it is expected to have a higher affinity for the membrane (Yang, Livingston & Freitas dos Santos, 2001).

Table 3.10 Rejections after 5h and 24h of operation at 10 bar and 27°C for the membranes screened using model mixture C.

	R_i (%)			
Membrane	**MY 5 h**	**BBR 5 h**	**MY 24 h**	**BBR 24 h**
PI2211-A	81.4	98.4	91.6	98.4
PI2211-B	77.9	98.2	90.8	98.4
TFNF-DK-A	99.1	98.0	98.7	98.1
TFNF-DK-B	95.4	97.2	96.3	97.8
DM150	87.6	96.2	95.4	98.5
TFC-MPD24h	94.8	98.3	94.7	97.6
TFRO-SE	92.9	93.5	95.5	95.2
TFRO-SG	97.8	97.1	98.6	97.4

From Table 3.10 it can be seen that the rejections either increased or maintained more or less constant after 24h of operation. An increase in rejection was already expected, as this is a consequence of membrane compaction (Gibbins et al., 2002, Yang, Livingston & Freitas dos Santos, 2001, Whu, Baltzis & Sirkar, 2000). The increase in rejection was particularly significant for PI2211 membrane, since compaction effects are also more significant for the looser membranes. From now on all comparisons in terms of rejections will be made relatively to the values obtained after 24 h, assuming that all membranes had already reached the maximum level of compaction at this point.

PI2211 membrane was the only membrane tested considering the purification stage, since it had already shown a good performance when screened against model mixture B. All the other membranes were tested for the solvent recovery stage, since this had been, so far, the hardest task of this work. It happens that this time, in opposition to what was observed for PI2211 membrane when DMF was used as solvent, the membrane did not completely rejected BBR. Plus, a higher rejection was obtained for MY (compare values presented in Table 3.10 and Table 3.8).

Some differences in the rejections were already expected since it is known that, for a given membrane, rejection depends on the solvent used. MeOH is a protic polar solvent and DMF an aprotic polar solvent, which can readily solvate anions and cations, respectively. Since both MY and BBR are negatively charged, it was expected them to have a larger diameter in MeOH than in DMF, and so a higher rejection in the former solvent. This was, however, only observed for MY. It happens that also the solute-membrane and solvent-membrane interactions affect solute transport, and separation is not always based on the sieving mechanism (Geens et al., 2005). In fact, Whu et al. (Whu, Baltzis & Sirkar, 2000) found a rejection of 94.8 % for BBR in MeOH when using a solvent resistant membrane with a MWCO three times higher than the MW of the compound, so it is not so unlikely the rejection of BBR in MeOH obtained in this study for PI2211 membrane.

It must be said, however, that MY rejections could have been underestimated in DMF. The rejections for MY in this solvent were obtained using a system like the one described in subsection 2.3.2.2 for which it was concluded, when using model mixture A, that the concentration polarization effects were important, leading to underestimation of the rejections.

In opposition to this, about the same rejections were obtained for DM150 membrane when using MeOH or DMF (compare values presented in Table 3.10 and Table 3.8), as if solvent had no influence on the membrane rejection. Nevertheless, it should be noted that the DM150 membrane rejections in DMF were determined using the system described in sub-section 2.3.2.2 after only 1h of operation, whereas the rejections in MeOH were determined in a cross-flow cell rig after 24h. Thus, it is likely that higher rejections would be obtained in DMF if the test have ran for a couple more hours.

A curious aspect is that the measured rejections of MY and BBR, for all the commercial TFC membranes tested, apart from being very similar among them, are sometimes higher for MY, the lower MW compound. This last phenomenon, already observed by other authors

(Geens et al., 2005, White, 2002), shows once again that the solute transport through membranes in organic solvents can't only depend on size exclusion mechanisms.

Despite the fact that PI2211 membrane did not completely rejected BBR it was decided to use this membrane for the purification of model mixture C. Therefore it was already not expected to obtain a final product free of impurities.

From the flux and rejection data, TFNF-DK membrane would be the best choice for solvent recovery. However, it has to be mentioned that both discs of TFNF-DK cracked after washing the membranes with pure MeOH. In fact, this membrane is known to have a polysulfone support, which normally has a limited solvent resistance, making it unsuitable for solvent intensive processes (White, 2006). The TFRO-SG was then chosen instead of TFNF-DK as it revealed the highest rejections for both compounds. However it was already known that by using this membrane in combination with PI2211 membrane in the closed-loop membrane process it would not be possible to recover all the product form the feed.

3.3.2.2. Purification using the single membrane process with PI2211 membrane

The permeate fluxes and rejection of MY and BBR obtained with this system are summarized in Table 3.11. The average MeOH permeability of the PI2211 discs tested in the membrane screening was (after two washings of 2h each) 9.54 ± 1.06 $L.m^{-2}.h^{-1}.bar^{-1}$ at 27 °C; for model mixture C the average permeability at steady state was 5.04 ± 0.45 $L.m-2.h^{-1}.bar^{-1}$ at 27 °C. Comparing these values with the permeabilities listed in Table 3.11, we can say that the disc selected for the purification process was less permeable. This shows once again the variability of the self-prepared membranes.

Although this membrane disc revealed to be less permeable than the discs tested during membrane screening, the estimated rejection for MY was lower than expected (Table 3.10: 91.2 ± 0.6%). On the other hand, BBR rejection was consistent with the previous results (Table 3.10: 98.4 ± 0.0%).

Table 3.11 Summary of the data recorded along the diafiltration of model mixture C using the single membrane process with a PI2211 membrane.

N	ΔP (bar)	J ($L.m^{-2}.h^{-1}$)[a] [B ($L.m^{-2}.h^{-1}.bar^{-1}$)]	R_{MY} (%)	R_{BBR} (%)
MeOH	30	222.35 [7.60][b]	-	-
1	31	83.53 [2.69]	84	95
2	30	81.18	85	99
3	30	81.18	85	98
4	30	81.18	84	99
5	30	78.82	85	98
6	30	77.65	85	98
7	30	75.29	82	97
8	30	74.12	83	98
9	30	71.76	83	97
10	30	71.76 [2.39]	84	98
			84 ± 1	98 ± 1

[a] Fluxes determined at 22 °C

[b] Permeability determined by plotting J_{MeOH} vs. ΔP: J_{MeOH}=7.60.ΔP, R^2=0.9965

The mass profiles of MY and BBR over the number of diafiltration volumes are presented in Figure 3.16. This time samples did not lose the blue color, at least to the same extent as when mixture A was used as model mixture, and that is why BBR data are finally shown. For precaution samples were kept in a cold room with the temperature set at 4 °C while they were not being analyzed, which may have help preserving its color.

The calculated curves were obtained considering an average of the experimental rejections obtained for each compound (see Table 3.11), which perfectly fit to the experimental data in the membrane cell (Figure 3.16-b).

Since this time samples were taken from the feed tank only in the beginning and at the end of the diafiltration, all the other data points from the experimental mass profiles in the feed tank (Figure 3.16-a) were estimated from the mass balance. As it can be seen the model seems to underestimate the mass profile of MY in the feed tank; only the first and last points of the experimental mass profile, the ones that were actually measured, are in accordance with the predicted curve. Similarly, only the initial and final points of BBR experimental mass profile fit to the calculated curve in the feed tank.

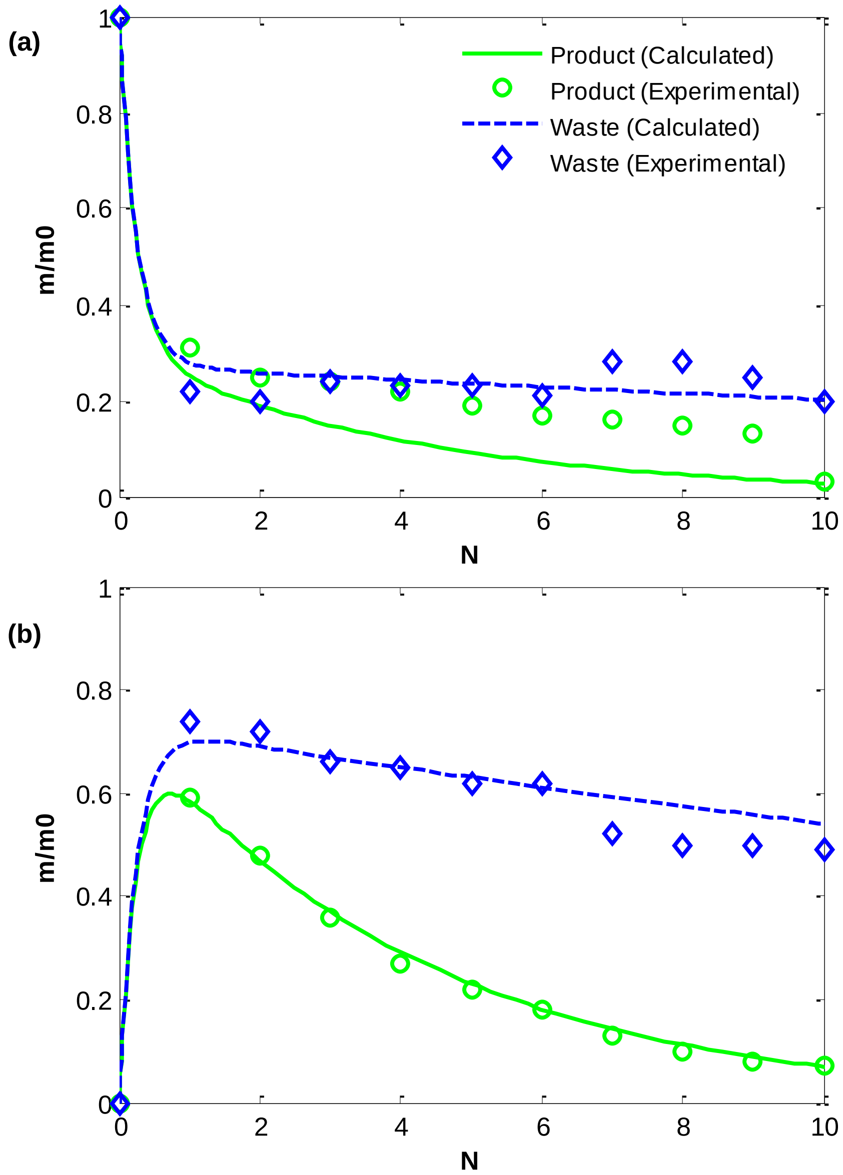

Figure 3.16 Calculated and experimental mass profiles of product (MY) and waste (BBR) in (a) feed tank and (b) membrane cell for the purification of model mixture C using single membrane process with a PI2211 disc at 30 bar and 22 °C.

From Figure 3.17 one can see that the permeate concentrations of MY are lower than what is predicted from the model. This may explain why the feed concentrations of MY (Figure 3.16-a) were estimated to be higher than what model predicts. This may also mean that MY was getting trapped on the membrane matrix, blocking the membrane pores and leading to the observed decrease in the flux (see Table 3.11).

In the case of BBR, it is difficult to say if the concentrations in the permeate were under or overestimated as they vary a lot. What can actually be seen is that BBR feed data (Figure 3.16-a) shifts around the calculated curve in the same way as the data from the membrane cell (Figure 3.16-b), but on the other way around. Feed data were then more sensible to oscillations in the concentration on the retentate side than in the permeate side, which makes sense as the measured concentration of BBR in the permeate was very low (< 0.01 g.L^{-1}).

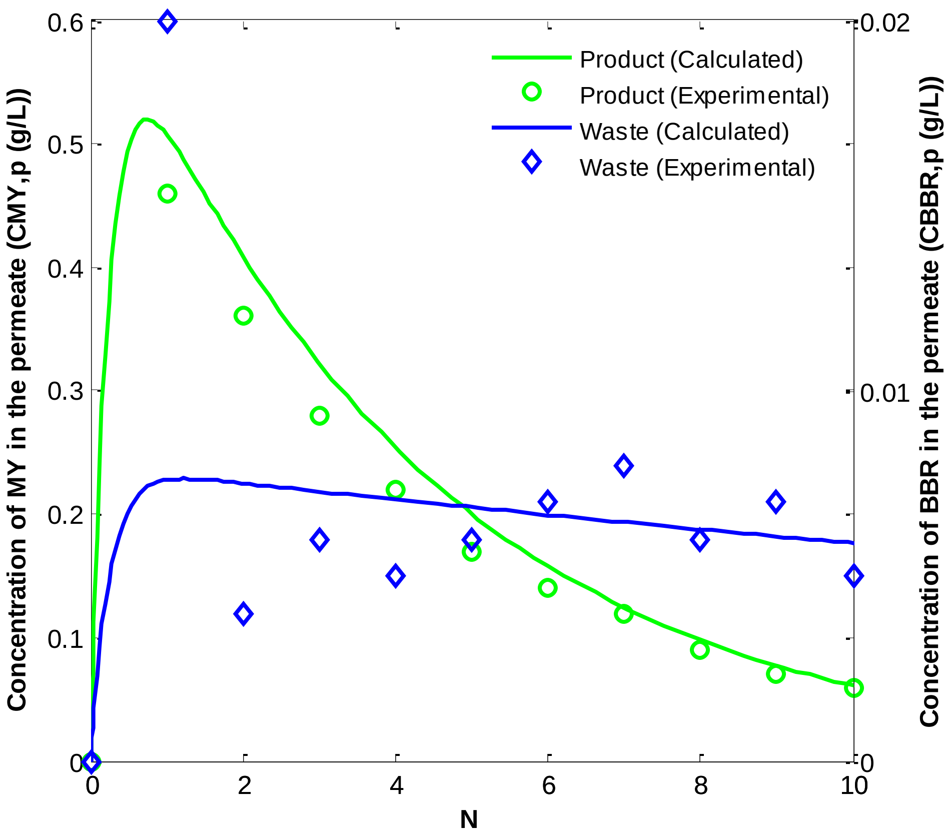

Figure 3.17 Calculated and experimental concentration profiles in the permeate for the purification of model mixture C using the single membrane process with a PI2211 disc at 30 bar and 22 °C.

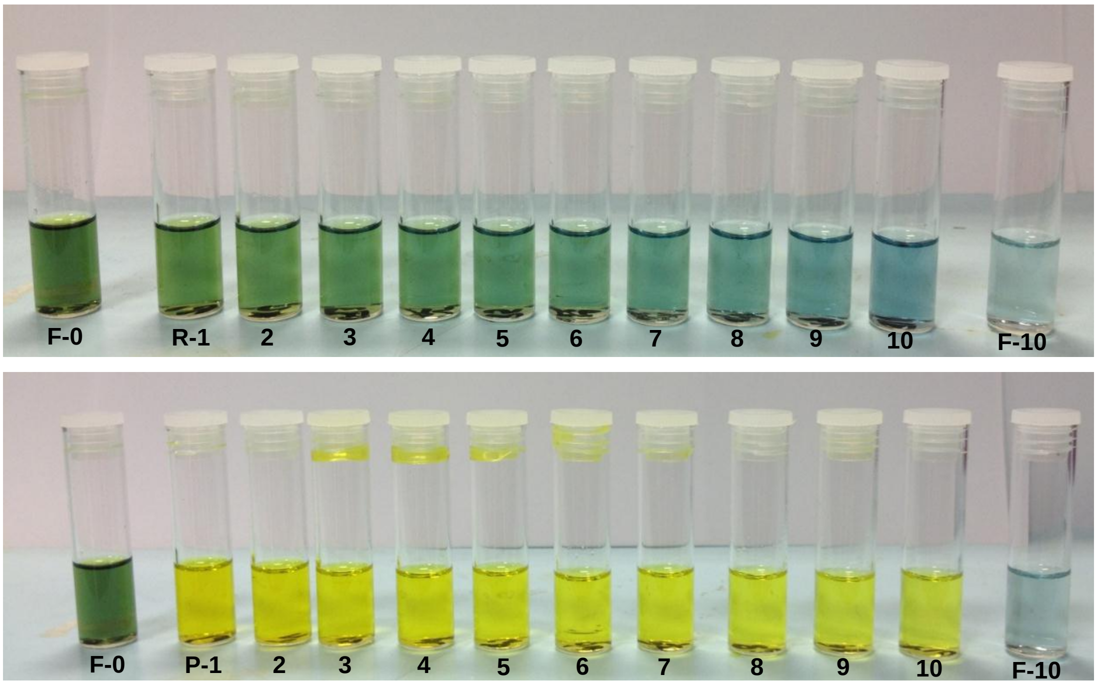

Figure 3.18 Photograph of the initial and final feed and of retentate and permeate samples at each diafiltration volume. Feed and retentate samples were 40 times diluted.

The course of the diafiltration of model mixture C using PI2211 membrane can also be assessed from Figure 3.18. The feed solution that was initially green because of the presence of the two dyes, MY (yellow) and BBR (blue), in a proportion of 10:1, turned blue after 10 volumes of solvent ran through the single membrane system. Retentate color also varied progressively from green to blue, as MY was being removed from the system. In the case of the permeate samples, the presence of BBR is almost imperceptible by eye, but it can be seen that permeate became actually less concentrated towards the end.

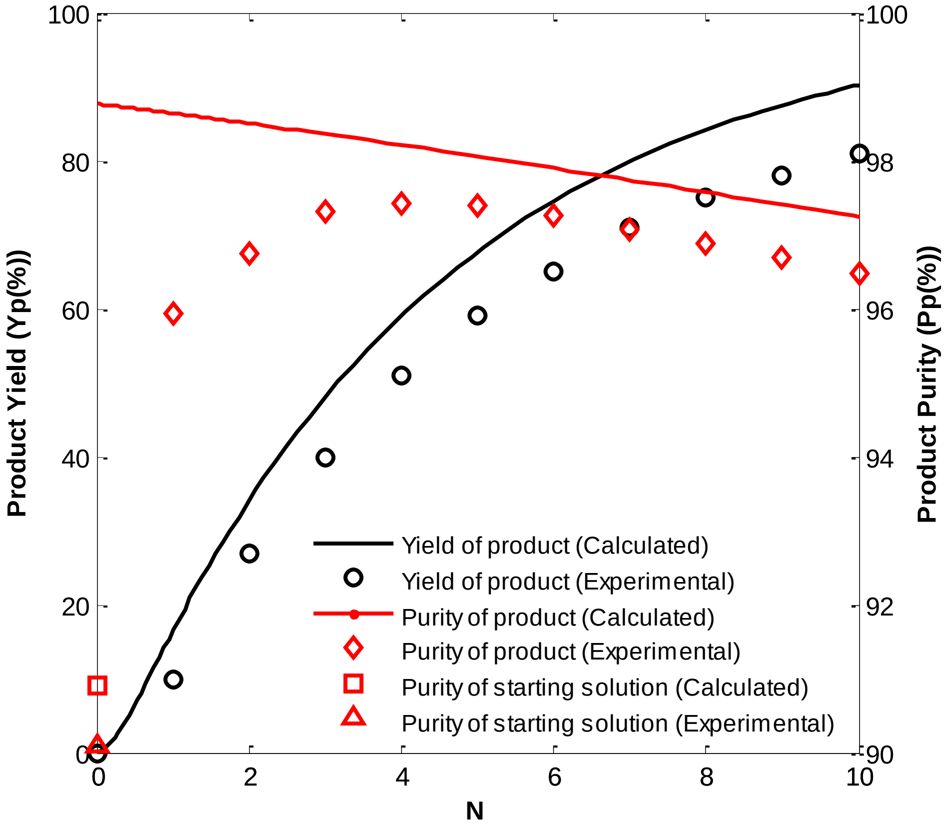

Figure 3.19 **Yield and purity profiles for the purification of model mixture C using single membrane process with a PI2211 disc at 30 bar and 22 °C.**

In Figure 3.19 are shown the yield and purity profiles for this same diafiltration. Both profiles were obtained based on the permeate data shown in Figure 3.17, which, as referred before, was underestimated for MY. This may explain why the calculated yield and purity profiles overestimate the experimental profiles. The difference between the experimental and calculated purity for the first volumes may have to do with the limitations of the trapezoidal rule, used to estimate the amount of solute that permeated through the membrane between two volumes (equation 3-3).

Overall, we can say from the experimental data that after 10 volumes, which required 1.9 L of MeOH, about 81% of the product was recovered with a purity of 96%. Although this corresponds to an increase in purity of 7% relatively to the purity of the starting solution, this could not be enough for some pharmaceutical applications for which purity needs to be most of the times around 99%.

After this diafiltration, the same PI2211 membrane disc was used in combination with a TFRO-SG membrane disc in a closed-loop process to purify model mixture C. The results obtained with this system will be shown on the next sub-section and then compared in terms of yield, purity and amount of solvent saved with the results obtained for the former diafiltration.

3.3.2.3. Purification using the closed-loop membrane process with PI2211 membrane for purification and TF-ROSG for solvent recovery

The permeate fluxes and rejection of MY and BBR obtained with this system are summarized in Table 3.12. This time the permeability of PI2211 membrane for mixture C was higher compared to the previous diafiltration. Since the membrane disc was the same this may have happened because the recycle ratio was higher (0.55 ± 0.01) than in the previous diafiltration (0.34 ± 0.04), which may have reduced the concentration polarization effects by increasing the hydrodynamics of the system. In turn, the rejections revealed to be lower than expected from the previous experiments, but are in accordance with the higher permeability encountered for this membrane.

Table 3.12 Summary of the data recorded along the purification of model mixture C using the closed-loop membrane process with a PI2211 membrane disc for purification and a TFRO-SG membrane disc for solvent recovery.

				PI2211		TFRO-SG	
N	**ΔP_1 (bar)**	**ΔP_2 (bar)**	**J ($L.m^{-2}.h^{-1}$)[a] [B($L.m^{-2}.h^{-1}.bar^{-1}$)]**	**$R_{MY,1}$ (%)**	**$R_{BBR,1}$ (%)**	**$R_{MY,2}$ (%)**	**$R_{BBR,2}$ (%)**
MeOH	10	20	77.65/69.41 [7.60[b]/3.54[c]]	-	-	-	-
1	9	21	55.29 [6.14/2.63]	84	96	81	28
2	9	21	54.12	83	97	75	53
3	9	21	52.94	72	97	78	51
5	9	21	52.94	70	96	79	58
7	9	21	50.59 [5.62/2.41]	63	96	82	69
				74 ± 9	96 ± 1	79 ± 3	52 ± 8

[a] Fluxes determined at 25 °C

[b] Permeability determined by plotting J_{MeOH} vs. ΔP: $J_{MeOH}=7.60.\Delta P$, $R^2=0.9965$

[c] Permeability determined by plotting J_{MeOH} vs. ΔP: $J_{MeOH}=3.54.\Delta P$, $R^2=0.9985$

The permeability of the TFRO-SG disc used is higher than expected from the screening (1.89 $L.m^{-2}.h^{-1}.bar^{-1}$ for Mix C at 27 °C) and, accordingly to this the calculated rejections for MY and BBR are lower than the rejections determined during the screening (98.6% for MY and 97.4% for BBR). Again, and in opposition to what was expected from the differences between the MW of the two compounds, a higher rejection was obtained for MY.

In general, the rejections varied considerably along the process. However, an increasing trend was only observed for the rejections of TFRO-SG membrane. Since the flux also dropped over time, this could mean that TFRO-SG membrane continued to be compacted during the process. In order to have reproducible results the membranes should have been pre-conditioned with pure solvent until a steady flux was obtained (Gibbins et al., 2002).

Figure 3.20 shows the mass profiles of MY and BBR in the feed tank, first and second membrane cells. The model that considers the calculated rejections (Model 1) underestimates the mass profiles in the feed tank, but overestimates the mass profiles in the second membrane unit. In the case of the first membrane cell, Model 1 overestimates the BBR mass profile, while underestimates the MY profile for the first 3 volumes. On the other hand, Model 2, that considers corrected rejections for both compounds, gives a good fitting between the MY profiles in the first and second membrane units and also between the BBR profiles in the first membrane unit, but largely overestimates the mass profile for BBR in the second membrane unit. Since the feed data points were estimated from the mass balance, it was not possible to have a good fitting between the calculated and experimental curves in the feed tank, in particularly for BBR. It seems then that BBR concentrations in the first and/or in the second membrane unit were not properly measured, leading to such these inconsistencies.

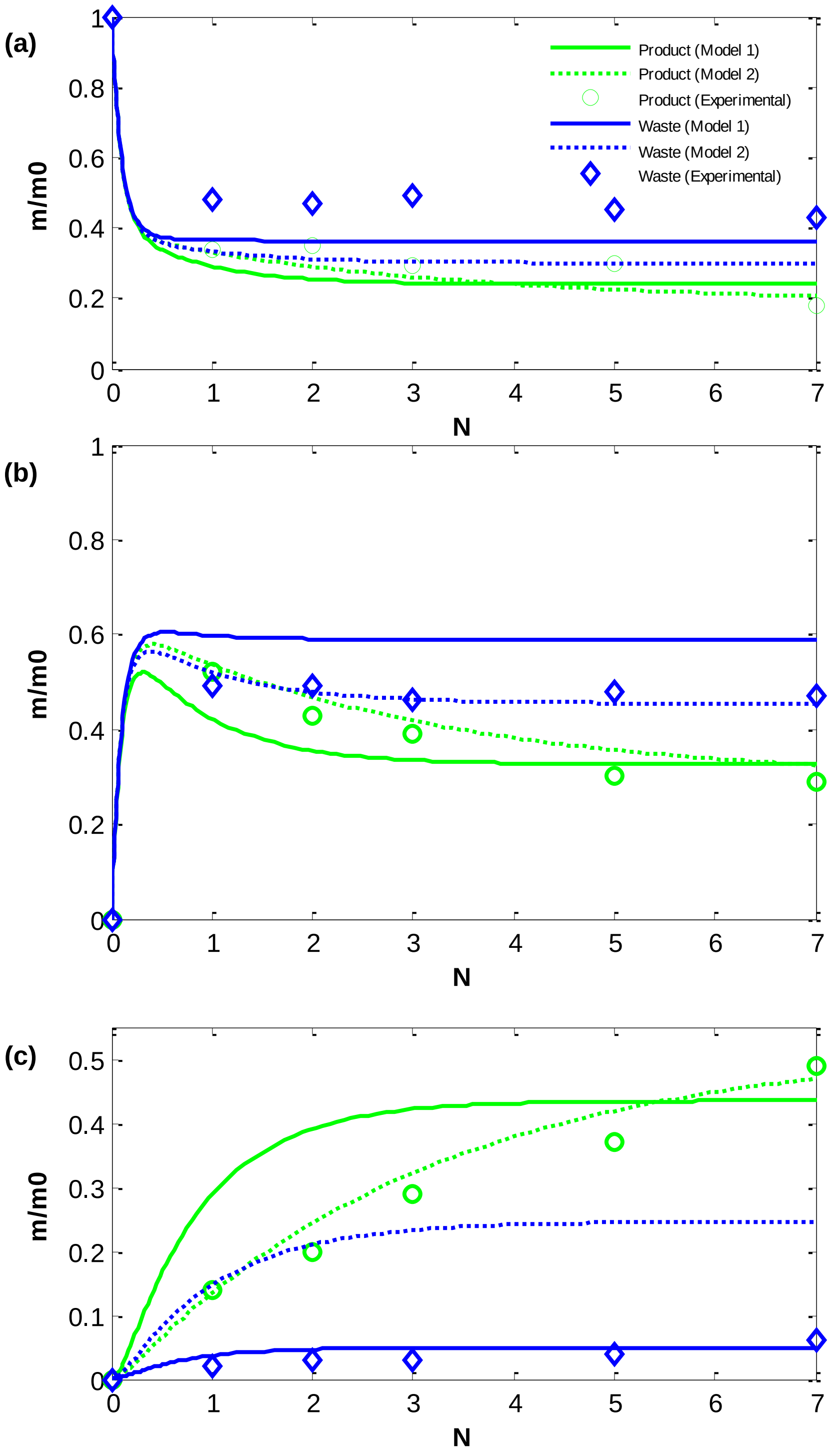

Figure 3.20 Calculated and experimental mass profiles of the product (MY) and waste (BBR) in (a) feed tank, (b) membrane cell 1 and (c) membrane cell 2 for the purification of model mixture C using the closed-loop membrane process with a PI2211 and a TFRO-SG disc at 25 °C. Curve fitting was done by assigning different values to the rejections: Model 1- $R_{MY,1}$=74%,/$R_{BBR,1}$=96%, and $R_{MY,2}$=79%/$R_{BBR,2}$=52%, Model 2-$R_{MY,1}$=91%/$R_{BBR,1}$=87% and $R_{MY,2}$=96%/$R_{BBR,2}$=76%.

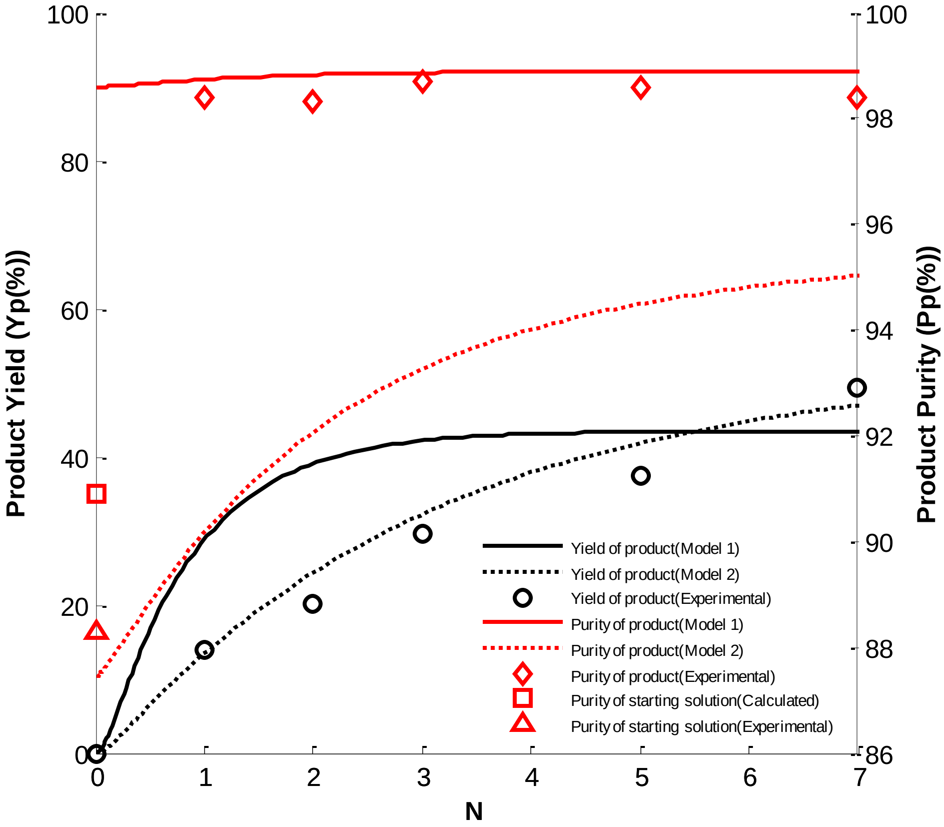

Figure 3.21 Yield and purity profiles for the purification of model mixture C using closed-loop membrane process with a PI2211 and a TFRO-SG disc at 25 °C. Curve fitting was done by assigning different values to the rejections: Model 1- $R_{MY,1}$=74%,/$R_{BBR,1}$=96%, and $R_{MY,2}$=79%/$R_{BBR,2}$=52%, Model 2-$R_{MY,1}$=91%/$R_{BBR,1}$=87% and $R_{MY,2}$=96%/$R_{BBR,2}$=76%.

The yield and purity profiles are presented in Figure 3.21. Experimental profiles reveal that about 49% of the product was recovered with a final purity of about 98% after 7 diafiltration volumes. The process was stopped at this point because from Model 1, the model used to make predictions during the experimental work, it would not be possible to effectively recover more product. This model, however, overestimates the observed yield profile. This makes sense as the yield depends on the mass of MY accumulated in the second membrane unit, and Model 1 also overestimates the mass profile inside the second membrane cell. On the other hand, Model 2 gives a good fitting between the experimental and calculated yield profiles, as this is the model that also best describes the MY mass profile in membrane cell 2 (see Figure 3.20-c).

The experimental purity profile follows the trend predicted by Model 1 but shows that purity was always slightly below what was expected from the model. Model 2, on the other hand, predicts a purity profile with a completely different trend that nothing has to do with the experimental data, as this model overestimates the amount of BBR in the second membrane unit relatively to the measured values (see Figure 3.20-c).

After stopping the closed-loop process, the two cells were disconnected and the purification continued without recovering the solvent, in order to have results comparable with the ones obtained for the single membrane process using PI2211 membrane. The data for this diafiltration is summarized by Table 3.13 and Figure 3.22, which presents the yield ad purity profiles.

The permeabilty of PI2211 membrane for model mixture C is much more consistent with the permeability encountered for this same membrane when using the single membrane process for purification (see Table 3.11). This time the recycle ratio was 0.37 ± 0.01, pretty similar to the ratio applied to the single membrane process (0.34 ± 0.04), which means that concentration polarization effects actually have a big impact in the performance of the single and closed-loop membrane processes.

The average rejections encountered for MY and BBR are also in accordance with the average rejections obtained for the previous diafiltration using single membrane process with PI2211 membrane (Table 3.11: 84 ± 1 % for MY and 98 ± 1 for BBR).

Table 3.13 Summary of the data recorded along the purification of model mixture C using the single membrane process with a PI2211 membrane disc after disconnecting the second cell from the system.

N	**ΔP_1 (bar)**	**J ($L.m^{-2}.h^{-1}$)[a] [B ($L.m^{-2}.h^{-1}.bar^{-1}$)]**	**$R_{MY,1}$ (%)**	**$R_{BBR,1}$ (%)**
1	30	76.47 [2.55]	83	96
2	30	75.29	83	97
3	30	72.94	84	96
4	30	71.76	85	97
5	30	74.12	84	97
6	30	75.29	84	97
7	30	75.29	85	97
8	30	75.29 [2.51]	85	98
			84 ± 1	97 ± 1

[a] Fluxes measured at 27 °C

From the experimental data presented in Figure 3.22 we can see that by running this diafiltration for 8 more volumes, which required 1.4 L of pure MeOH, it was possible to increase the yield from 49% to about 83%. However, purity got compromised, and dropped from 98 to about 96%. From the model it was expected that purity dropped even further, down to about 92%. However, this was not observed, perhaps because, as it can be seen from Figure 3.23, the BBR concentrations in the permeate were underestimated relatively to what was expected from the model.

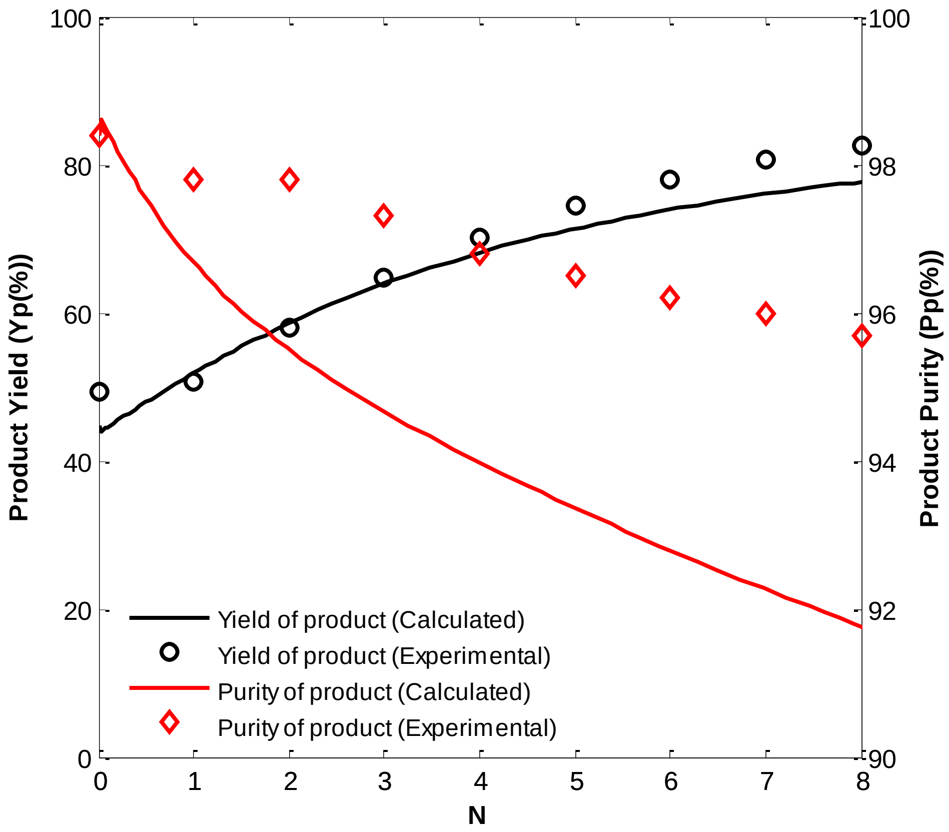

Figure 3.22 Yield and purity profiles for the purification of model mixture C after disconnecting the second cell from the system PI2211/TFRO-SG.

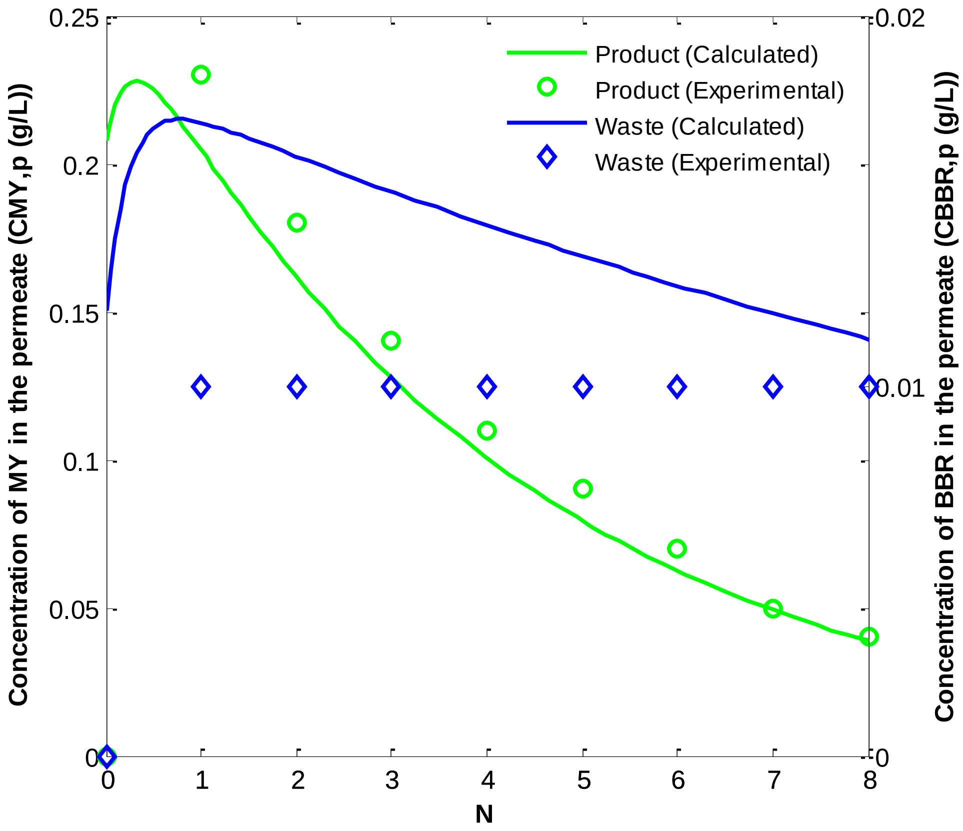

Figure 3.23 Experimental and calculated concentration profiles for the product (MY) and waste (BBR) in the permeate.

The performance of the two processes used to purify mixture C using PI2211 is summarized in Table 3.14. As it can be seen, by running a diafiltration with solvent recovery using the closed-loop process, it was possible to recover the same amount of product as with a single membrane process, without compromising the purity, and at the same time reduce the use of solvent in 36%.

Table 3.14 Comparison between the performance of the single membrane process with PI2211 membrane and the closed-loop membrane process with PI2211 and TFRO-SG membranes.

					PI2211		TFRO-SG	
Process	**Y_P (%)**	**P_P (%)**	**Vp (L)**	**Solvent saved (%)**	**$R_{MY,1}$ (%)**	**$R_{BBR,1}$ (%)**	**$R_{MY,2}$ (%)**	**$R_{BBR,2}$ (%)**
SM-PI2211	81	96	1.9	-	84	98	-	-
CL-PI2211/TFRO-SG	81	96	1.2[b]	36	91/84[c]	-/97[c]	96	-

[a] SM: single membrane; CL: closed-loop.
[b] Solvent only required after disconnect the cells
[c] Rejection before disconnect the cells/ Rejection after disconnect the cells

In section 3.1 it was concluded that the maximum yield obtained with the closed-loop membrane process is highly dependent on the membrane used for solvent recovery, that need to be the tightest possible in order to recover the maximum amount of product. From the results obtained so far with model mixture C it also became clear the importance of having a membrane able to completely reject the impurities in the purification stage (if they have a higher MW than the product). Consequently, and as a last attempt to find a membrane that complete rejected BBR, PBI 24xDBX membrane was applied on the purification of model mixture C using the single membrane process. The results for this diafiltratration are shown in the next subsection.

3.3.2.4. Purification using single membrane process with PBI 24xDBX membrane

The permeate fluxes and rejection of MY and BBR obtained with this system are summarized in Table 3.15. Again, a big difference between the MeOH and mixture C permeabilities was observed. In opposition to what happened in all other diafiltrations, this time an increase in the membrane flux over time was observed. This suggests that PBI 24xDBX disc did not compact during the diafiltration process. The flux could have increased because of a reduction of osmotic pressure, as MY was being removed from the system.

Table 3.15 Summary of the data recorded along the purification of model mixture C using the single membrane process with a PBI 24xDBX membrane.

N	ΔP (bar)	J (L.m-2.h-1)[a] [B ($L.m^{-2}.h^{-1}.bar^{-1}$)]	R_{MY} (%)	R_{BBR} (%)
MeOH	20	105.9[b] [5.3[c]]	-	-
1	20	21.8 [1.09]	96	100
2	20	22.4	96	100
3	21	23.2	96	100
5	21	22.9	96	100
7	21	24.1	96	100
9	20	24.1	95	100
11	21	24.1	95	100
13	21	26.3	95	100
14	21	25.9 [1.23]	95	100
			95 ± 0.5	100 ± 0

[a] Fluxes measured at 23°C
[b] Flux measured at 22 °C
[c] Permeability determined at 22 °C by plotting J_{MeOH} vs. ΔP: $J_{MeOH}=5.31.\Delta P$, $R^2=0.9998$

The mass profiles of the product (MY) and waste (BBR) are shown in Figure 3.24. Model 1 predicts mass profiles pretty consistent to what was observed for MY. Nevertheless, it was possible to have a better fitting between the calculated and experimental curves by correcting the MY rejection to 94%. This means that the rejection of the product was once again overestimated once again.

From the experimental mass profiles of BBR it seems that it was slightly washed away from the system, in opposition to what was expected from the calculated rejections. In fact, a better fitting between the calculated and experimental mass profiles was obtained by decreasing BBR rejection down to 98.5% (Model 2). BBR rejections were probably overestimated because this compound was present in the permeate in very tiny amounts, which made difficult to obtain the area of its characteristic peak in the chromatogram.

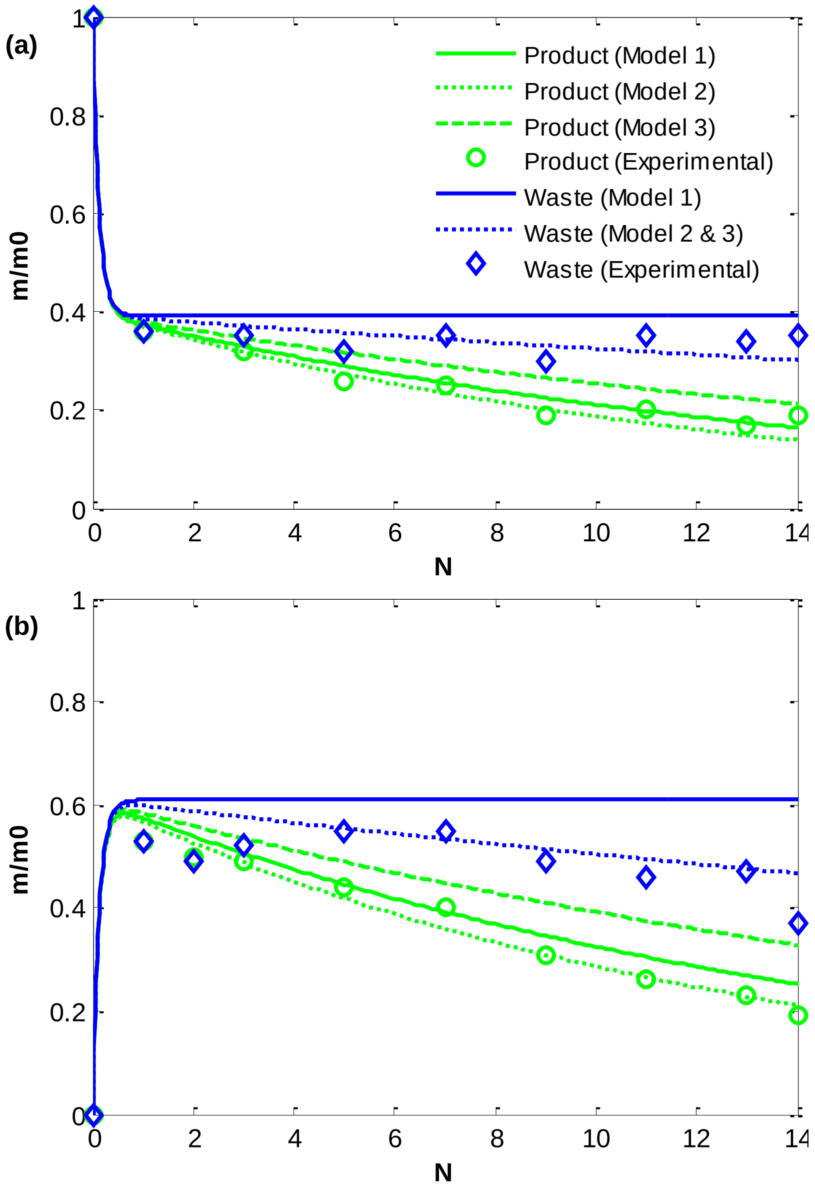

Figure 3.24 Calculated and experimental mass profiles of product (MY) and waste (BBR) in (a) feed tank and (b) membrane cell for the purification of model mixture C using single membrane process with a PBI 24xDBX disc at 21 bar and 23 °C. Curve fitting was done by assigning different values to R_{MY} and R_{BBR}: Model 1- R_{MY}=95%/R_{BBR}=100%; Model 2- R_{MY}=94%/R_{BBR}=98.5%; Model 3- R_{MY}=96.5%/R_{BBR}=98.5%.

The yield and purity profiles are presented in Figure 3.25. This time the experimental yield was determined in two different ways, based on the permeate concentrations (equation 3-6) - Yield of product (P) - and on the amount of MY removed from the feed and membrane cell (equation 3-4) - Yield of product (F+R). As it can be seen, neither Model 1 nor Model 2 gives a good fitting between the calculated yield profiles and the yield data calculated from the permeate concentrations. That is why a third model, Model 3, was proposed. This model gives a good description of the yield profile obtained from the permeate concentrations, although it leads to an overestimation of MY mass profiles (see Figure 3.24).

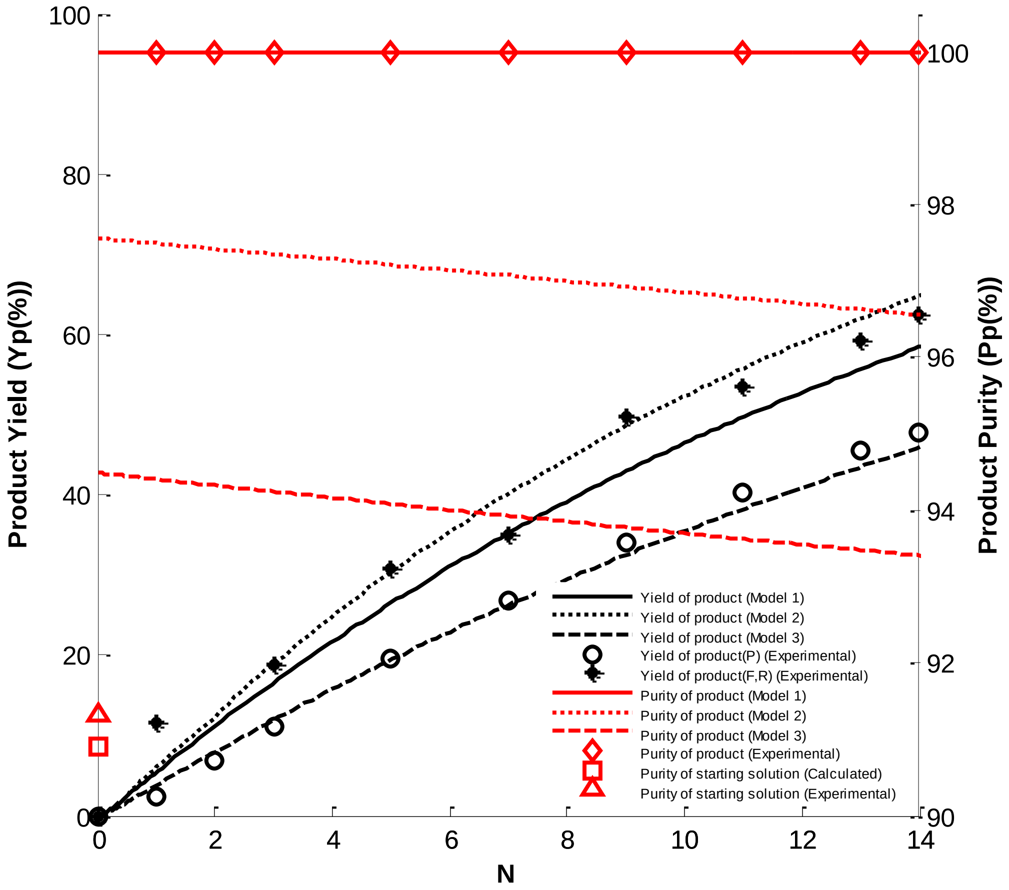

Figure 3.25 Yield and purity profiles for the purification of model mixture C using single membrane process with a PBI 24xDBX disc at 21 bar and 23 °C. Curve fitting was done by assigning different values to R_{MY} and R_{BBR}: Model 1- R_{MY}=95%/R_{BBR}=100%; Model 2- R_{MY}=94%/R_{BBR}=98.5%; Model 3- R_{MY}=96.5%/R_{BBR}=98.5%.

From Figure 3.26 it can be seen that Model 3 is the only model that gives a permeate concentration profile consistent with the measured concentrations of MY in the permeate, which may explain why Model 3 describes the Yield of product (P) so good. On the other hand, by calculating the yield based on the total amount of MY removed from the system (feed tank + membrane cell), we get a curve that is well described by Model 2. It seems then the permeate concentrations were not only underestimated for BBR, as discussed before, but also for MY. The underestimation can have two more possible explanations. One is the entanglement of the solutes in the membrane matrix, although this is not in accordance with the observed fluxes that, in this case, should have decreased due to pore blocking and hindered transport within the pores. The other reason is related to the membrane-solvent and membrane-solute interactions. It is possible that MeOH had a higher transport rate through the membrane, comparing to the solutes, and so that their permeate concentrations were lower than expected. An underestimation of the permeate concentrations can lead to and overestimation of the membrane rejections, which was in fact the case for this diafiltration.

The purity profiles predicted by Model 1 completely overlaps the experimental purity values, as this model considers that BBR was completely rejected by the membrane. However, we already concluded from the experimental mass profiles that this was not true, and that PBI

24xDBX membrane let some BBR permeate through it. Therefore, a purity profile like the one predicted from Model 2 should have been obtained.

From the experimental data, validated by Model 2, 62% of product was recovered after 14 diafiltration volumes by using the single membrane process with PBI 24xDBX membrane. This required the use of 2.7 L of fresh MeOH. Since no BBR was detected on the permeate by HPLC analysis, a product 100% pure was expected. However, mass profiles in the feed tank and membrane cell reveal that some BBR was actually removed from the system. Therefore, it is most likely that the product have been recovered with a purity of about 97%, as predicted by Model 2.

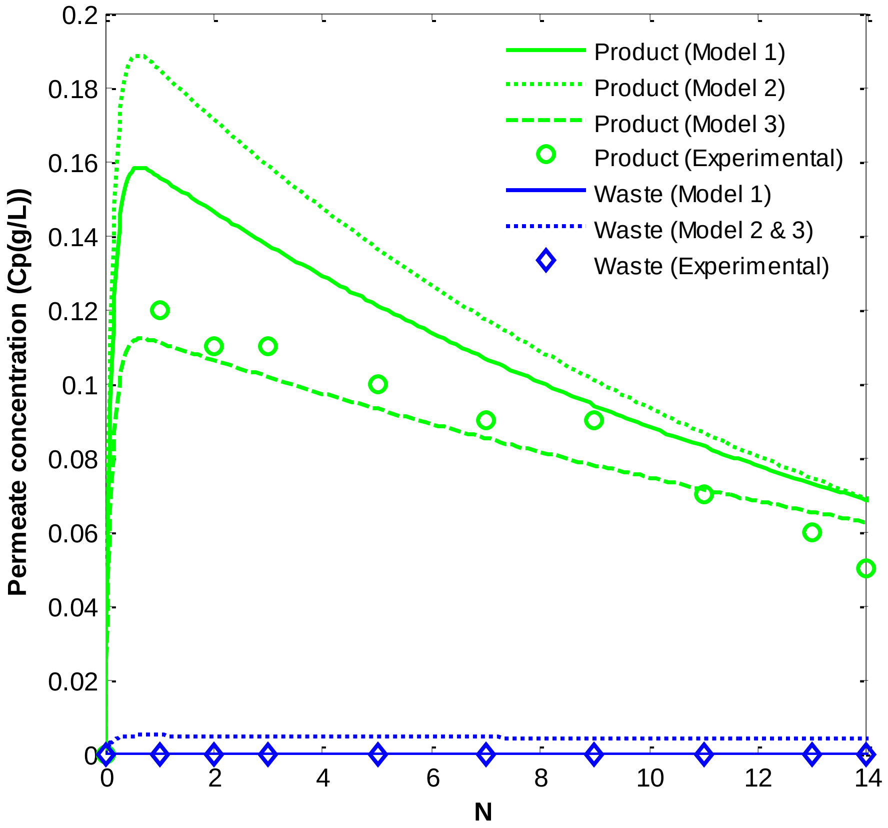

Figure 3.26 Experimental and calculated concentration profiles for the product (MY) and waste (BBR) in the permeate. Curve fitting was done by assigning different values to R_{MY} and R_{BBR}: Model 1- R_{MY}=95%/R_{BBR}=100%; Model 2- R_{MY}=94%/R_{BBR}=98.5%; Model 3- R_{MY}=96.5%/R_{BBR}=98.5%.

Despite this membrane did not complete rejected BBR it was decided to apply it in the closed-loop process. For the solvent recovery stage, another PBI membrane was considered. PBI 26xDBB membrane was chosen only because it was expected from the polymer concentration to be tighter than PBI 24xDBX when exposed to the same conditions. The results will be shown hereafter.

3.3.2.5. Purification using the closed-loop membrane process with PBI 24xDBX membrane for purification and PBI 26xDBB for solvent recovery

The permeate fluxes and rejection of MY and BBR obtained with this system are summarized in Table 3.16. Since PBI 26XDBB membrane is less permeable than PBI 24xDBX membrane, the flux was limited by the membrane used in the second stage.

Table 3.16 Summary of the data recorded along the purification of model mixture C using the closed-loop membrane process with a PBI 24xDBX membrane disc for purification and a PBI 26xDBB membrane disc for solvent recovery.

				PBI 24xDBX		**PBI 26xDBB**	
N	**ΔP_1 (bar)**	**ΔP_2 (bar)**	**J ($L.m^{-2}.h^{-1}$)[a] [B ($L.m^{-2}.h^{-1}.bar^{-1}$)]**	**$R_{MY,1}$ (%)**	**$R_{BBR,1}$ (%)**	**$R_{MY,2}$ (%)**	**$R_{BBR,2}$ (%)**
MeOH	10	15	51.76[b]/10.20[c] [5.31[d]/0.66[e]]	-	-	-	-
0.2	10	21	14.94 [1.49/0.71]	-	-	97	99
0.4	10	21	12.35	-	-	88	97
0.6	10	21	12.06	87	89	91	97
1.0	10	20	11.76	89	-	94	98
1.5	11	19	10.59	93	97	94	96
2.3	10.5	19.5	11.18	89	96	95	96
3	10.5	19.5	10.59	93	101	94	96
5	10	20	9.41	88	95	94	98
7	10	20	10.59	94	101	95	99
11	10	20	10.59	93	99	95	98
15	10	20	8.82	92	99	96	99
29	9	21	8.82 [0.98/0.42]	92	99	96	98
				91 ± 2	97 ± 4	94 ± 2	98 ± 1

[a] Fluxes determined at 24°C; [b] Flux determined at 22 °C; [c] Flux determined at 27 °C
[d] Permeability determined at 22 °C by plotting J_{MeOH} vs. ΔP: $J_{MeOH}=5.31.\Delta P$, $R^2=0.9998$
[e] Permeability determined at 22 °C by plotting J_{MeOH} vs. ΔP: $J_{MeOH}=0.66.\Delta P$, $R^2=0.9949$

Although consistent, the average rejections obtained for PBI 24xDBX are slightly lower than the rejections obtained for this same membrane in the previous diafiltration (Table 3.15: 95 ±

0.5 % for MY and 100 ± 0% for BBR). Higher rejections were obtained for PBI 26xDBB, which is also consistent with what was expected from the relative composition of these membranes in terms of polymer concentration. This is also in accordance to what we were looking for in terms of process feasibility, as the membrane used for solvent recovery needs to be the tightest as possible.

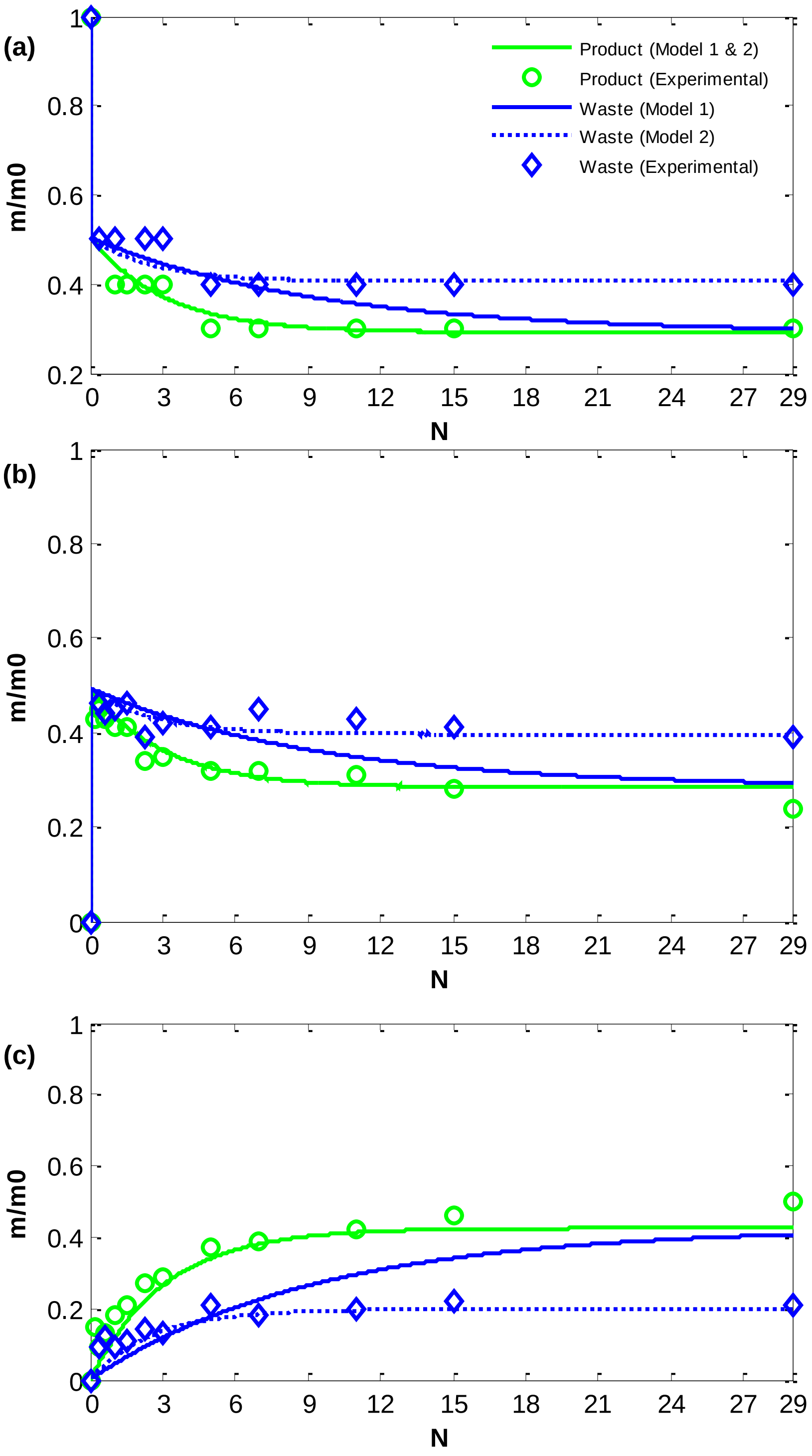

Figure 3.27 Calculated and experimental mass profiles of the product (MY) and waste (BBR) in (a) feed tank, (b) membrane cell 1 and (c) membrane cell 2 for the purification of model mixture C using closed-loop membrane process with a PBI 24xDBX and a PBI 26xDBB disc. Curve fitting was done by assigning different values to R_{MY} and R_{BBR}: Model 1- $R_{MY,1}$=91%, $R_{BBR,1}$=97%, $R_{MY,2}$=94% and $R_{BBR,2}$=98%; Model 2- $R_{MY,1}$=91% and $R_{BBR,1}$=95%, $R_{MY,2}$=94% and $R_{BBR,2}$=90%.

As it can be seen from Figure 3.27, a good fitting was obtained between the calculated and experimental mass profiles for MY, considering an average of the calculated rejections (Model 1). However, the same did not happen for BBR. Model 1 seems to underestimate the mass profile of BBR in the feed and first membrane cell and overestimate the mass profile in the second membrane cell after 6-7 volumes. To have a good fitting the rejections of PBI 24xDBX and PBI 26xDBB membranes for BBR needed to be corrected to 95 and 90%, respectively (Model 2). These rejections are lower than the calculated, which mean that they were overestimated. This may have happened again because of an underestimation of the BBR concentration in the permeate of the second membrane. However, it is still hard to explain why the corrected rejection of BBR is lower for PBI 26xDBB membrane, which is supposed to be the tightest of the two membranes used.

From Figure 3.28 it can be seen that Model 1 gives a great description of the yield profile. Not so good is the purity profile predicted from this model, as it nothing has to do with the experimental data. However, by using the corrected values of BBR rejections (Model 2) a more realistic purity profile was obtained.

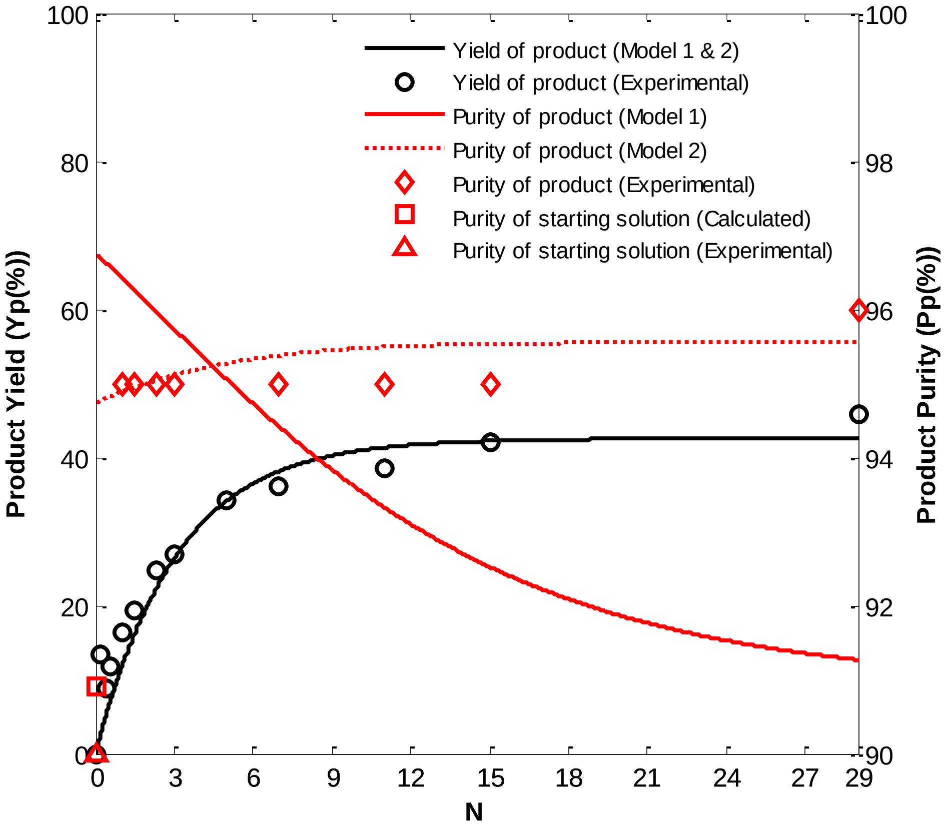

Figure 3.28 Yield and purity profiles for the purification of model mixture C using closed-loop membrane process with a PI2211 and a TFRO-SG disc. Curve fitting was done by assigning different values to R_{MY} and R_{BBR}: Model 1- $R_{MY,1}$=91%, $R_{BBR,1}$=97%, $R_{MY,2}$=94% and $R_{BBR,2}$=98%; Model 2- $R_{MY,1}$=91% and $R_{BBR,1}$=95%, $R_{MY,2}$=94% and $R_{BBR,2}$=90%..

By applying the closed-loop membrane process to mixture C (90% pure) it was possible to recover 45% of the product with a purity of about 96%, without adding more solvent. Once again it was not possible to reach the yield achieved by using the single membrane process. Thus, in order to have comparable results, the cells were disconnected and the diafiltration continued until the same amount of MY have been recovered. The data for this diafiltration is shown in Table 3.17 and Figure 3.29.

Table 3.17 Summary of the data recorded along the diafiltration of model mixture C using the single membrane process with a PBI 24xDBX membrane disc after disconnected the cells.

N	ΔP_1 (bar)	J (L.m-2.h-1)[a] [B(L.m^{-2}.h^{-1}.bar^{-1})]	$R_{MY,1}$ (%)	$R_{BBR,1}$ (%)
1	10	1.0 [0.1]	86	99
2	10	1.0	92	99
6	10	1.0	93	99
			90 ± 3	99 ± 0

[a] Fluxes measured at 25 °C

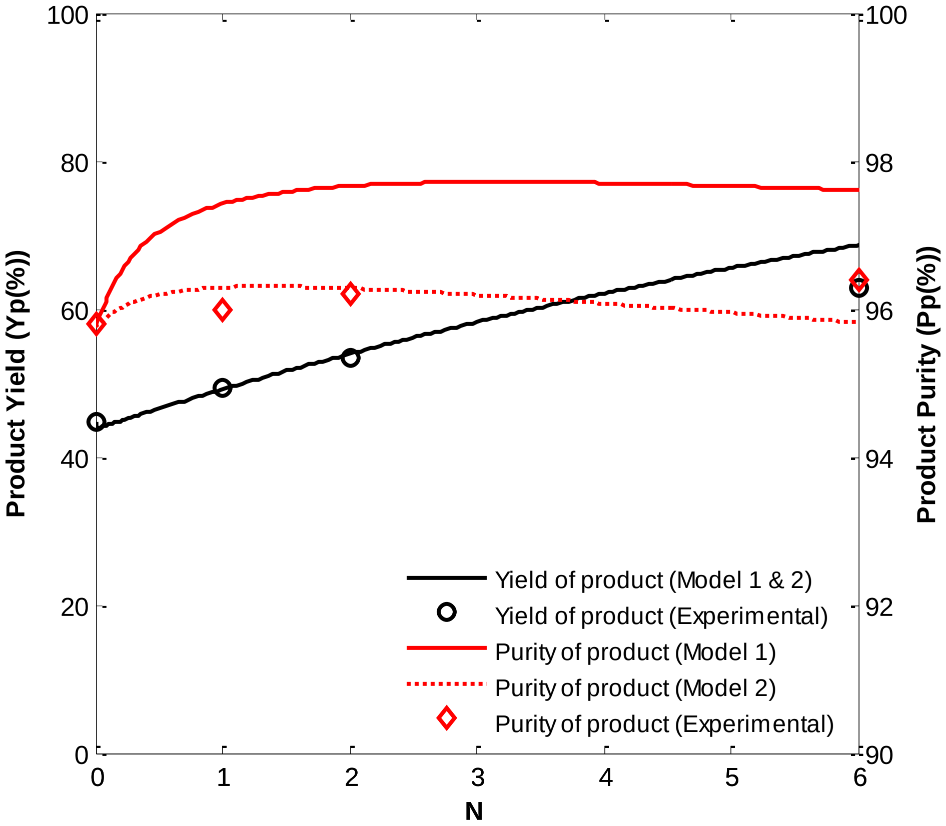

Figure 3.29 Yield and purity profiles for the purification of model mixture C after disconnecting the second cell from the system PBI 24xDBX/PBI 26xDBB. Curve fitting was done by assigning different values to R_{MY} and R_{BBR}: Model 1- $R_{MY,1}$=90%/$R_{BBR,1}$=99%; Model 2- $R_{MY,1}$=90%/$R_{BBR,1}$=98%;

Despite Model 1 gives a good fitting between the calculated and experimental yield profiles, the rejection of BBR needed to be corrected to have a better description of the actual purity profile (Model 2). Six diafiltration volumes, which correspond to 1.1 L of pure MeOH were required to reach 63% yield and have a final purity of 96%.

The performance of the two processes used to purify mixture C using PBI 24xDBX is summarized in Table 3.18. As it can be seen, the closed-loop membrane process allowed to save 59% of the solvent required to perform a conventional diafiltration and achieve about the same yield and purity.

Table 3.18 Comparison between the performance of the single membrane process with PBI 24xDBX membrane and the closed-loop membrane process with PBI 24xDBX and PBI 26xDBB membranes.

					PBI 24xDBX		PBI 26xDBX	
Process[a]	**Y_P (%)**	**P_P (%)**	**V_p (L)**	**Solvent saved (%)**	**$R_{MY,1}$ (%)**	**$R_{BBR,1}$ (%)**	**$R_{MY,2}$ (%)**	**$R_{BBR,2}$ (%)**
SM-PBI 24xDBX	62	97	2.7	-	94	98.5	-	-
CL-PBI 24xDBX/PBI 26xDBB	63	96	1.1[b]	59	91/90[c]	95/98[c]	94	90

[a] SM: single membrane; CL: closed-loop.
[b] Solvent only required after disconnect the cells
[c] Rejection before disconnect the cells/ Rejection after disconnect the cells

3.3.3. Conclusions

The change of solvent from DMF to MeOH resulted in a bad strategy to fully demonstrate the feasibility of the closed-loop membrane process. By using MeOH all the membranes tested revealed to be too loose for both the purification and the solvent recovery stage, probably due to a higher contribution of the convective flow, as MeOH was found to be more permeable than DMF. Like this both the yield (< 90%) and the purity (~96%) achieved by using the considered membrane systems (PI2211/TF-ROSG and PBI 24xDBX/PBI 26xDBB) ended up to be too low for a pharmaceutical application.

Chapter 4

Membrane cascade

A complete separation between two compounds in a liquid mixture is only achievable by OSN if one of the compounds is completely retained and the other is allowed to pass through unhindered. However not impossible, as it was shown for model mixture A, it is not always easy to find a membrane with that characteristics for a real separation problem, especially for those encountered in the synthesis of APIs where molecules can have different physical and chemical properties and where separation is not only based on steric effects.

Oligonucleotides (short chains of DNA and RNA) and peptides have a lot of potential therapeutic applications, so there has been a great effort to develop efficient large-scale processes to synthesize these compounds. OSN was already successfully used for in-cycle purification during both oligonucleotide and peptide synthesis (So et al., 2010). However, these processes still require a large amount of solvent, and a long filtration period (Kim, 2011).

It was already proved in this study that the closed-loop membrane process can considerably reduce the amount of solvent required by continuous diafiltration process, by proper selection of the membranes. The use of a membrane cascade for purification, instead of a single membrane unit, would allow to use looser membranes, and consequently to speed up the process without compromising the yield and purity.

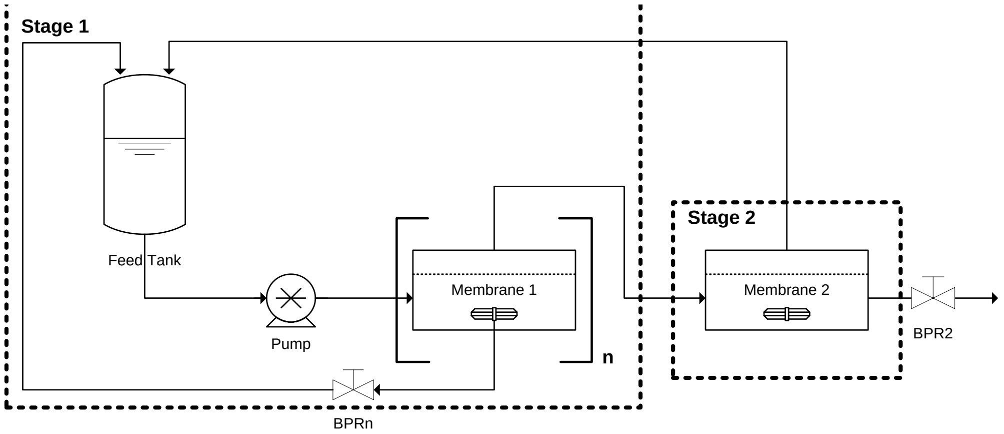

Figure 4.1 Schematic representation of the closed-loop membrane process integrating a cascade of n membrane units for purification.

The proposed design for the closed-loop membrane process integrating a membrane cascade of n membrane units for purification is shown in Figure 4.1. Like for the simple closed-loop membrane process, stage 1 is enriched in the component with the highest rejection, while stage 2 gets enriched in the component with the lowest rejection.

To assess the potential of integrating a membrane cascade on the closed-loop membrane process for improve its separation performance towards a crude product from an actual oligonucleotide synthesis step, simulations were carried on using the performance data from the single membrane purification experiments.

Before performing the diafiltration over the crude product, membranes were screened using model mixtures D1 and D2, to select the most suitable membrane for the cascade purpose. These results will be shown bellow in the first section of this chapter, together with the results for the single membrane purification using the chosen membrane.

4.1. SINGLE MEMBRANE EXPERIMENTS

4.1.1. Experimental

4.1.1.1. Membrane screening

Screening 1

Four different membranes, PI2321, PI2341, PBI 17xDBX and TFC-HDA membrane, were screened against model mixture D1 on an 8-cell cross-flow rig like the one described in section 3.3.1. The rig was first washed three times with 1.5 L of MeCN at 20 bar for 2h. Then two discs of each membrane to be screened were loaded onto the system and washed for 2h at 10 bar and 25 °C. After washing, the system was drained and reloaded with 1.5 L of model mixture D1, polyethylene glycol 400 (PEG400), polyethylene glycol 2000 (PEG2000) and polyethylene glycol 8000 (PEG8000) (1 $g.L^{-1}$ each) in MeCN. The screening test was carried out at 10 bar and 25 °C for 24 h. Samples were taken from the feed and each permeate line after 5 and 24 hours of operation and analyzed by HPLC.

Screening 2

This time the same membranes, except TFC-HDA that was replaced by PI2210 membrane, were screened against model mixture D2. The rig was again washed two times with 1.5 L of MeCN at 20 bar for 2h. Then two discs of each membrane to be screened were loaded to the system and washed for 2h at 10 bar and 25 °C. After washing, the system was drained and reloaded with 1.5 L of model mixture D2, a mixture similar to mixture D1 to which the succinate nucleotide (0.2 $g.L^{-1}$) was added. Samples were taken from the feed and each permeate line after 2 and 16 hours of operation and analyzed by HPLC.

4.1.1.2. Purification using single membrane system

The system described in sub-section 2.3.2.2 was used to diafilter the product crude from the synthesis of oligonucleotides. A disc of PI2341, the membrane selected from the screening tests, was loaded onto the cell and washed with pure MeCN at 6-8 bar until no PEG400 trace was detected in the permeate by HPLC analysis. During washing the pump flow rate was set at 48 $mL.min^{-1}$, since the MeCN flux was extremely high. After washing the system, the solvent feed tank was replaced by a 250 mL flask containing a 0.1 $g.L^{-1}$ solution of the crude product from an oligonucleotide synthesis step, and the diafiltration started. At this point the pump flow rate was reduced to 9 $mL.min^{-1}$, and the system components stirred at 250 rpm.

4.1.2. Results & Discussion

4.1.2.1. Membrane screening

Screening tests were made in order to select the better membrane to separate an oligonucleotide intermediate (polymer), with a MW of 6900 g.mol^{-1}, from the excess nucleotides (monomer), which have a MW of 700 g.mol^{-1}. A good membrane for this purpose is a membrane with a MWCO much lower than 6900 in order to completely retain the polymer, which should be relatively easy for OSN membranes, but simultaneously with a MWCO sufficiently higher than 700, so the monomer can easily permeate through the membrane.

Screening 1

Figure 4.2 shows the flux profile for each membrane tested in using model mixture D1. For most of the membranes, steady state was observed after 5 h of continuous operation.

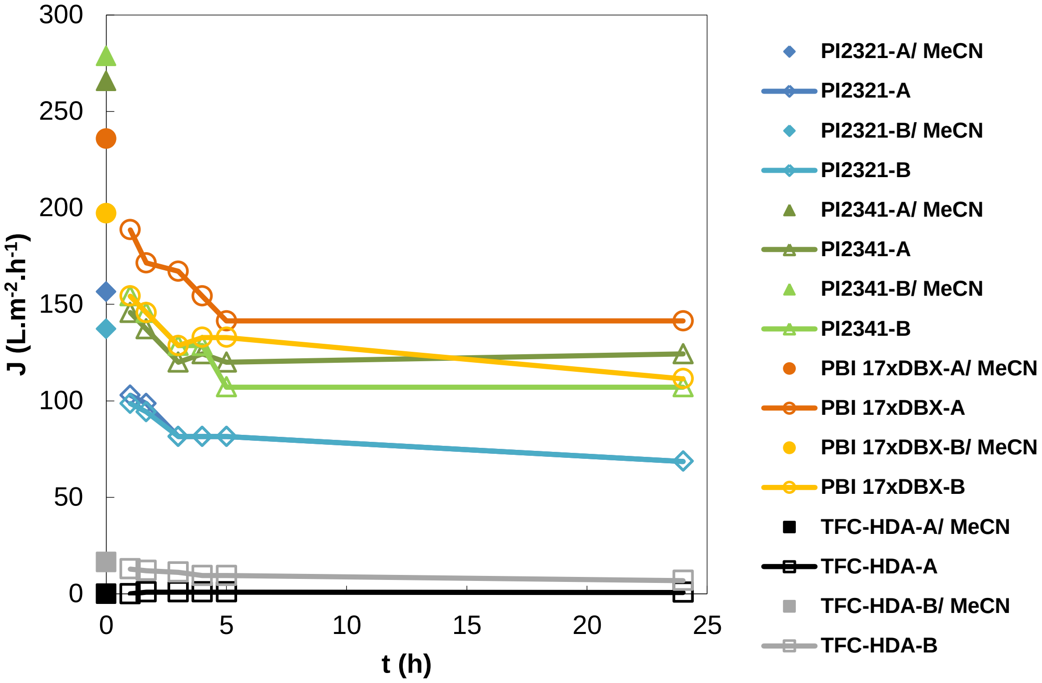

Figure 4.2 Flux profiles over time at 10 bar and 25°C for the membranes screened using model mixture D1. The flux at time 0 is the flux of pure MeCN.

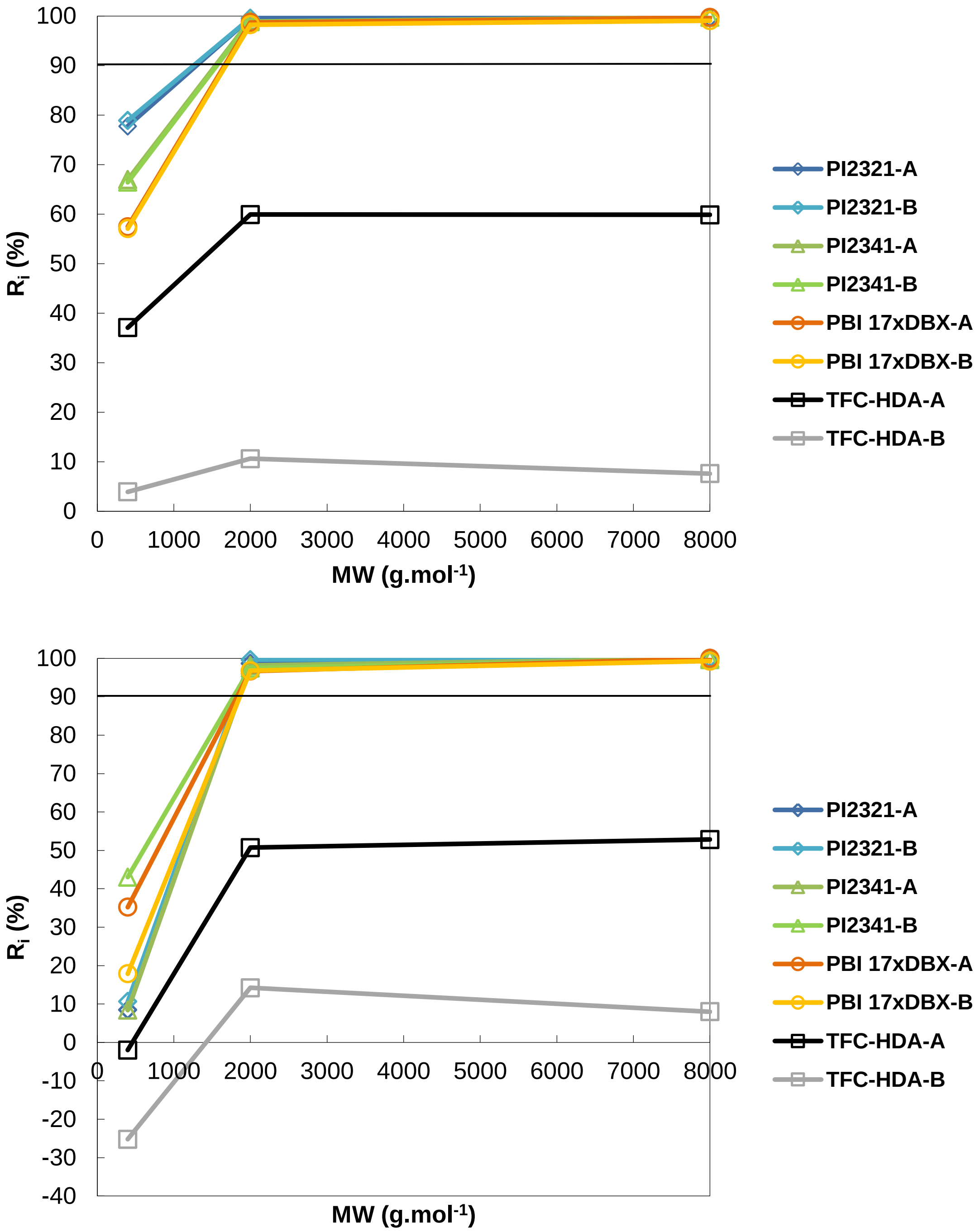

Figure 4.3 Rejection curves in for the membranes screened in MeCN at 10 bar and 25°C after a) 5 hours and b) 24 hours of continuous operation.

The rejection curves after 5 and 24 hours are presented in Figure 4.3. We can see that all the curves from Figure 4.3-b are dislocated to the bottom, comparing to those in Figure 4.3-a. This was due to a problem in the HPLC that did not allow for a proper analysis of the samples. Nevertheless, we can see that PI2321, PI2341, and PBI 17xDBX membranes showed a sufficiently low MWCO, between 1000 and 2000, to retain the polymer. Both PI2341 and PBI 17xDBX membranes have the higher MWCO in this range, which is also convenient to allow the monomer to be easily washed away from the system. Plus they presented the highest fluxes from all the membranes screened. The screening using model mixture D2 allowed to decide between the two.

Screening 2

The flux profile for the membranes screened against model mixture D2 is presented in Figure 4.4. The fluxes higher than 500 L.m^{-2}.h^{-1} exhibited by some membranes for MeCN are not shown. In this case, steady state was achieved after 2 h, except for the PI2210 membrane, a very loose membrane for which the flux continued to drop, probably due to compaction. The fluxes measured for PI2321 membrane using this model mixture are consistent with the results from the previous screening, but are relatively lower for PI2321 and PBI 17xDBX membranes.

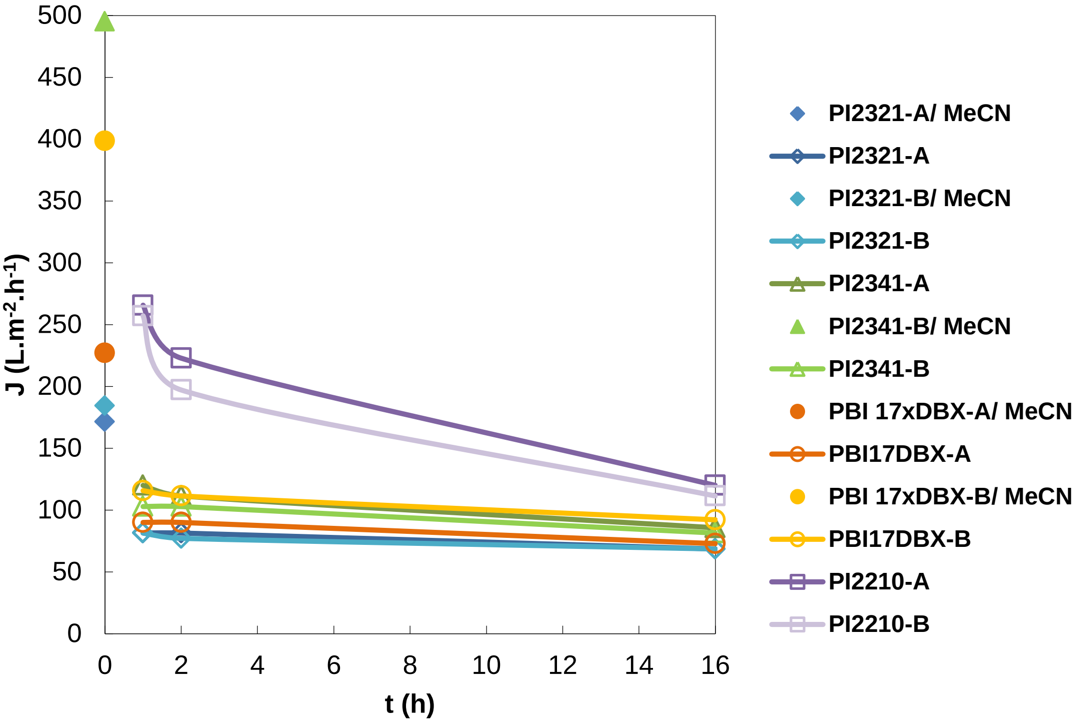

Figure 4.4 Flux profiles over time at 10 bar and 25°C for the membranes screened using model mixture D2. The flux at time 0 is the flux of pure MeCN.

Table 4.1 summarizes the rejections of the membranes for each compound present in model mixture D2. Once again, the rejections for PEG400 were too low due to a problem with the HPLC that was affecting the chromatograms at lower retention times. That is why the samples taken after 16 hours were not analyzed and that is why these results are not shown.

Despite the monomer has a lower molecular weight than PEG2000 or PEG8000, a higher rejection was obtained for this compound. This has to do with its negative charge that does not allow the separation to be based only in the size. From all the membranes tested, PI2210 and PI2341 membranes presented the lowest rejection for this compound. Although the difference between the rejection of the monomer and PEG8000 was larger for PI2210 membrane, PI2341 membrane presented the highest rejection for the higher MW compound. Thus, it was decided to apply PI2341 membrane on the diafiltration of the crude product.

Table 4.1 Rejections after 2h of operation at 10 bar and 25 °C for the different membranes tested against model mixture D2.

Membrane	R_i (%)			
	PEG400	**PEG2K**	**PEG8K**	**Monomer**
PI2321-A	10.3%	92.6%	99.6%	≥99.7%
PI2321-B	43.0%	92.3%	99.3%	≥99.7%
PI2341-A	20.6%	91.8%	99.7%	94.2%
PI2341-B	23.9%	89.8%	99.7%	95.2%
PBI 17xDBX-A	26.4%	93.6%	99.7%	≥99.7%
PBI 17xDBX-B	29.5%	89.4%	99.7%	≥99.7%
PI2210-A	13.2%	73.5%	74.1%	67.9%
PI2210-B	12.7%	79.0%	84.6%	73.4%

4.1.2.2. Purification using single membrane process

The permeate fluxes and rejections of PI2341 membrane during the diafiltration process are summarized in Table 4.2. The flux is a bit lower than expected from the screening tests. However, the average rejection obtained for the monomer is quite consistent with the rejections obtained for the second screening test (see Table 4.1).

Table 4.2 Performance data for the purification of the product crude using PI2341 membrane at 21 °C.

			R_i (%)	
N	**ΔP (bar)**	**J ($L.m^{-2}.h^{-1}$)[a] [B ($L.m^{-2}.h^{-1}.bar^{-1}$)]**	**Monomer**	**Polymer**
1	10	55.29 [5.53]	94.5	95.6
2	13	67.06	96.3	96.4
3	13	67.06	96.6	96.3
4	13	67.06	-	-
5	13	67.06	-	-
6	13	58.82	92.0	95.4
7	13	58.82	-	-
8	13	58.82	-	-
9	14	65.88	-	-
10	15	69.41 [4.63]	93.9	93.7
			94.6 ± 1.9	95.5 ± 1.1

The mass profiles for both the polymer (product) and the monomer (waste) are shown in Figure 4.5. As it can be seen, no separation would be achieved if the membrane had in fact rejections of 94.6 and 95.5% for the monomer and the product, respectively. By correcting the rejections of the polymer and the monomer to 92 and 84% a better fitting between the calculated curve and the experimental data was obtained. These were assumed as the real rejections and used in the cascade simulations presented in the next section.

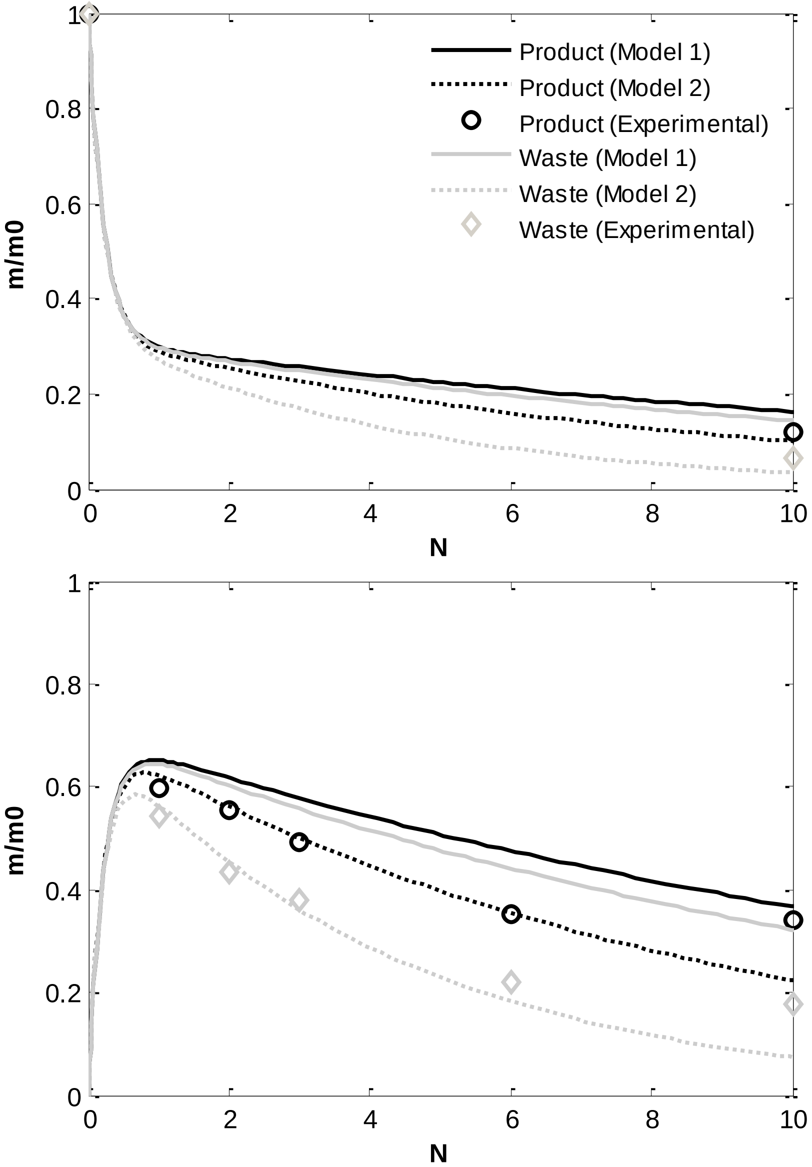

Figure 4.5 Experimental and calculated mass profiles for the polymer (product) and monomer (waste) using the single membrane process with a PI2341 membrane at 10-15 bar and 21 °C. Calculated curves were obtained considering the an average of the calculated rejections, $R_{polymer}=95.5\%$ and $R_{monomer}=94.6\%$. (Model 1) and corrected values, $R_{polymer}=92\%$ and $R_{monomer}=84\%$. (Model 2).

4.2. MEMBRANE CASCADE MODELLING

The closed-loop membrane process integrating a membrane cascade for purification was modeled by writing a mass balance around the separation stage (Stage 1) and the solvent recovery stage (Stage 2). The concentration profiles of the product and impurity in stages 1 and 2 were calculated in MATLAB using the process model described in Appendix C and by assuming feed concentrations of 0.05 g.L^{-1} for both compounds, that all membrane units in stage 1 were characterized by the corrected rejections obtained for the PI2341 membrane, and that a tight membrane with a rejection of 100% for both monomer and polymer was used for solvent recovery. The concentration profiles were then used to determine the yield and purity profiles. Since the product is, in this case, the compound with the highest rejection, the yield and purity of product were calculated using the concentrations in the first stage:

$$Y_P = \frac{C_{R1,i} . V_1}{C_{F,i,0} . V_F} \times 100 \qquad \textbf{4.1}$$

$$P_P = \frac{C_{R1,i}}{\sum C_{R1,i}} \times 100 \qquad \textbf{4.2}$$

where $C_{R1,i}$ is the concentration of component i in the first stage, $C_{F,i,0}$ is the initial concentration of component i in feed tank, V_1 is the volume of system 1 and V_F is the volume of the feed tank.

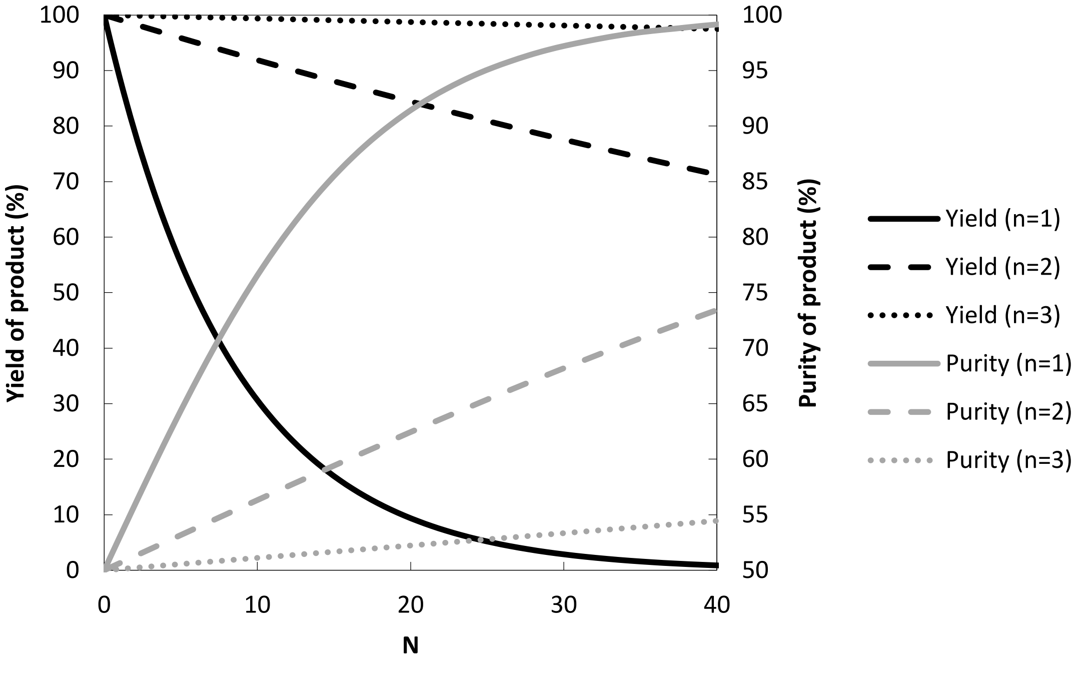

Figure 4.6 Yield and purity profiles as a function of the number of membrane units used for purification. Simulations performed by assuming that $R_{polymer}$=92% and $R_{monomer}$=84%..

In Figure 4.6 are presented the yield and purity profiles as a function of the number of units used for purification, n. As it can be seen, the yield increases from about 1% to 97% after 40 volumes by increasing the number of purification units from 1 to 3. However, the purity gets really compromised and drops from 99% to a little more than 54% after the same number of volumes. With a cascade with only 2 membrane units it is also possible to increase the yield comparing to a single membrane unit, but even so the purity obtained, ~73%, is too low for an API intermediate.

Table 4.3 presents the overall rejections, $R_{cascade,i}$, of the separation stage as a function of the number of membrane units used for purification. This parameter can be calculated by

$$R_{i,cascade}=1-(1-R_i)^n \tag{4.3}$$

if it is assumed that all the membranes in the cascade have the same rejection, R_i (see Appendix C).

As it can be seen from Table 4.3 the rejection of the separation stage increases exponentially with the number of modules; this increase is desirable for the product but not for the impurity as like this it makes it difficult of being washed away from the purification stage in a feasible time scale.

Table 4.3 Overall rejections, $R_{cascade,i}$, of the separation stage as a function of the number of membrane units used for purification.

	$R_{cascade,i}$ (%)	
n	**Monomer**	**Polymer**
1	84.0	92.0
2	97.4	99.4
3	99.6	99.9

It seems then that to achieve simultaneously a high product yield and purity it is important to use membranes with a high rejection for the product, but is also necessary that the membrane have a low rejection for the impurity.

4.3. CONCLUSIONS

In this chapter it was proposed the integration of a membrane cascade in the closed-loop membrane process, to improve the separation performance realized by a single membrane. As case study it was used a crude product from an actual oligonucleotide synthesis step, containing oligonucleotide intermediates (polymer) and nucleotides (monomer).

Simulations showed that it is possible to increase the yield by increasing the number of membrane units in the cascade. However this increase is accompanied by a prohibitive decrease in the product purity. Consequently it was not possible to show any advantages of increasing the number of modules for purification in the closed-loop membrane process by using the PI2341 membrane.

The drop in purity was found to be related with the increase of the overall rejections with the number of membrane units, and not with a loss of selectivity. Since this increase is something unavoidable in a cascade and desirable when the product is the compound with the higher MW, it was concluded that the feasibility of the cascade depends on the membrane applied on it that should present a large difference between the rejections of the two compounds to be separated.

It should be mentioned that the simulations performed were based on a simplistic model that considers the whole cascade unit as one system, not taking into account all the process parameters and variables that may possibly affect the cascade performance. A model resultant from the mass balance around each component of the process would allow for a more realistic description, and consequently for a better assessment of the factors affecting the cascade yield and purity.

Chapter 5

Conclusion Remarks and Future Work

Two model mixtures of dyes with MW in the OSN range were diafiltered in a closed-loop membrane system using solvents widely used in the pharmaceutical industry, *N,N*-dimethylformamide (DMF), in model mixture A, and methanol (MeOH), in model mixture C. These mixtures were so challenging in terms of separation that it was necessary to disconnect the two membrane units at some point and continue the diafiltration using only the first membrane, which required using fresh solvent. With model mixture A it was possible to show a reduction of 43% in the solvent consumption, comparing to the amount of solvent required by a single membrane process, and meet the yield (> 90%) and purity (>99%) targets, by using two crosslinked polyimide membranes. Unfortunately, the separation between the two model compounds got even more challenging by using MeOH as solvent. Consequently, and despite the high percentage of solvent savings (59%) achieved by using a combination of two crosslinked polybenzimidazole membranes, the yield and specially the purity (~96%) turned out to be too low to show the feasibility of the process.

Although the concept of the closed-loop membrane process for the purification of API was demonstrated with this work, it was found that to operate the process without the need for extra solvent, the membrane used in the solvent recovery stage must be as tight as possible, so only the solvent can permeate through it. Plus, in order to meet the high standards of purity demanded by the pharmaceutical industry it is also important for the membrane used in the purification stage to have a high rejection for the higher MW compound.

A cascade of membranes was considered to improve the separation in the closed-loop membrane process. The effect of increasing the number of membrane units for purification was assessed through simulations using the performance data from single membrane experiments over an actual separation challenge – the crude product of an intermediate synthesis step for the production of oligonucleotides, where the impurities (excess nucleotides) have a MW lower than the product (oligonucleotide intermediate). It can be concluded that the feasibility of a membrane cascade for purification of APIs depends on the membrane selected for that purpose, which should have a large difference between the rejections of the two compounds to be separated. However, a more detailed process model should be developed in order to better understand the parameters influencing its performance. After this the concept of the process should be experimentally demonstrated.

References

Agrawal, R. (1997) A simplified method for the synthesis of gas separation membrane cascades with limited numbers of compressors. *Chemical Engineering Science.* 52 (6), 1029-1044.

Agrawal, R. (1996) Membrane Cascade Schemes for Multicomponent Gas Separation. *Industrial & Engineering Chemistry Research.* 35 (10), 3607-3617.

Agrawal, R. & Xu, J. (1996a) Gas separation membrane cascades II. Two-compressor cascades. *Journal of Membrane Science.* 112 (2), 129-146.

Agrawal, R. & Xu, J. (1996b) Gas-separation membrane cascades utilizing limited numbers of compressors. *AIChE Journal.* 42 (8), 2141-2154.

Baker, R. W. (2006) Membrane Technology in the Chemical Industry: Future Directions. In: Anonymous *Membrane Technology.* , Wiley-VCH Verlag GmbH & Co. KGaA. pp. 305-335.

Baker, R. W. (2004) *Membrane Technology and Applications.* 2nd edition. , John Wiley & Sons, Ltd.

Barker, P. E. & Till, A. (1992) Using multistage techniques to improve diafiltration fractionation efficiency. *Journal of Membrane Science.* 72 (1), 1-11.

Bellona, C. & Drewes, J. E. (2005) The role of membrane surface charge and solute physico-chemical properties in the rejection of organic acids by NF membranes. *Journal of Membrane Science.* 249 (1–2), 227-234.

Benedict, M., Pigford, T. H. & Levi, H. W. (1981) *Nuclear Chemical Engineering.* 2nd edition. , McGraw-Hill.

Bhanushali, D., Kloos, S. & Bhattacharyya, D. (2002) Solute transport in solvent-resistant nanofiltration membranes for non-aqueous systems: experimental results and the role of solute–solvent coupling. *Journal of Membrane Science.* 208 (1–2), 343-359.

Boam, A. & Nozari, A. (2006) Fine chemical: OSN – a lower energy alternative. *Filtration & Separation.* 43 (3), 46-48.

Bowen, W. R. & Welfoot, J. S. (2002) Modelling the performance of membrane nanofiltration—critical assessment and model development. *Chemical Engineering Science.* 57 (7), 1121-1137.

Carey, J. S., Laffan, D., Thomson, C. & Williams, M. T. (2006) Analysis of the reactions used for the preparation of drug candidate molecules. *Organic & Biomolecular Chemistry.* 4 (12), 2337-2347.

Carl Roth. (2012) *Technical Info- Coomassie Brilliant Blue and mechanisms of protein staining and Bradford-assay.* [Online] Available from: http://www.carlroth.com/website/de-ch/pdf/Coomassie_E.pdf .

Caus, A., Braeken, L., Boussu, K. & Van der Bruggen, B. (2009) The use of integrated countercurrent nanofiltration cascades for advanced separations. *Journal of Chemical Technology & Biotechnology.* 84 (3), 391-398.

Constable, D. J. C., Jimenez-Gonzalez, C. & Henderson, R. K. (2007) Perspective on Solvent Use in the Pharmaceutical Industry. *Organic Process Research & Development.* 11 (1), 133-137.

Cuperus, F. P. & Smolders, C. A. (1991) Characterization of UF membranes: Membrane characteristics and characterization techniques. *Advances in Colloid and Interface Science.* 34 (0), 135-173.

de la Garza, A. (1963) A generalization of the matched abundance-ratio cascade for multicomponent isotope separation. *Chemical Engineering Science.* 18 (2), 73-82.

Deen, W. M. (1987) Hindered transport of large molecules in liquid-filled pores. *AIChE Journal.* 33 (9), 1409-1425.

Dijkstra, M. F. J., Bach, S. & Ebert, K. (2006) A transport model for organophilic nanofiltration. *Journal of Membrane Science.* 286 (1–2), 60-68.

Dunn, P. J., Wells, A. & Williams, M. T. (2010) *Green Chemistry in the Pharmaceutical Industry.* Weinheim, Wiley-VCH.

Evangelista, F. (1987) Approximate design method for reverse osmosis plants equipped with imperfectly rejecting membranes. *Industrial & Engineering Chemistry Research.* 26 (6), 1109-1116.

Evonik Industries. (2012) *About DuraMem and PuraMem.* [Online] Available from: http://duramem.evonik.com/product/duramem-puramem/en/about/pages/default.aspx .

Ferry, J. D. (1936) *Statistical evaluation of sieve constants in ultrafiltration.*

Florian, E., Modesti, M. & Ulbricht, M. (2007) Preparation and Characterization of Novel Solvent-Resistant Nanofiltration Composite Membranes Based on Crosslinked Polyurethanes. *Industrial & Engineering Chemistry Research.* 46 (14), 4891-4899.

Geens, J., Hillen, A., Bettens, B., Van der Bruggen, B. & Vandecasteele, C. (2005) Solute transport in non-aqueous nanofiltration: effect of membrane material. *Journal of Chemical Technology & Biotechnology.* 80 (12), 1371-1377.

Gevers, L. E. M., Vankelecom, I. F. J. & Jacobs, P. A. (2006) Solvent-resistant nanofiltration with filled polydimethylsiloxane (PDMS) membranes. *Journal of Membrane Science.* 278 (1–2), 199-204.

Ghazali, N. F., Ferreira, F. C., White, A. J. P. & Livingston, A. G. (2006) Enantiomer separation by enantioselective inclusion complexation–organic solvent nanofiltration. *Tetrahedron: Asymmetry.* 17 (12), 1846-1852.

Ghosh, R. (2003) Novel cascade ultrafiltration configuration for continuous, high-resolution protein–protein fractionation: a simulation study. *Journal of Membrane Science.* 226 (1–2), 85-99.

Gibbins, E., D'Antonio, M., Nair, D., White, L. S., Freitas dos Santos, L. M., Vankelecom, I. F. J. & Livingston, A. G. (2002) Observations on solvent flux and solute rejection across solvent resistant nanofiltration membranes. *Desalination.* 147 (1–3), 307-313.

Golemme, G. & Drioli, E. (1996) *Polyphosphazene membrane separations—Review.* Springer Netherlands.

Gryta, M., Karakulski, K. & Morawski, A. W. (2001) Purification of oily wastewater by hybrid UF/MD. *Water Research.* 35 (15), 3665-3669.

Halle, E. V. & Shacter, J. (2000) Diffusion Separation Methods. In: Anonymous *Kirk-Othmer Encyclopedia of Chemical Technology.* , John Wiley & Sons, Inc.

He, Y., Li, G., Wang, H., Jiang, Z., Zhao, J., Su, H. & Huang, Q. (2010) Diafiltration and water recovery of Reactive Brilliant Blue KN-R solution by two-stage membrane separation process. *Chemical Engineering and Processing: Process Intensification.* 49 (5), 476-483.

Higuchi, A., Higuchi, Y., Furuta, K., Yoon, B. O., Hara, M., Maniwa, S., Saitoh, M. & Sanui, K. (2003) Chiral separation of phenylalanine by ultrafiltration through immobilized DNA membranes. *Journal of Membrane Science.* 221 (1–2), 207-218.

Hoover, K. C. & Hwang, S. (1982) Pervaporation by a continuous membrane column. *Journal of Membrane Science.* 10 (2–3), 253-271.

Hwang, S. T. & Kammermeyer, K. (1975) *Membranes in Separations.* , Wiley.

Hwang, S. & Kammermeyer, K. (1965) Operating lines in cascade separation of binary mixtures. *The Canadian Journal of Chemical Engineering.* 43 (1), 36-39.

Hwang, S. & Ghalchi, S. (1982) Methane separation by a continuous membrane column. *Journal of Membrane Science.* 11 (2), 187-198.

Kale, V., Katikaneni, S. & Cheryan, M. (1999) *Deacidifying rice bran oil by solvent extraction and membrane technology.* Springer Berlin / Heidelberg.

Kedem, O. & Katchalsky, A. (1958) Thermodynamic analysis of the permeability of biological membranes to non-electrolytes. *Biochimica Et Biophysica Acta.* 27 (0), 229-246.

Keurentjes, J. T. F., Linders, L. J. M., Beverloo, W. A. & Van 'T Riet, K. (1992) Membrane cascades for the separation of binary mixtures. *Chemical Engineering Science.* 47 (7), 1561-1568.

Kim, J. (2011) *Development of Scalable Oligunucleotide Synthesis Process Combined with Organic Solvent Nanofiltration (OSN) Technology - First Year Assessment Transfer Report.* Chemical Engineering Department - Imperial College London, .

Kimmerle, K., Bell, C. M., Gudernatsch, W. & Chmiel, H. (1988) Solvent recovery from air. *Journal of Membrane Science.* 36 (0), 477-488.

Köseoglu, S. & Engelgau, D. (1990) *Membrane applications and research in the edible oil industry: An assessment.* Springer Berlin / Heidelberg.

Kothe, K. D., Chen, S., Kao, Y. K. & Hwang, S. T. (1989) A study of the separation behavior of different membrane columns with respect to ternary gas mixtures. *Journal of Membrane Science.* 46 (2–3), 261-281.

Krass, A. S. (1983) *Uranium enrichment and nuclear weapon proliferation.* New York, International Publications Service, Taylor & Francis.

Krstić, D. M., Tekić, M. N., Zavargo, Z. Z., Djurić, M. S. & Ćirić, G. M. (2004) Saving water in a volume-decreasing diafiltration process. *Desalination.* 165 (0), 283-288.

Laguntsov, N. I., Gruzdev, E. B., Kosykh, E. V. & Kozhevnickov, V. Y. (1992) The use of recycle permeator systems for gas mixture separation. *Journal of Membrane Science.* 67 (1), 15-28.

Lightfoot, E. N. (2005) Can Membrane Cascades Replace Chromatography? Adapting Binary Ideal Cascade Theory of Systems of Two Solutes in a Single Solvent. *Separation Science and Technology.* 40 (4), 739-756.

Lightfoot, E. N., Root, T. W. & L. O'Dell, J. (2008) Emergence of Ideal Membrane Cascades for Downstream Processing. *Biotechnology Progress.* 24 (3), 599-605.

Lin, J. C. T., Peeva, L. G. & Livingston, A. G. (2006) Separation of pharmaceutical process-related impurities by an organic solvent nanofiltration membrane cascade. *AIChe Annual Meeting. 2006,* San Francisco pp.12-17.

Lin, J. C. & Livingston, A. G. (2007) Nanofiltration membrane cascade for continuous solvent exchange. *Chemical Engineering Science.* 62 (10), 2728-2736.

Livingston, A. G., Peeva, L., Han, S., Nair, D., Luthra, S. S., White, L. & Freitas dos Santos, L. M. (2003) Membrane Separation in Green Chemical Processing. *Annals of the New York Academy of Sciences.* 984 (1), 123-141.

Luo, J., Ding, L., Qi, B., Jaffrin, M. Y. & Wan, Y. (2011) A two-stage ultrafiltration and nanofiltration process for recycling dairy wastewater. *Bioresource Technology.* 102 (16), 7437-7442.

Luthra, S. S., Yang, X., Freitas dos Santos, L. M., White, L. S. & Livingston, A. G. (2002) Homogeneous phase transfer catalyst recovery and re-use using solvent resistant membranes. *Journal of Membrane Science.* 201 (1–2), 65-75.

Luthra, S. S., Yang, X., Freitas, d. S., White, L. S. & Livingston, A. G. (2001) Phase-transfer catalyst separation and re-use by solvent resistant nanofiltration membranes. *Chemical Communications.* (16), 1468-1469.

Malik, P. K. & Sanyal, S. K. (2004) Kinetics of decolourisation of azo dyes in wastewater by UV/H2O2 process. *Separation and Purification Technology.* 36 (3), 167-175.

Maskan, F., Wiley, D. E., Johnston, L. P. M. & Clements, D. J. (2000) Optimal design of reverse osmosis module networks. *AIChE Journal.* 46 (5), 946-954.

Mason, E. A. & Lonsdale, H. K. (1990) Statistical-mechanical theory of membrane transport. *Journal of Membrane Science.* 51 (1–2), 1-81.

McCandless, F. P. (1990) Comparison of countercurrent recycle cascades with continuous membrane columns for gas separations. *Industrial & Engineering Chemistry Research.* 29 (10), 2167-2170.

McCandless, F. P. (1985) A comparison of some recycle permeators for gas separations. *Journal of Membrane Science.* 24 (1), 15-28.

McCandless, F. P. & Herbst, S. (1990) Counter-current recycle membrane cascades for the separation of the boron isotopes in BF3. *Journal of Membrane Science.* 54 (3), 307-319.

Mohanty, K. & Ghosh, R. (2008) Novel tangential-flow countercurrent cascade ultrafiltration configuration for continuous purification of humanized monoclonal antibody. *Journal of Membrane Science.* 307 (1), 117-125.

Mulder, M. (1996) *Basic principles of membrane technology.* , Kluwer Academic.

Mulherkar, P. & van Reis, R. (2004) Flex test: a fluorescent dextran test for UF membrane characterization. *Journal of Membrane Science.* 236 (1–2), 171-182.

Mulholland, K. L. & Dyer, J. A. (2001) Process analysis via waste minimization: Using DuPont's methodology to identify process improvement opportunities. *Environmental Progress.* 20 (2), 75-79.

Muller, A., Daufin, G. & Chaufer, B. (1999) Ultrafiltration modes of operation for the separation of α-lactalbumin from acid casein whey. *Journal of Membrane Science.* 153 (1), 9-21.

Musale, D. A. & Kumar, A. (2000) Solvent and pH resistance of surface crosslinked chitosan/poly(acrylonitrile) composite nanofiltration membranes. *Journal of Applied Polymer Science.* 77 (8), 1782-1793.

Ohno, M., Morisue, T., Ozaki, O. & Miyauchi, T. (1978a) Comparison of Gas Membrane Separation Cascades Using Conventional Separation Cell and Two-Unit Separation Cells. *Journal of Nuclear Science and Technology.* 15 (5), 376-386.

Ohno, M., Morisue, T., Ozaki, O. & Miyauchi, T. (1978b) Gas Separation Performance of Tapered Cascade with Membrane. *Journal of Nuclear Science and Technology.* 15 (6), 411-420.

Overdevest, P. E. M., Hoenders, M. H. J., van't Riet, K., van der Padt, A. & Keurentjes, J. T. F. (2002) Enantiomer separation in a cascaded micellar-enhanced ultrafiltration system. *AIChE Journal.* 48 (9), 1917-1926.

Pathare, R. & Agrawal, R. (2010) Design of membrane cascades for gas separation. *Journal of Membrane Science.* 364 (1–2), 263-277.

Peeva, L. G., Gibbins, E., Luthra, S. S., White, L. S., Stateva, R. P. & Livingston, A. G. (2004) Effect of concentration polarisation and osmotic pressure on flux in organic solvent nanofiltration. *Journal of Membrane Science.* 236 (1–2), 121-136.

Peng, H. & Tremblay, A. Y. (2008) The selective removal of oil from wastewaters while minimizing concentrate production using a membrane cascade. *Desalination.* 229 (1–3), 318-330.

Peng, H., Tremblay, A. Y. & Veinot, D. E. (2005) The use of backflushed coalescing microfiltration as a pretreatment for the ultrafiltration of bilge water. *Desalination.* 181 (1–3), 109-120.

Rama, L. P., Cheryan, M. & Rajagopalan, N. (1996) Solvent recovery and partial deacidification of vegetable oils by membrane technology. *Lipid / Fett.* 98 (1), 10-14.

Rauf, M. A., Ashraf, S. & Alhadrami, S. N. (2005) Photolytic oxidation of Coomassie Brilliant Blue with H2O2. *Dyes and Pigments.* 66 (3), 197-200.

Rautenbach, R. & Albrecht, R. (1985) The separation potential of pervaporation : Part 2. Process design and economics. *Journal of Membrane Science.* 25 (1), 25-54.

Reddy, K. K., Kawakatsu, T., Snape, J. B. & Nakajima, M. (1996) Membrane Concentration and Separation of L-Aspartic Acid and L-Phenylalanine Derivatives in Organic Solvents. *Separation Science and Technology.* 31 (8), 1161-1178.

Reichardt, C. C. (2010) *Solvents and Solvent Effects in Organic Chemistry4e.* , wiley.

Richard Bowen, W. & Doneva, T. A. (2000) Atomic force microscopy studies of nanofiltration membranes: surface morphology, pore size distribution and adhesion. *Desalination.* 129 (2), 163-172.

Robeson, L. M. (1991) Correlation of separation factor versus permeability for polymeric membranes. *Journal of Membrane Science.* 62 (2), 165-185.

Robinson, J. P., Tarleton, E. S., Millington, C. R. & Nijmeijer, A. (2004) Solvent flux through dense polymeric nanofiltration membranes. *Journal of Membrane Science.* 230 (1–2), 29-37.

Rundquist, E. M., Pink, C. J. & Livingston, A. G. (2012) Organic solvent nanofiltration: a potential alternative to distillation for solvent recovery from crystallisation mother liquors. *Green Chemistry.* 14 (8), 2197-2205.

Savelski, M. J., Slater, C. S., Hounsell, G., Pilipauskas, D. & Urbanski, F. (2008) 12th Annual ACS Green Chemistry and Engineering Conference. *2008,* Washington, DC pp.133.

Schmidt, M., Mirza, S., Schubert, R., Rödicker, E. H., Kattanek, S. & Malisz, J. (1999) Nanofiltrationsmembranen für Trennprobleme in organischen Lösungen. *Chemie Ingenieur Technik.* 71 (3), 199-206.

See Toh, Y. H., Lim, F. W. & Livingston, A. G. (2007) Polymeric membranes for nanofiltration in polar aprotic solvents. *Journal of Membrane Science.* 301 (1–2), 3-10.

See Toh, Y. H., Loh, X. X., Li, K., Bismarck, A. & Livingston, A. G. (2007) In search of a standard method for the characterisation of organic solvent nanofiltration membranes. *Journal of Membrane Science.* 291 (1–2), 120-125.

See Toh, Y. H., Silva, M. & Livingston, A. (2008) Controlling molecular weight cut-off curves for highly solvent stable organic solvent nanofiltration (OSN) membranes. *Journal of Membrane Science.* 324 (1–2), 220-232.

Sengupta, A. & Sirkar, K. K. (1987) Ternary gas mixture separation in two-membrane permeators. *AIChE Journal.* 33 (4), 529-539.

Sereewatthanawut, I., Lim, F. W., Bhole, Y. S., Ormerod, D., Horvath, A., Boam, A. T. & Livingston, A. G. (2010) Demonstration of Molecular Purification in Polar Aprotic Solvents by Organic Solvent Nanofiltration. *Organic Process Research & Development.* 14 (3), 600-611.

Seyler, C., Capello, C., Hellweg, S., Bruder, C., Bayne, D., Huwiler, A. & HungerbÃ¼hler, K. (2006) Waste-Solvent Management as an Element of Green Chemistry:â€‰ A Comprehensive Study on the Swiss Chemical Industry. *Industrial & Engineering Chemistry Research.* 45 (22), 7700-7709.

Sheth, J. P., Qin, Y., Sirkar, K. K. & Baltzis, B. C. (2003) Nanofiltration-based diafiltration process for solvent exchange in pharmaceutical manufacturing. *Journal of Membrane Science.* 211 (2), 251-261.

Shi, D., Kong, Y., Yu, J., Wang, Y. & Yang, J. (2006) Separation performance of polyimide nanofiltration membranes for concentrating spiramycin extract. *Desalination.* 191 (1–3), 309-317.

Slater, C. S., Savelski, M. J., Taylor, S., Kiang, S., LaPorte, T. & Spangler, L. (2007) American Institute of Chemical Engineerings Annual Meeting. *2007,* Salt Lake City pp.233f.

Snape, J. B. & Nakajima, M. (1996) Processing of agricultural fats and oils using membrane technology. *Journal of Food Engineering.* 30 (1–2), 1-41.

So, S., Peeva, L. G., Tate, E. W., Leatherbarrow, R. J. & Livingston, A. G. (2010) *Membrane enhance peptide synthesis.* The Royal Society of Chemistry.

Sterlitech Corporation. (2012) *Bench scale equipment - Flat sheet membranes.* [Online] Available from: http://www.sterlitech.com/bench-scale-equipment/flat-sheet-membranes.html .

Thomas, P. (January 3, 2012) *Solvent Recovery at Pfizer: A Continuous Solution for Small Waste Streams.* [Online] Available from: http://www.sustainableplant.com/2012/01/solvent-recovery-at-pfizer-a-continuous-solution-for-small-waste-streams/?show=all .

Valtcheva, I. B., Kumbharkar, S. C., Kim, J. F., Peeva, L. G. & Livingston, A. G. (2012) Development of organic solvent nanofiltration membranes for the application in extreme pH conditions. *Euromembrane. 23-27 September, London.*

Van der Bruggen, B., Geens, J. & Vandecasteele, C. (2002) Influence of organic solvents on the performance of polymeric nanofiltration membranes. *Separation Science and Technology.* 37 (4), 783-797.

Van der Bruggen, B., Mänttäri, M. & Nyström, M. (2008) Drawbacks of applying nanofiltration and how to avoid them: A review. *Separation and Purification Technology.* 63 (2), 251-263.

Vandezande, P., Gevers, L. E. M. & Vankelecom, I. F. J. (2008) Solvent resistant nanofiltration: separating on a molecular level. *Chemical Society Reviews.* 37 (2), 365-405.

Vankelecom, I. F. J., De Smet, K., Gevers, L. E. M., Livingston, A., Nair, D., Aerts, S., Kuypers, S. & Jacobs, P. A. (2004) Physico-chemical interpretation of the SRNF transport mechanism for solvents through dense silicone membranes. *Journal of Membrane Science.* 231 (1–2), 99-108.

Vanneste, J., De Ron, S., Vandecruys, S., Soare, S. A., Darvishmanesh, S. & Van der Bruggen, B. (2011) Techno-economic evaluation of membrane cascades relative to simulated moving bed chromatography for the purification of mono- and oligosaccharides. *Separation and Purification Technology.* 80 (3), 600-609.

Villani, S. & Becker, E. W.,. (1979) *Uranium enrichment.* Berlin; New York, Springer-Verlag.

Ward, R. A., Klein, E., Feldhoff, P. W. & Turnham, T. J. (1987) Ultrafiltration: separation enhancement by counter-current cascading. *Journal of Membrane Science.* 33 (1), 97-111.

White, L. S. (2006) Development of large-scale applications in organic solvent nanofiltration and pervaporation for chemical and refining processes. *Journal of Membrane Science.* 286 (1–2), 26-35.

White, L. S. (2002) Transport properties of a polyimide solvent resistant nanofiltration membrane. *Journal of Membrane Science.* 205 (1–2), 191-202.

White, L. S. & Nitsch, A. R. (2000) Solvent recovery from lube oil filtrates with a polyimide membrane. *Journal of Membrane Science.* 179 (1–2), 267-274.

Whu, J. A., Baltzis, B. C. & Sirkar, K. K. (2000) Nanofiltration studies of larger organic microsolutes in methanol solutions. *Journal of Membrane Science.* 170 (2), 159-172.

Wong, H., Pink, C. J., Ferreira, F. C. & Livingston, A. G. (2006) Recovery and reuse of ionic liquids and palladium catalyst for Suzuki reactions using organic solvent nanofiltration. *Green Chemistry.* 8 (4), 373-379.

Xu, J. & Agrawal, R. (1996) Gas separation membrane cascades I. One-compressor cascades with minimal exergy losses due to mixing. *Journal of Membrane Science.* 112 (2), 115-128.

Yan, Z. & Kao, Y. (1989) Comparative study of two-membrane permeators for gas separations. *Journal of Membrane Science.* 42 (1–2), 147-168.

Yang, X. J., Livingston, A. G. & Freitas dos Santos, L. (2001) Experimental observations of nanofiltration with organic solvents. *Journal of Membrane Science.* 190 (1), 45-55.

Appendix A.

HPLC Calibration Curves

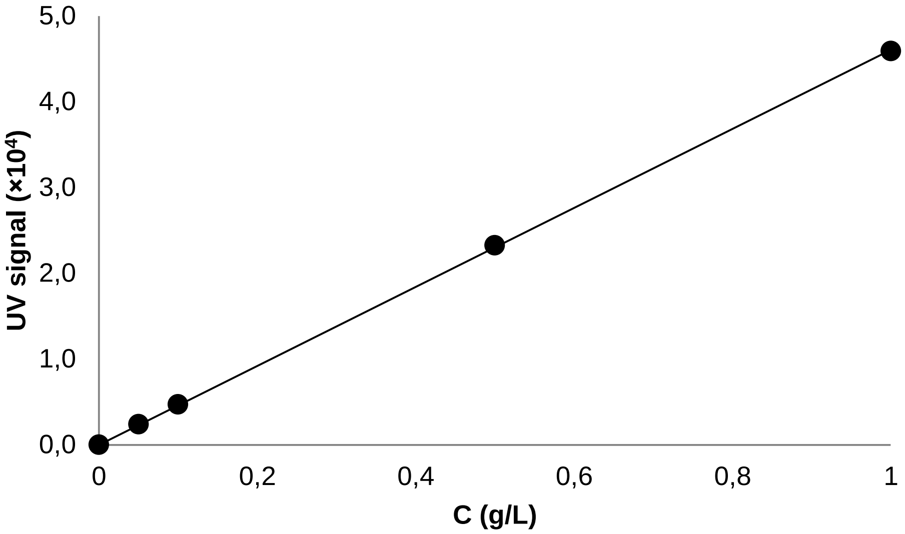

Figure A - 1 Calibration curve for MY in MeOH (T=30 °C; Retention time=6.6 min): y=4.60x with R^2=0.9999.

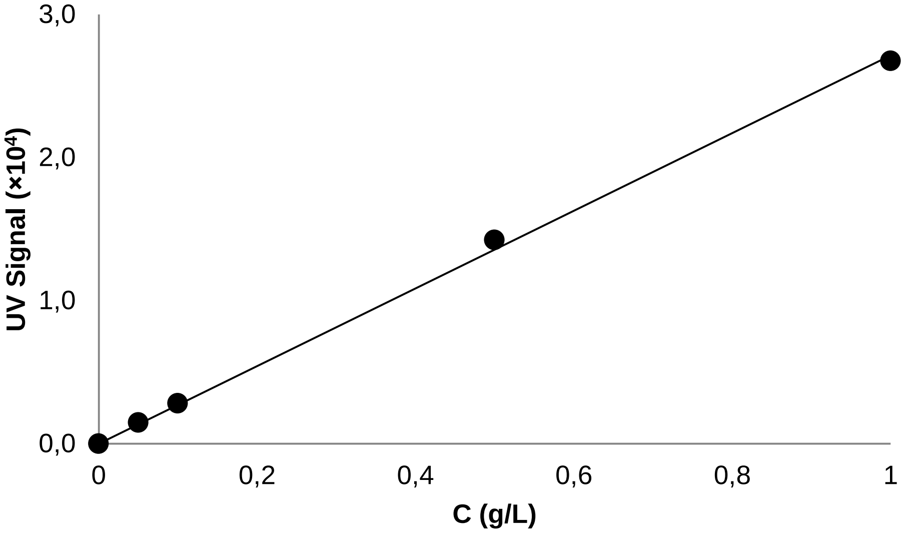

Figure A - 2 Calibration curve for BBR in MeOH (T=30 °C; Retention time=17.4 min): y=2.71x with R^2=0.9988.

Appendix B.

Effect of temperature on the visible spectra of MY and BBR compounds

A sample of 1g/L was prepared for each dye. The two samples were analyzed in three different days by UV/Vis Spectroscopy. The maximum absorption wavelength of MY and BBR is at 435 and 600 nm, respectively, so both absorb in the visible range. The spectra obtained on Day 2 are shifted to the left when compared to the other. Plus, the absorbance of BBR increased from Day 1 to Day 2 and decreased back to the initial value on Day 3 (see Figure B-1 and Figure B-2). Since Day 2 was much warmer than the other days, it is possible that the absorbance of these two compounds, mostly BBR, depends a lot on temperature. Thus, the HPLC should be used instead of the UV/Vis spectrophotometer as this system allows to have control over the temperature at which samples are analyzed.

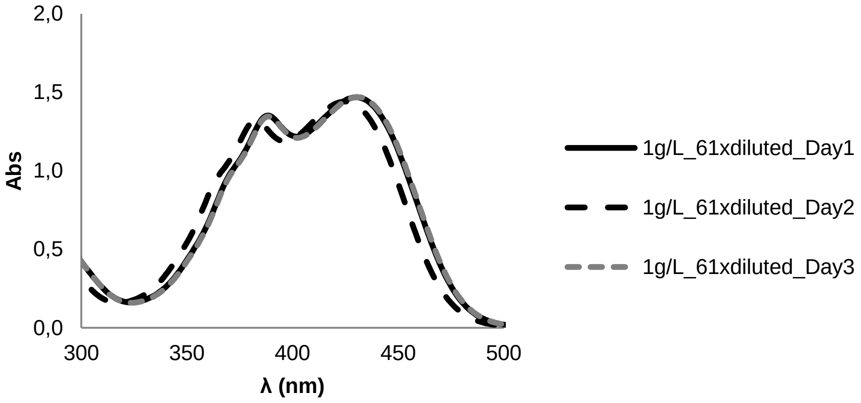

Figure B - 1 UV/Vis Spectra for a 1g/L sample of MY in MeOH at different days.

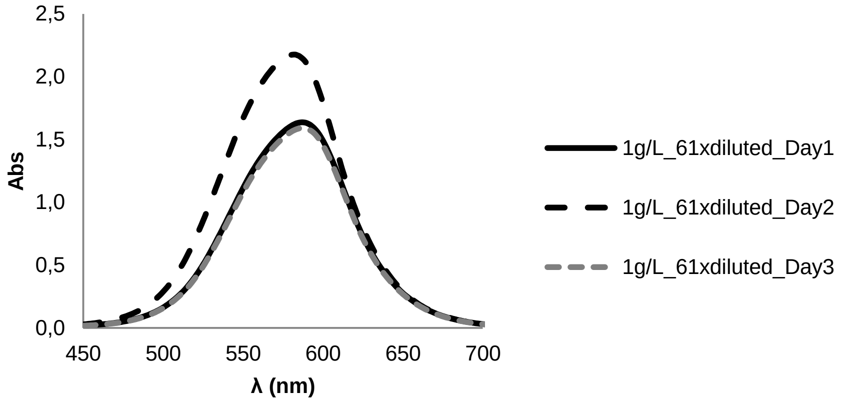

Figure B - 2 UV/Vis Spectra for a 1g/L sample of BBR in MeOH at different days.

Appendix C.

Process Modeling

A simple process model based on mass balances at steady state was developed for each of the systems studied in this work. The following assumptions were made:

- The systems operate at constant volume.
- The fluxes and rejections are constant with respect to time.
- The concentration of the solutes has no influence on rejection.
- Solutes are no interactive.
- Concentration polarization and fouling effects are not taken into account.

C.1 SINGLE MEMBRANE SYSTEM

The single membrane system can also be modeled by writing a mass balance around the feed tank and the membrane cell. According to the above assumptions, the mass balance over the feed tank yields,

$$\frac{dC_{F,i}}{dt}=\frac{1}{V_F}[Q_R.C_{R,i}-Q_F.C_{F,i}] \qquad \text{C.1-1}$$

where V_F is the feed tank volume, Q_R and Q_F are the retentate and feed volumetric flow rates, respectively, and $C_{R,i}$ and $C_{F,i}$ are the concentration of species i in the retentate and feed, respectively. On the other hand, the mass balance over the membrane unit gives,

$$\frac{dC_{R,i}}{dt}=\frac{1}{V_R}[Q_F.C_{F,i}-Q_{R.}C_{R,i}-Q_P.C_{P,i}] \qquad \text{C.1-2}$$

where V_R is the volume of the membrane cell, Q_P is the permeate volumetric flow rate, and $C_{P,i}$ is the concentration of species i in the permeate. Substituting $C_{P,i}$=(1-R_i).$C_{R,i}$ and $Q_P = J.A$ into this equation gives,

$$\frac{dC_{R,i}}{dt}=\frac{1}{V_R}[Q_F.C_{F,i}-(Q_R+J.A.(1-R_i)).C_{R,i}] \qquad \text{C.1-3}$$

The calculated mass profiles of each one of the species in solution were obtained by numerically solve the differential equations A.1.1 and A.1.3 in MATLAB® using ODE45 function.

C.2 CLOSED-LOOP MEMBRANE PROCESS

The closed-loop membrane system can be modeled by writing a mass balance around the feed tank and membranes cells 1 and 2. Since $Q_{R2}=0$, then $J_1=J_2=J$, and the mass balances yield,

$$\frac{dC_{F,i}}{dt}=\frac{1}{V_F}[Q_{R1}.C_{R1,i}+J.A.C_{R2,i}.(1\text{-}R_{i,2})\text{-}Q_F.C_{F,i}] \quad \textbf{C.2-1}$$

$$\frac{dC_{R1,i}}{dt}=\frac{1}{V_{R1}}[Q_F.C_{F,i}\text{-}(Q_{R1}+J.A.(1\text{-}R_{i,1})).C_{R1,i}] \quad \textbf{C.2-2}$$

$$\frac{dC_{R2,i}}{dt}=\frac{J.A}{V_{R2}}[C_{R1,i}(1\text{-}R_{i,1})\text{-}C_{R2,i}(1\text{-}R_{i,2})] \quad \textbf{C.2-3}$$

These three ordinary differential equations were also solved using the ODE45 function from MATLAB®, in order to describe the concentration profiles of the different species in the feed tank, membrane cell 1 and membrane cell 2.

By rearranging equation A.2.3 in order to make $R_{i,1}$ the subject we obtain:

$$R_{i,1}=1\text{-}\frac{V_2\frac{dC_{R2,i}}{dt}+J.A.C_{R2}.(1\text{-}R_{i,2})}{J.A.C_{R1}} \quad \textbf{C.2-4}$$

This equation was used to calculate the observed rejection of the membranes from the membrane cell 1.

C.3 MEMBRANE CASCADE

The membrane cascade can be modeled by doing a mass balance around the separation stage (Stage 1) and the solvent recovery stage (Stage 2). Assuming that $J_1=J_2=J$, then we obtain the following equations:

$$\frac{dC_{R1,i}}{dt}=\frac{J.A}{V_{R1}}[C_{R2,i}.(1-R_{i,2})-C_{R1,i}.(1\text{-}R_{i,cascade})] \quad \textbf{C.3-1}$$

$$\frac{dC_{R2,i}}{dt}=\frac{J.A}{V_{R2}}[C_{R1,i}.(1\text{-}R_{i,cascade})\text{-}C_{R2,i}.(1-R_{i,2})] \quad \textbf{C.3-2}$$

where in this case J_1 is the flux of the final permeate from stage 1 and $R_{i,cascade}$ is the overall rejection of a cascade with n membrane units and is given by

$$R_{i,cascade}=1-\prod_{j=1}^{n}(1-R_{i,j}) \tag{C.3-3}$$

where $R_{i,j}$ is the rejection of species i in the membrane unit j. If it is assumed that all the membranes used in the separation stage have the same rejection, then we obtain:

$$R_{i,cascade}=1-(1-R_i)^n \tag{C.3-4}$$

Equations C.3.3 and C.2.4 are only valid if all compounds in system 1 are well-mixed, which is only possible if it was assumed infinite recycle ratio from each membrane unit in system 1.

Equations C.3.1 and C.3.2 were solved using the ODE45 function from MATLAB®, in order to obtain the concentration profiles of the different species in the stages 1 and 2.